DEHYDROGENATION OF N-PROPANOL TO PROPIONALDEHYDE OVER A COPPER CHROMITE CATALYST

MARINA HOP BSc Hons (Applied Chemistry)

Submitted to the University of Cape Town in fulfilment of the requirements for the degree of Masters of Science (Applied Science)

1 February 1998

TABLE OF CONTENTS

ACKNOWLEDGEMENTS

I would like to thank my husband, Darren, for his support and faith in me. I would also like to thank SASOL for their financial support. In particular, I would like to thank the staff of Sastech R & D who, although too numerous to mention individually, assisted, advised and guided me through this work. I would also like to thank my supervisor, Prof. M. Dry, for his assistance.

SYNOPSIS

Methyl methacrylate (MMA) is widely used for a range of polymer products. MMA can be produced from propionaldehyde via the BASF process. n-Propanol is readily available in South Africa as a byproduct of Fischer-Tropsch synthesis. This prompted an investigation into the production of propionaldehyde by the dehydrogenation of n-propanol. There is presently no established technology for the dehydrogenation of n-propanol to propionaldehyde and there has been very little work carried out on the effect of process variables on propionaldehyde yield.

The emphasis of the current work was optimising propionaldehyde production. A commercial copper-chromite catalyst (G-13), for the dehydrogenation of ethanol to acetaldehyde, was used for the purposes of this study. Typical operating conditions of 250°C, 1 atmosphere pressure, 1:1 molar ratio of n-propanol to water and a liquid hourly space velocity of 1 hr^{-1} were used. Significant byproduct formation occurred (between 64% and 93% n-propanol selectivity to byproducts) despite the addition of water to the n-propanol feed in an attempt to reduce the formation of condensation products. The copper-chromite catalyst deactivated rapidly with time-on-line. The catalytic activity reduced to half the initial value after seven days on line. The reaction conditions (temperature, water partial pressure and liquid hourly space velocity) were varied in order to optimise the propionaldehyde yield. A maximum propionaldehyde selectivity of 32 mole % was achieved at a reaction temperature of 219°C, a water partial pressure of 0.8 atmospheres and a liquid hourly space velocity of 1.1 hr^{-1}. The rapid deactivation of this particular catalyst together with the low propionaldehyde yield make the process unattractive for industrial applications.

LIST OF FIGURES

LIST OF TABLES

NOMENCLATURE

Abbreviations:

ACH	=	Acetone cyanohydrin
BET	=	Brunauer, Emmett and Teller
CI	=	Chemical ionisation
EI	=	Electron-impact ionisation
FID	=	Flame ionisation detector
GC	=	Gas chromatography
ID	=	Internal diameter
LHSV	=	Liquid hourly space velocity
MMA	=	Methyl methacrylate
NA	=	Not analysed
PONA	=	Paraffins, olefins, naphthenes, aromatics
SEM	=	Scanning electron microscopy
STP	=	Standard temperature and pressure
TCD	=	Thermal conductivity detector
TOF	=	Turn over frequency
TPD	=	Temperature programmed desorption
TPR	=	Temperature programmed reduction
XRD	=	X-ray diffraction

A	=	Cross sectional area of tube
A_0	=	Pre-exponential factor
Av	=	Average
D_p	=	Diameter of catalyst particle
d_p	=	Diameter of particle
d_t	=	Diameter of tube
E_A	=	Activation energy
F	=	Feed rate of alcohol
$\Delta G°$	=	Standard Gibb's free energy
hr^{-1}	=	Per hour
$\Delta H°$	=	Standard reaction enthalpy
$\Delta H°_f$	=	Standard enthalpy of formation
k	=	Rate constant
K_a	=	Equilibrium constant for adsorption of alcohol
K_A	=	Adsorption constant for acetaldehyde
K_C	=	Equilibrium constant for the adsorption of methylethylketone
k_D	=	Mass transfer coefficient
K_e	=	Equilibrium constant for the dehydrogenation of ethanol
K_p	=	Thermodynamic equilibrium constant in terms of partial pressures
L	=	Tube length
m	=	Mass flow rate
M_i	=	Molar mass of component i
N	=	Rate of mass transfer per unit area
n	=	Moles

n_T = Total number of moles

n_s = Number of surface copper atoms per gram of catalyst

n_1 = Sample size for experiment A

n_2 = Sample size for experiment B

P = Pressure at which reaction takes place

P_0 = Pressure at time zero

p = Partial pressure of a gas

p_{ROH} = Partial pressure of alcohol

P_A = Partial pressure of acetaldehyde

p_A = Partial pressure of secondary butanol

p_B = Partial pressure of component B

p_c = Partial pressure of methylethylketone

P_E = Partial pressure of ethanol

P_H = Partial pressure of hydrogen

PrOH = n-Propanol

r = Rate of reaction

R = Gas constant

R_e = Reynold's number

R_f = Response factor

r_e = Rate of reaction

r_p = Reaction rate impeded by mass transfer

s_1^2 = Sample variance for experiment A

s_2^2 = Sample variance for experiment B

$\Delta S°$ = Standard reaction entropy

S_x = Area available to mass transfer

t_{test} = Test statistic

T = Temperature

u = Superficial fluid velocity

V_0 = Initial rate of reaction

W = Catalyst mass

x = Sample value

$\bar{x}$ = Mean of experiment A

X = g.mole of feed converted divided by g.mole of feed

y = Mean of experiment B

y_i = Mole fraction of component i

Greek Symbols:

ε = Void fraction

$\hat{\sigma}^2$ = Estimated population variance

η = Effectiveness factor

η_i = Viscosity of pure component i

μ_1 = Population variance for experiment A

μ_2 = Population variance for experiment B

μ_{mix} = Viscosity of low pressure gas mixture

ρ_f = Density of fluid

ϕ_{ij} = Parameter to account for differences in molecular masses of components in a gas mixture

Σ = The sum of

1. INTRODUCTION

1.1. SCOPE OF THE CURRENT WORK

Methyl Methacrylate (MMA) is used extensively in a range of polymer products [1]. The MMA market has shown a sustained growth rate in recent years which has lead to the development of processes based on a variety of different feedstocks. The conventional route to MMA is via the acetone cyanohydrin route. This accounts for the majority of the world production at present [2]. The other processes of significance are C4 (isobutylene, isobutanol or tertiary butanol) direct oxidation, the propylene process and the BASF propionaldehyde route. Ethylene hydroformylation is used in the BASF process to produce propionaldehyde which is then condensed with formaldehyde to produce methacrolein. Direct oxidation of methacrolein produces methacrylic acid which undergoes acid catalysed esterification with methanol to give MMA.

Propionaldehyde can be produced by the dehydrogenation of n-propanol which offers an alternative to the ethylene hydroformylation step. Propanol is readily available as a byproduct of the Fischer-Tropsch process making this an attractive route for the production of MMA.

There is presently no established technology for the dehydrogenation of propanol to propionaldehyde. However, the commercial production of acetaldehyde by the dehydrogenation of ethanol is well documented [3]. Some work has also been carried out on the dehydrogenation of iso-propanol [4], [5]. Copper is widely used as a catalyst for the dehydrogenation of alcohols [6], [7]. However, very little work has been done on the dehydrogenation of n-propanol over copper catalysts and in particular over copper-chromite catalysts. Some work has been carried out by Connett [8] who studied the mechanism of n-propanol dehydrogenation over copper oxide catalysts. Chhabra et al [9] studied the reaction mechanism, equilibrium constant and activation energy for the dehydrogenation of n-propanol over a copper supported on kieselguhr catalyst. Despite these studies very little work has been carried out concerning the effect of process variables in the context of an industrially applicable process. The lack of literature available on the dehydrogenation of n-propanol over copper-chromite catalysts and the interest expressed in

establishing a process for the production of MMA from an alternative, readily available feedstock, have prompted the work discussed below. The aims of the current study were;

(i) to establish suitable operating conditions at which acceptable conversions and selectivities could be obtained over a commercial copper-chromite catalyst

(ii) the optimisation of the operating conditions in order to maximise the production of propionaldehyde to make the process viable for industrial application.

In order to optimise propionaldehyde production the following were investigated:

(i) The reactor system was checked to ensure that it was inert and that reproducible results could be obtained.

(ii) The presence or absence of mass transfer effects were investigated.

(iii) The effect of temperature profiles through the catalyst bed were investigated and minimised.

(iv) Effects of catalyst aging with time-on-line were investigated.

(v) The products of n-propanol dehydrogenation were identified and the mechanisms by which byproduct formation takes place were investigated in order to understand the factors influencing propionaldehyde formation.

(vi) The operating conditions were optimised by means of a matrix experimental design.

1.2. THE CHEMISTRY OF PROPIONALDEHYDE

Propionaldehyde is a highly reactive chemical intermediate and is used primarily in the preparation of C_3 and C_6 compounds. It is used as a source of propyl groups during chemical synthesis. The α-hydrogen of propionaldehyde can be replaced by formaldehyde via the Aldol condensation reaction to produce methacrolein in the manufacture of methyl methacrylate for the polymer industry [10]. Propionaldehyde is converted into 1-propanol, propionic acid and trimethylolethane (trihydroxymethyl ethane) and finds application in the pharmaceutical industry as the tranquillizer meprobmat, as well as in the agricultural chemical field. It is used as a rubber additive and in corrosion inhibitors.

Its highly reactive chemical nature is due to the polarity of the carbonyl group and the acidity of the α-hydrogen atoms. These reactive centres allow propionaldehyde to undergo oxidation and polymerisation readily. Propionaldehyde commonly undergoes the following reactions;

(i) Oxidation;

The aldehyde undergoes liquid phase catalytic and non-catalytic oxidation to produce propionic acid which is used as a crop preservative as well as in the manufacture of herbicides. The sodium and calcium salts are used as food preservatives [11].

(ii) Condensation and Addition;

Propionaldehyde can undergo self-Aldol condensation to produce 3-hydroxy-2-methyl pentanal which dehydrates to form 2-methyl-2-pentenal when heated, or cross-Aldol condensation with other aldehydes or ketones, in the presence of an aqueous alkali or acid.

Propionaldehyde undergoes Aldol condensation with formaldehyde in the production of 2-hydroxymethyl-2-methyl-1,3-propanediol for the manufacture of alkyl resins.

1.3. THE PRINCIPLE PROCESSES FOR THE COMMERCIAL PRODUCTION OF ALDEHYDES

1.3.1. Hydroformylation

Propionaldehyde is commercially produced by the hydroformylation of ethylene. The annual production of propionaldehyde using this method was estimated to be approximately 170 000 tons in 1993 [12].

The hydroformylation (oxo) process involves the reaction of an olefin (usually an α-olefin) with carbon monoxide and hydrogen in the presence of a homogeneous catalyst to produce an aldehyde or alcohol with one additional carbon atom [13][14].

The process was discovered by Roelen of Ruhrchemie in 1938 [14]. However, commercial scale production only began in 1948 in America [13]. The process made use of cobalt catalysts until the mid-1970's when Union Carbide and Celanese independently developed Rhodium-based catalysts which are more active and selective for the aldehyde [14].

The oxo process is catalysed by transition metal catalysts but only cobalt and rhodium complexes

are used commercially [13].

Cobalt catalysts used for the hydroformylation of olefins can be divided into unmodified catalysts and modified cobalt catalysts. The unmodified cobalt catalyst required high CO partial pressures in order to ensure a good yield of straight chain product. The conventional cobalt catalyst required reaction temperatures of 100-180°C, 20-25 MPa pressure and 0,1-1 weight percent Co to α-olefin with a residence time of 1-2 hours and a ratio of H_2:CO of 1:1 [13]. The byproducts include acetals, diols and esters. In 1963 Shell introduced the first commercial cobalt/phosphene-ligand catalyst for the production of 1-butanol. The introduction of an organophosphine ligand gives rise to the formation of a catalyst complex which improves the selectivity for the straight chain alcohol. The modified catalyst is also more thermally stable and can be used at lower reactor pressures (2-10 MPa) which has reduced capital and operating costs. However the ligand modified catalyst is less active than the unmodified catalyst and requires a higher reaction temperature (150-210°C). The modified catalyst also has significant hydrogenation activity to convert the aldehyde directly to the corresponding alcohol and isomerisation activity to convert internal olefins to terminal olefins. The modified catalyst system makes use of 2:1 H_2:CO ratio [13]. The hydroformylation of ethylene gives 90% conversion to propionaldehyde with 2-3% of the ethylene being converted to condensation products [15]. Byproducts of the Co modified catalyst include almost 10% paraffins but less acetals, diols and esters compared to the conventional process because of the lower aldehyde concentrations as a result of the hydrogenation activity of the modified Co catalyst. Rhodium is more catalytically active than cobalt and favours aldehyde formation. The unmodified rhodium catalyst favours branched products while the rhodium carbonyl-phosphine complex catalysts favour linear products. The reaction condition are 100°C and 1,5 MPa with a CO partial pressure of less than 0,3 MPa and a hydrogen partial pressure of less than 1,4 MPa. Union Carbide has made use of modified rhodium catalysts for ethylene hydroformylation since 1975 [13]. Hydroformylation of ethylene produces 98-99% propionaldehyde, 0,5-1% ethane and 0,5-1% heavy ends [15].

Hydroformylation is a complex process which proceeds stepwise through a series of consecutive reactions. Most of these reactions are reversible and there appears to be more than one rate limiting step in the overall reaction mechanism. The reaction is highly exothermic with about 125 kJ/mol of energy released. The most crucial process variables are reaction temperature and the CO and H_2

partial pressure [13]. The process does suffer from several problems. These include catalyst sensitivity to poisons such as strong acids, cyanides, sulphur, oxygen and dienes. The combination of high pressure and relatively high temperature and long residence times make the process expensive from an operations point of view. Another problem facing the process is the cost of the catalyst and deposition of cobalt metal on the process equipment. This makes the addition of surfactants necessary further increasing the operating cost of the process. It is also difficult to recover the catalyst from homogeneous solution which makes separation procedures expensive.

In the South African context ethylene is expensive compared to n-propanol. This together with the problems associated with the hydroformylation process, have prompted an investigation into other routes for the production of propionaldehyde. The commercial production of acetaldehyde is well documented [3][11][16] and will be described below since the production of propionaldehyde is likely to follow a similar route.

1.3.2. Catalytic Dehydrogenation of Ethanol

In the dehydrogenation process ethanol is vaporised and passed over a chromium-activated copper catalyst at 270 to 300 °C and 1 atmosphere pressure. The conversion is between 30 and 50 mole percent and the selectivity to the aldehyde is between 90 and 95 mole percent [17].

1.3.3. Oxidation of Ethanol

The commercial production of acetaldehyde by oxidation of ethanol is well established [16]. Ethanol oxidation is carried out in the vapour phase over a copper or silver catalyst at 300 to 500 °C in the presence of air. The oxidation is controlled by diluting the ethanol with steam. Conversions of between 45 and 50 mole percent are achieved and the selectivity for the aldehyde is in the range of 94 to 96 mole percent.

The oxidation and dehydrogenation processes have been combined in a process developed by Braunschweigische Maschineenbauanstalt. This has solved the problem of heat supply during dehydrogenation and heat removal during oxidation. Air, ethanol and steam are passed over a silver catalyst at 375 to 550 °C to produce acetaldehyde [3] [18].

1.3.4. Direct Oxidation of Ethylene

The Wacker-Hoechst process for the oxidation of ethylene to acetaldehyde makes use of an aqueous solution of palladium chloride and cupric chloride as catalyst [11]. The palladium chloride converts the ethylene to acetaldehyde generating palladium metal and hydrogen chloride in the process. The cupric chloride then reacts with the palladium to reform the palladium chloride catalyst. The cupric chloride is in turn regenerated with oxygen and hydrogen chloride. The Wacker-Hoechst process has to a large extent replaced the other processes for the production of acetaldehyde. There are two variations of the process, a single stage process and a double stage process, however the basic principle remains the same for both processes.

1.3.5. Acetylene Hydration

Acetaldehyde has been produced commercially by the hydration of acetylene since 1916. However, this process has been surpassed by the direct oxidation of ethylene.

1.4. METHYL METHACRYLATE (MMA)

Methyl methacrylate (MMA) is widely used in the polymer industry for a range of products from acrylic sheets and surface coatings to synthetic latex and moulded products [1]. Expected expansion of the local MMA market together with the availability of n-propanol as a byproduct of the Fischer Tropsch reaction, have made the development of an alternative route for the production of MMA highly attractive.

Traditionally MMA has been produced via the acetone cyanohydrin (ACH) process and most of the MMA produced worldwide is still made via this process. Undesirable byproducts of the process (ammonium sulphate) and the dangers involved in handling hydrogen cyanide have prompted efforts to develop alternative routes for the production of MMA.

1.4.1. C_4 Direct Oxidation Route

Isobutylene, isobutanol or tertiary butanol are used as raw materials and are oxidised over

multicomponent metal catalysts (containing bismuth, molybdenum and several other metal promoters [19]), to methacrolein which is further oxidised to methacrylic acid [1]. MMA is produced by the esterification of methacrylic acid with methanol. Nihon Methacryl Monomer (a joint venture between Sumitomo and Nippon Shokubai) and Mitsubishi Rayon have commercial plants which utilise this route [19].

1.4.2. The Propylene Process

This process involves the reaction of propylene, carbon monoxide and water in the presence of a strong acid catalyst (such as sulphuric acid, hydrogen fluoride and boron fluoride) [19] to give isobutyric acid. This is followed by oxidative dehydrogenation. The process is not in commercial operation at present but patents are held by Röhm, Ashland Oil, Sinclair Refining and Chemical Systems [19].

1.4.3. The Propionaldehyde Route

BASF produce propionaldehyde by ethylene hydroformylation. The propionaldehyde is condensed with formaldehyde to give methacrolein. Methacrolein is catalytically oxidised in air to produce methacrylic acid which undergoes catalysed esterification with methanol to give MMA [1]. Propionic acid can also be used as a feedstock for the production of MMA via methyl propionate or methacrylic acid intermediates.

Amoco have developed a variation of this process which uses a silica-supported cesium ion catalyst for the vapour condensation of formaldehyde with propionic acid to form methacrylic acid. The propionic acid for the reaction is produced from ethylene via the modified Monsanto acetic acid process [1]. Alternately propionic acid can be produced by the oxidation of propionaldehyde.

Despite these new developments none of the newer processes are sufficiently superior to the acetone cyanohydrin process to warrant scrapping the existing plants [19]. Alternate technology is being used for any new plants that are to be built in the future.

1.5. DEHYDROGENATION OF ALCOHOLS BY COPPER CATALYSTS

Copper has been widely used as a catalyst in both supported and unsupported forms. Supported copper catalysts are used extensively in the dehydrogenation of lower alcohols to aldehydes and ketones [6].

1.5.1. The Effect of Chrome Promoter on the Life of Copper Catalysts

Copper remains one of the most active and widely used industrial catalysts for the dehydrogenation of ethanol [20]. However, copper sinters above 300 °C [21] and exhibits low activity below 210 °C [9]. According to Pines et al [22] and Tonner et al [23] copper chromite catalysts were first developed by Homer Adkins in 1931 to increase the stability of the catalyst with respect to sintering and fouling. Fresh copper catalysts deactivate with time but if chromium is added the activity has been found to remain fairly constant [20].

Prasad et al [20] studied the activity of a 16,1 % copper; 83,9 % silica catalyst. The catalyst showed deactivation from 78,6 mole % conversion to 47,5 mole % over a 100 hour period. Comparison of the fresh and spent catalysts by means of XRD and SEM showed a growth in the crystallite size after reaction. A catalyst with 16,1 % copper; 1,4 % Cr_2O_3 and 82,5 % SiO_2 gave conversions of 82,4 mole % which decreased to 68,5 mole % over 100 hours on line. It was found that the copper surface area of the promoted catalyst was almost double that of the unpromoted catalyst. Prasad et al found that the chromia in a copper-chromite catalyst doesn't undergo sintering at the reaction temperature used in their study (310°C) i.e. it has a low mobility at this temperature. The deactivation that took place was mainly due to carbon deposition on the active surface of the catalyst. The amount of carbon present amounted to 1,06 weight percent [20]. Madhusudhan Rao et al [24] also found that chromium-containing copper catalysts showed very high copper surface areas compared to catalysts without chromium. Chromia appeared to maintain the dispersion of the metallic copper when the CuO was reduced during pretreatment. It is thought that chromia interferes with the regular crystal growth of the copper. Chromia particles act as barriers between crystallites of copper maintaining dispersion. They found that the mean particle size of spent copper catalysts containing SiO_2 and Cr_2O_3 was between 5 and 6 nm compared to 38 nm for copper catalysts supported on SiO_2 alone. They presented these results as evidence for the effectiveness

of chromium in controlling the growth rate of copper crystallites.

Tonner et al [23] in contrast, postulated that the presence of chromia prolonged catalyst activity by promoting the breakdown of carbonaceous polymerisation products during the dehydrogenation of methanol over a copper catalyst. They observed that at high hydrogen partial pressures the catalyst reduces completely to copper supported on chromia.

The reaction can be written as follows;

$$CuO + H_2 \rightarrow Cu + H_2O \quad (1)$$

$$Cu + CuCr_2O_4 \rightarrow Cu_2Cr_2O_4 \quad (2)$$

$$Cu_2Cr_2O_4 + H_2 \rightarrow 2Cu + Cr_2O_3 + H_2O \quad (3)$$

Reaction (1) and (2) occur very rapidly and reaction (3) occurs more slowly. At low hydrogen partial pressures (101 kPa) reaction (3) doesn't proceed to completion and the active form of the catalyst is likely to consist of copper supported on cuprous chromite ($Cu_2Cr_2O_4$) or copper/chromia surrounding a core of $CuCr_2O_4$ [25]. They did find however, that copper chromite catalysts exhibit a reduction in activity compared to unpromoted copper catalysts. They suggested that this was due to an electronic interaction between the catalyst and the chromium support. The high copper surface area and the good copper dispersion compensated for any loss in activity [26]. Doca and Segal [27] tested Cu/Cr catalysts with a chrome content ranging from 0,5 to 1,5 atomic mass % and found that the catalysts containing chrome had a lower initial activity compared to pure copper, but the stability of the chrome-containing catalysts during dehydrogenation, was better than that of the copper catalysts.

1.5.2. Active Sites for the Dehydrogenation of Primary Alcohols

There are two schools of thought regarding the valence state of copper in the sites possessing dehydrogenation activity [5]. The research group at ICI support the view that Cu^0 metallic sites play a central role while Klier and co-workers [28] support the view that Cu^+ ions, dispersed in zinc oxide, play a key role in the activity of the catalyst. This prompted Cunningham et al [5] to study the dehydrogenation of 2-propanol over unsupported CuO, Cu_2O and copper metal. They found that oxidised copper showed no activity over a 2 hour period. Exposure to 2-propanol resulted

in reduction of the CuO surface and development of dehydrogenation activity. Therefore dehydrogenation activity was not an intrinsic property of the CuO surface. Cu_2O showed greater resistance to reduction by the alcohol than CuO. This agrees with work carried out by Pepe et al who found that fully oxidised copper was inactive [4]. Cunningham et al found that prereduced copper showed an initial conversion of 23 % which declined to an insignificant level after five hours of exposure to 2-propanol. They proposed that to maintain high activity, Cu^0 and "oxidised" copper sites must be present simultaneously. This was borne out by the high conversions obtained (96,5%) with a physical mixture of $Cu^{II}O$ and metallic copper. The catalyst mixture showed a decline in conversion to 81% over a 5 hour period.

Cunningham et al concluded that the working surface of the catalyst consists of a mixture of copper valence states. They ruled out short-range interactions on the basis that the amount of oxygen required to enhance dehydrogenation activity or reverse deactivation was orders of magnitude greater than reported in the literature for oxygen chemisorption on copper. They put forward long range transfer events such as oxygen, hydrogen or alcohol spillover between metallic and oxidised sites as an explanation for the observed results.

From 2-propanol adsorption isotherms it was found that metallic copper had a higher coverage of 2-propanol than the number of copper sites available and that the amount of 2-propanol adsorbed increased with the percentage of surface that was reduced. From this they concluded that the alcohol underwent migration from the metallic sites to the oxidised locations.

Cunningham investigated these hydrogen spillover effects and found that hydrogen spillover did indeed occur during TPR studies of a physical mixture of Cu^0 and CuO [5]. This is in agreement with results obtained by Pepe et al [4] for CuO/Al_2O_3 catalysts where they found that hydrogen was activated on an Al^{3+} site on Al_2O_3 as H^- H^+ pairs, via reverse spillover, and then transferred to the neighbourhood of Cu^{2+} O^{2-} pairs. Reduction was found to be less hindered when there was more copper since the transfer distance was smaller.

Pepe et al [4] refute the hypothesis of Cunningham and co-workers of a mixed valence state model [5]. Pepe et al studied the dehydrogenation of 2-propanol over copper on γ-Al_2O_3 catalysts and found that fully oxidised copper was inactive and that a large increase in the Cu(I) content doesn't

cause an increase in the activity. However, an increase in the surface content of Cu(0) parallels the increase in k_{sp} (kinetic constant per catalyst surface area). From this they infer that the Cu(0) species is the only one responsible for dehydrogenation with the reduced copper being formed in situ on being exposed to 2-propanol. This is in agreement with work carried out by Volta et al [29].

Schulz and Cox [30] studied the reaction of n-propanol on single Cu_2O crystals. They found that propanol adsorbs dissociatively on $Cu_2O(100)$ to form a propoxy surface intermediate via the loss of an acidic proton at the -OH group. The production of propionaldehyde was found to occur over a wide temperature range. This is thought to be due to reactions occurring at different surface sites and to the presence of multiple reaction pathways.

The scheme proposed by Schulz and Cox is given in Figure 1.1.

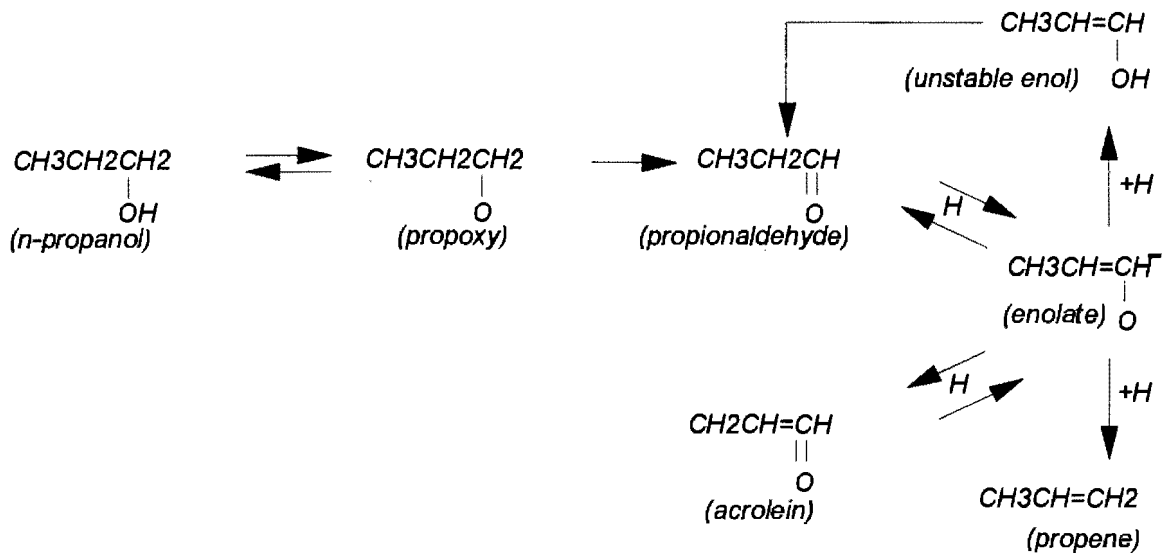

Figure 1.1. Reaction Mechanism for n-Propanol Proposed by Schulz and Cox.

1.5.3. Effect of Copper Content on Dehydrogenation Activity

Shivaraj et al studied the effect of copper loading in Cu-Al_2O_3 catalysts on the dehydrogenation of ethanol. The catalyst was prereduced in situ in hydrogen for 5 hours at 250°C [7]. Using XRD they were unable to detect a copper containing phase with a copper loading of less than 22 weight percent indicating that copper is present as a highly dispersed phase or in an amorphous state on the γ-Al_2O_3. CuO was detected for a copper loading of 22 to 34 weight percent. They observed

a maximum rate of reaction of ethanol at a copper loading of 5 weight percent after which the rate decreased as the copper loading on the copper-alumina catalyst was increased up to 16 weight percent. Thereafter the rate only changed marginally with further increase in copper content. The alumina support was found to have only dehydration activity in the temperature range 225 to 300°C and dehydrogenation only became evident on addition of copper. High activity at low copper loading may be due to the combined rates of dehydrogenation by the copper species and the dehydration due to γ-Al_2O_3. With an increase in copper loading the dehydration activity of the alumina was suppressed. Catalysts with more that 22 weight percent copper showed good dehydrogenation activity and selectivity to acetaldehyde [7].

Pepe et al [4] showed that Cu-Al_2O_3 exhibited only dehydrogenation activity below 170°C and dehydration and dehydrogenation activity above 170°C. They also observed a decrease in the dehydration activity as the copper loading was increased and was minimal for catalysts containing more than 24 weight percent copper. The catalyst selectivity for acetaldehyde increased from 28 % with a copper loading of 4 weight percent, to 94 % for a copper loading of 9 weight percent and remained between 98 and 100 % with further increases in copper loading.

Sivaraj et al found that the total surface area decreased with an increase in Cu loading due to filling of the γ-Al_2O_3 pores. The copper metal surface area increased with copper loading up to 22 weight percent copper and remained constant up to a loading of 24 weight percent after which the surface area decreased slightly due to the formation of large crystallites and blocking of the pores of the support. The maximum copper surface area (41 m^2Cu/g of catalyst) is lower than the theoretical value of 140 m^2Cu/g of catalyst which is available for monolayer coverage of the support [7].

The surface areas of copper catalysts prepared by various methods have been reviewed by Shivaraj and Kantarao [7]. Kaushik et al found that as copper metal loading increased the spinel Cu-Al_2O_3 phase disappeared and segregation of CuO occurred [31].

1.6. KINETICS AND REACTION MECHANISM FOR THE DEHYDROGENATION OF ALCOHOLS

Using Hougan-Watson mechanisms, Shiau and Chen [21] proposed that the dehydrogenation of

ethanol takes place at a single site where product hydrogen gets adsorbed on the catalyst surface and the adsorption of ethanol is the controlling step of the reaction. They proposed the following overall rate equation;

$$-r_E = \frac{k(P_E - \frac{P_A P_H}{K_E})}{1 + K_A P_A}$$

Where

r_E= rate of reaction

P_E= partial pressure of ethanol

P_A= partial pressure of acetaldehyde

P_H= partial pressure of hydrogen

K_A= adsorption constant for acetaldehyde =$3{,}665 \times 10^{-2}$ exp (4538,3/RT)

K_E= equilibrium constant for dehydrogenation of ethanol

k = $1{,}01 \times 10^6$ exp (-15749/RT)

Doca and Segal [27] however, believe that the desorption of the product aldehyde is the rate limiting step. Gulkava and Kraus [32] used a Langmuir-Hinshelwood-type rate equation for the dehydrogenation of primary and secondary alcohols over a $ZnO\text{-}Cr_2O_3$ catalyst. The equation was of the form;

$$r_A = \frac{k\, K_A\, p_{ROH}}{1 + K_A\, p_{ROH}}$$

Where

k = rate constant

K_A = adsorption constant for acetaldehyde

p_{ROH} = partial pressure of the alcohol

For both primary and secondary alcohols the rate of reaction decreases with increase in the electronegativity of the substituents on the alcohol molecule e.g. for R_1 and R_2 in $R_1\text{-CHOH-}R_2$. For example the reaction rate decreases in the following order as the electronegativity increases from left to right, 2-methyl-1-propanol > n-propanol > ethanol > 2-methoxyethanol > 2-

phenoxyethanol > 2,2,2-trifluoroethanol. The steric effects were found to be negligible. The decrease in reactivity of the alcohols with increase in electronegativity indicates that the displacement of electrons has an unfavourable influence on the reactivity. They put this forward as evidence for the carbonyl mechanism which involves the fission of the O-H and C_α-H bond. The splitting off of a hydrogen atom from the α-carbon is thought to be the rate determining step. The carbonyl mechanism can be represented as shown in Figure 1.2.;

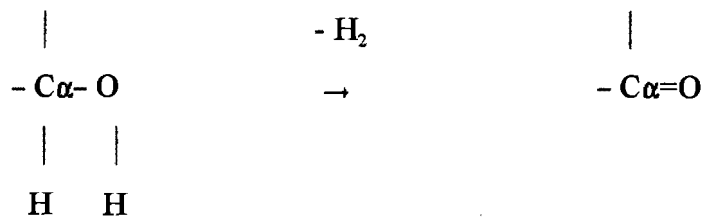

Figure 1.2. Carbonyl Mechanism.

Connett [8] studied the performance of a calcium phosphate/copper oxide catalyst for the dehydrogenation of propanol. The values obtained for K_p differ from those obtained by Buckley and Cox [33]. Connett suggests that the value obtained by Buckley and Cox for K_p is low due to undetected byproducts which give a higher apparent proportion of propanol in the equilibrium mixture. The byproduct concentration was found to increase with temperature making the error in log K_p greater at higher temperatures (Table 1.1.)

Table 1.1. Values of K_p Obtained by Two Different Research Groups [8]

Temperature (K):	K_p as determined by Connet	K_p as determined by Buckley and Cox
473,0	0,0222	0,0154
524,3	0,1430	0,0856

Chhabra et al [9] studied a copper on kieselguhr catalyst (50,6% Cu as CuO; 29,2% Si as SiO_2; 4,2% Al_2O_3 and 1,0% CaO) for the dehydrogenation of propanol. The results are given in Table 1.2.

Table 1.2. Equilibrium Constants (K), Equilibrium Conversions (X_E) and Reaction Velocity Constant (k) as Obtained by Chhabra et al [9].

Temperature (K):	K:	X_E:	k:
498	0,554	0,600	4,0836
523	1,485	0,773	11,150
548	2,967	0,865	19,997
573	4,619	0,906	33,005

The activation energy E_A was found to be 13,68 kcal/g.mol. The pre-exponential factor was found to be A= 53,9x10^5. The values of K obtained by Chhabra et al appear to be an order of magnitude larger than those obtained by Connett. Since the units for each of the variables used in the calculation were not published it is difficult to speculate as to the reason for this discrepancy.

They proposed the following rate expression;

$$-X - 2\ln(1-X) = 53900e^{-\frac{13680}{1,98T}} \cdot \frac{1}{0,0082T} \cdot \frac{W}{F}$$

Where; X = g.mole converted/g.mole feed

W/F = g catalyst/g.mole feed/hr

W = catalyst mass (g)

F = feed rate of alcohol (mole/hr)

The most probable mechanism for the dehydrogenation reaction was established by calculating the coefficients of different rate controlling mechanisms at the temperatures studied, using a method of least squares to find the best fit. Using this method Chhabra et al [9] suggested that a surface

reaction occurring on dual sites was the most probable mechanism for the dehydrogenation of ethanol, propanol and butanol. This type of reaction can occur homolytically or heterolytically as is illustrated in Figure 1.3.

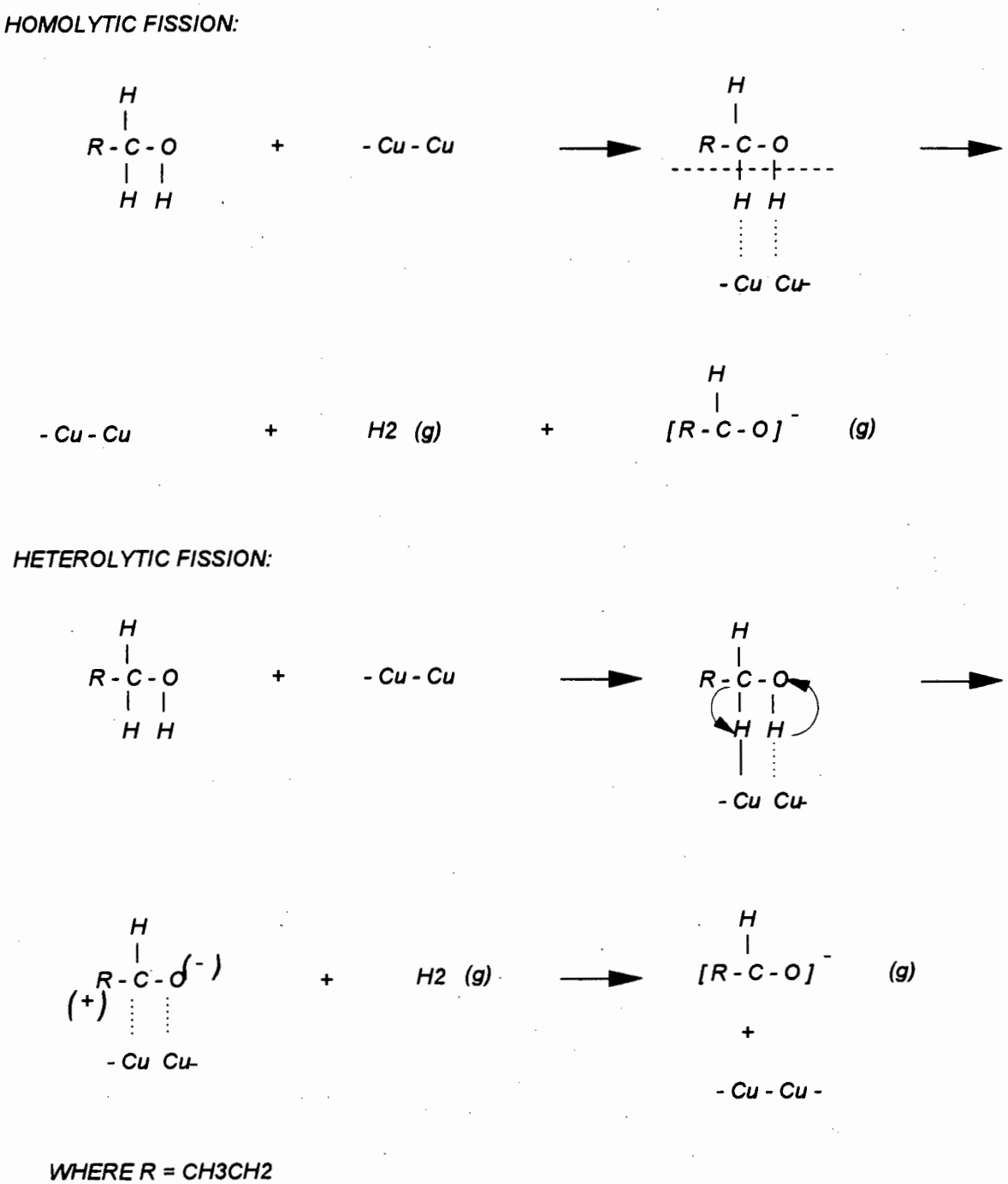

Figure 1.3. Schematic Representation of Homolytic and Heterolytic Fission.

Echevin and Teichner studied the dehydrogenation of secondary butanol over Cu/Al_2O_3 catalyst with copper loadings ranging from 0,4 to 7,1 mass % [34]. They found that for all catalysts studied the Arrhenius plots were all parallel indicating that the activation energy is independent of the catalyst used (E_0=12,5 kcal/mol) and only the pre-exponential factors differed. If this was indeed the case then the catalyst activity should depend directly on the number of active sites present.

A plot of the rate of conversion (mol/s/g. catalyst) versus the number of atoms of Cu/g catalyst was found to give a straight line with the slope of the line corresponding to the turn over frequency (TOF) (i.e. the number of decomposed alcohol molecules per copper atom per second). The TOF was $2,7x10^{-3}$ molecules/Cu atom/second and the pre-exponential factor was found to be $A_0=5,01x10^{-21}$ x n_s where n_s is the number of surface copper atoms per gram of catalyst. An equation for the initial rate of reaction (V_0) (at 178,3°C) was put forward, $V_0=5,01x10^{-21}$ x n_s x $e^{-12500/RT}$. In the initial stages the reaction appeared to be zero order at high alcohol partial pressures and it was assumed that under these conditions the surface is saturated with alcohol.
The reaction rate was found to be independent of hydrogen partial pressure for all the catalysts studied. An increase in the partial pressure of the reaction product, methyl ethyl ketone, was found to cause the reaction rate to decrease. They proposed that the heat of adsorption of the ketone was greater than that of the alcohol and it therefore adsorbed competitively on the catalyst inhibiting the dehydrogenation reaction. They proposed the following general rate equation;

$$V = \frac{V_0 K_A p_A}{1 + K_A p_A + K_C p_C}$$

Where;

V_0 = initial rate of reaction

K_A = equilibrium constant for adsorption of alcohol

p_A = partial pressure of secondary butanol

K_C = equilibrium constant for adsorption of methylethylketone

p_C = partial pressure of methylethylketone

Kanoun et al [35] studied the dehydrogenation of ethanol to acetaldehyde over modified copper catalysts containing vanadium, copper and zinc in varying proportions. The catalysts were activated

in hydrogen at 300°C for 3 hours. The feed was a mixture of ethanol (4,51 kPa) and hydrogen (97,33 kPa) which was fed over 20 g of catalyst at 1 atmosphere and a gas flowrate of 60 ml/min to maintain the conversion below 1% and the selectivity close to 100%. They found that the reaction for the conversion of ethanol to acetaldehyde is structure insensitive over vanadium-copper, and zinc-copper binary catalysts as well as vanadium-zinc-copper ternary catalysts. Kanoun et al [36] substituted zirconium in the place of zinc and the reaction was also found to be structure insensitive. Pure copper and the ternary catalysts were found to have the same activation energy of 20 kcal/mole for ethanol dehydrogenation, but different pre-exponential factors with the pre-exponential factor for copper being smaller than for the other catalysts since the copper metal in the ternary catalysts was more dispersed than in the pure copper catalyst [35].

Vanadium or zinc are thought to affect the performance of the catalyst by exerting a structural effect by increasing the copper dispersion. Although they found that the TOF (molecules of acetaldehyde produced per surface copper atom per second) for the copper catalyst was higher than for the ternary catalysts, the atomic rate (TOF x dispersion) was lower for copper than for the other catalysts due to the lower dispersion [35]. This was true for the mechanical binary mixtures indicating co-operative and synergic effects between copper metal and vanadium or zinc oxide. The active sites appear to be copper metal [35].

1.7. EFFECT OF PROCESS VARIABLES:

1.7.1. Water

Chhabra and Venkateswarlu [9] found that if 14% water was added to ethanol feed, the water helped to maintain higher catalytic activity for longer periods of time. No mention is made as to the effect of water on the selectivity to byproducts but it is possible that the addition of water may have an effect on the position of the equilibrium in byproduct formation reactions. Water is a product of the Aldol condensation reaction which is the most significant route for the formation of byproducts. The addition of water to the feed probably affects byproduct formation by driving the equilibrium reaction towards the reactants and away from the byproducts. This may account for the effect observed by Chhabra and Venkateswarlu.

Results published by Chinchen et al [37] show that hydrogen reduction of dehydrogenation catalysts (Cu/ZnO) in the presence of steam results in a lower metal surface area than in the absence of steam and that the reduction rate is retarded by the water vapour partial pressure. This is borne out by Pospisil et al [38] who observed a retarding effect on the reduction kinetics of copper catalysts in the presence of water vapour. Tonner et al [26] observed that high levels of water could be tolerated by commercial copper chromite catalysts as well as impregnated copper on silica, magnesia or chromia catalysts i.e. the catalysts were not poisoned by water. Water was added to the n-propanol feed during the present study to minimise the formation of Aldol condensation byproducts. The potential effect of water on the catalyst surface and therefore the activity of the catalyst must be borne in mind when interpreting the results.

1.7.2. Reaction Temperature

The selectivity for acetaldehyde was found to be almost 100% for reaction temperatures in the range between 250 and 275°C [7]. Condensation products are common at higher temperatures [18] and acetaldehyde selectivity decreases with an increase in temperature above 275°C [7]. However, Dunbar and Arnold [39] found that it was necessary to increase the temperature to between 300 and 320°C for n-propanol dehydrogenation over supported copper-chromium oxide catalysts although the dehydration activity also increased. This work was carried out in 1940 at which time the supports may have had a lower surface area than the supports available at the present moment. Supports currently available have high surface areas which lead to better copper dispersion and higher copper metal surface areas which give rise to more active catalysts.

1.7.3. Contact Time

If all other variables are kept constant the conversion, as expected, is found to increase with increase in contact time (W/F) (g catalyst/g.mole feed/hr) as shown in Table 1.3 [21].

Table 1.3. The Effect of Contact Time on Conversion as reported by Shiau and Chen [21]

Ethanol partial pressure (atm):	Time Factor (g-cat.hr/g mole)	Ethanol Conversion at 250°C (%)
0,25	2,0	12,3
0,25	3,0	18,5
0,25	4,0	24,1
0,25	5,0	30,2

No detail was given as to the effect of contact time on selectivity of ethanol to acetaldehyde.

2. EXPERIMENTAL PROCEDURES

2.1. CATALYST CHARACTERISATION

2.1.1. Catalyst Composition

The catalyst manufacturer (Süd-chemie) specified the following catalyst composition;

Copper	:	40 %
Chromium	:	26 %
Oxygen	:	34 %

The catalyst consisted of 3 x 3 mm tablets with a bulk density of 1,4 kg/l. The catalyst composition was verified by Atomic Absorption analysis and the results appear in section 3.1.1.

2.1.2. BET Surface area

BET surface area measurements were carried out using a SAP 2000 Micrometrics instrument with a Gemini 2375 surface analyser.

2.1.3. Temperature Programmed Desorption (TPD)

A Gemini 2375 instrument was used to perform ammonia and carbon dioxide desorption profiles. Approximately 0.1 g of catalyst was reduced in situ according to the reduction procedure outlined in section 2.2.3. The catalyst sample was allowed to cool to room temperature before exposing it to one of the adsorption gases for 10 minutes. A 5 mass % ammonia in helium mixture was used to measure the acidity of the catalyst surface and the basicity was measured by exposing the catalyst to high purity CO_2 (undiluted). The system was flushed for 10 minutes with helium (in the case of ammonia) or argon (in the case of CO_2) prior to increasing the temperature and recording the desorption profiles.

2.2. REACTOR SET-UP AND EXPERIMENTAL PROCEDURE

2.2.1. Reactor System

The reactor used for the dehydrogenation of n-propanol consisted of a 21,1 mm ID stainless steel tube with a total length of 290 mm of which the central part lies within the heating zone (237 mm) of the electrical heating element. The catalyst was loaded in the middle of the reactor tube (Fig. 2.1.). Carborundum powder (0,7 mm) was used to fill the reactor tube before and after the catalyst bed to act as a preheat zone ensuring that the feed was well heated and to limit the effect of heat loss from the ends of the reactor tube. The reactor tube was mounted in an aluminium block to ensure even heat distribution. Heating was provided by a 3 kW electric element mounted in refractory material. The entire arrangement was housed in a metal casing. The temperature was controlled by a Eurotherm temperature controller. A 1/8" stainless steel thermowell was fitted in the centre of the reactor tube to house a type K thermocouple. The temperature reading on the central thermocouple was used to set the power to the element. The reactor system used in the present study is shown schematically in Fig. 2.2. The propanol/water feed mixture was delivered to the preheater by means of a Lewa Type F1 positive displacement proportionating plunger pump. The feed was delivered to the pump from one of two calibrated feed pots (0-100 ml or 0-800 ml) depending on the desired feed flowrate. The feed entered the preheater at the bottom and the vaporised feed was removed overhead and introduced into the reactor by means of a well lagged transfer line. The exit stream from the preheater could be diverted away from the reactor via a bypass line which went directly to the product recovery section. This allowed the preheater to be heated up with feed flowing through it before the start of a run to allow stable conditions to be reached before switching over to reaction phase. The preheater was packed with stainless steel wire mesh rings, commonly used as a distillation packing. The preheater was heated by a band heater to the same temperature as the reactor. The temperature was controlled by means of a Eurotherm temperature controller with both the controlling and indicating thermocouples mounted horizontally through 1/8" Swagelok fittings in the side of the preheater.

Gases for catalyst pretreatment were delivered to the reactor via a Harris in-line regulator to a Krohne rotameter calibrated to deliver 0-5 l/hr of air at 20°C. The flowrate through the rotameter was controlled by a metering needle valve. The rotameter was calibrated with nitrogen and with a

2 % hydrogen (by volume) in nitrogen mixture. The calibration curves appear in Appendix 1.

A bypass valve after the reactor outlet made it possible to vent gases without having to go through the reactor tube. This was done during reduction when the preheater was switched on and allowed to reach temperature with feed flowing through it. The feed from the preheater could be collected in the product knock-out system while the reduction gases were vented separately.

During normal operation the reactor product went via a heated transfer line (traced with heating tape and controlled by a Eurotherm temperature controller) to an eight port G.C. sampling valve which was set to bypass the injection loop and allow product to go to a water cooled-condenser. The liquid product from the condenser was collected in a round bottom flask and the remaining vapour was carried over to a dry ice cold trap. The flow rate of the tail gas leaving the cold trap was measured using a soap bubble meter (graduated from 0 to 50 ml). The tail gas was sampled before being vented.

All tubing on the reactor system was 1/4" stainless steel and all components of the reactor system were 316 stainless steel. The transfer lines between the glassware used in the product recovery section consisted of *Tygon* tubing.

2.2.2. Catalyst Loading Procedure

The reactor tube was loaded from the bottom upwards as follows; a sieve was placed at the bottom of the reactor tube just above the product outlet to prevent carborundum powder from being flushed out of the reactor into the product lines. Carborundum (30 ml of 0,7 mm powder) was loaded into the bottom of the reactor followed by another sieve and then the desired amount of catalyst. This ensured that the catalyst bed was in the centre of the heated zone. Fine carborundum powder (0,2 mm) was loaded with the 3 x 3 mm catalyst to fill up the spaces between the catalyst pellets (typically 3 ml carborundum to 25 ml catalyst). This was followed by more of the course carborundum powder to fill up the remaining space in the reactor tube. The tube was sealed and placed inside the aluminium block inside the heating element arrangement.

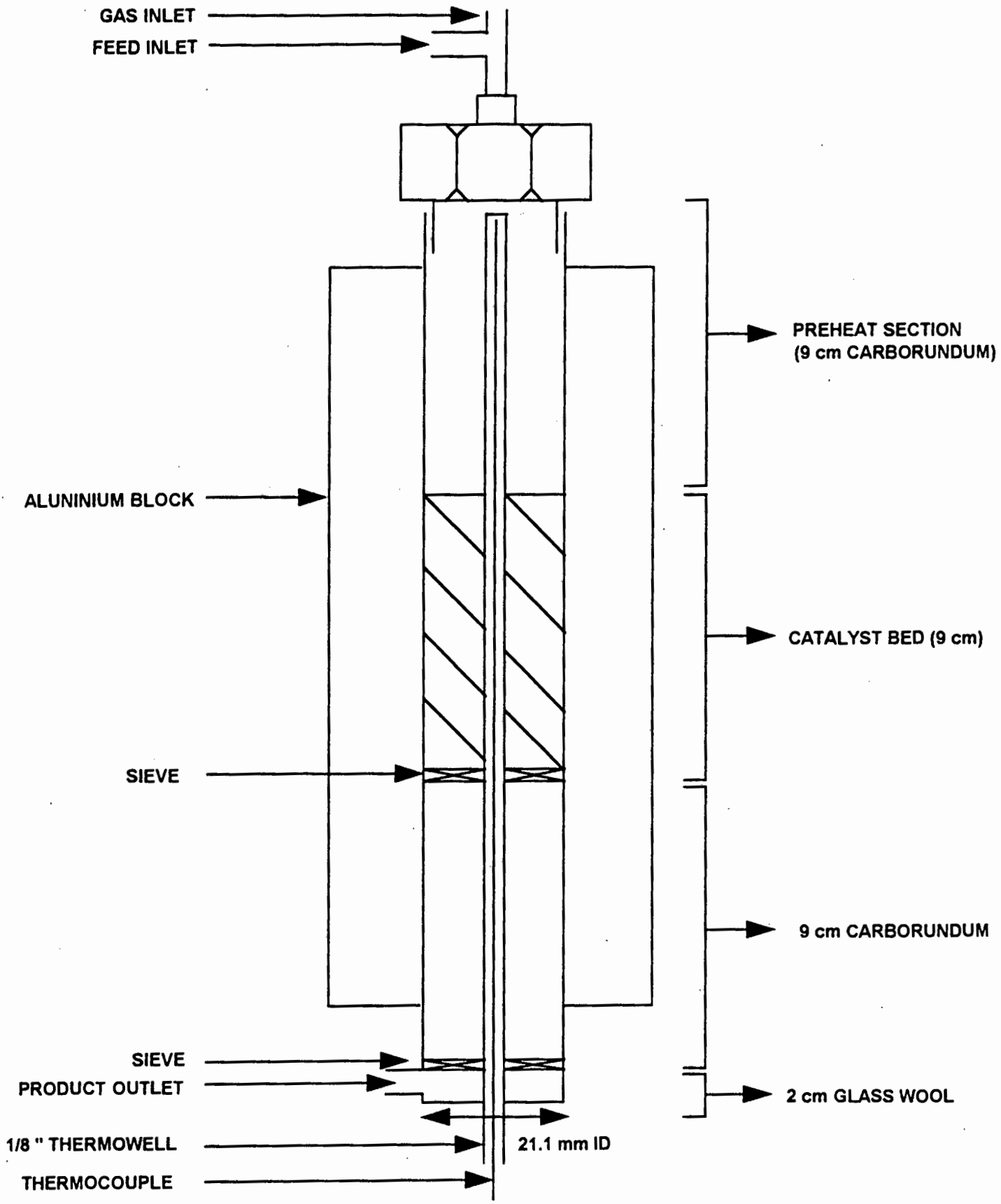

Figure 2.1. Schematic Diagram of Reactor Tube.

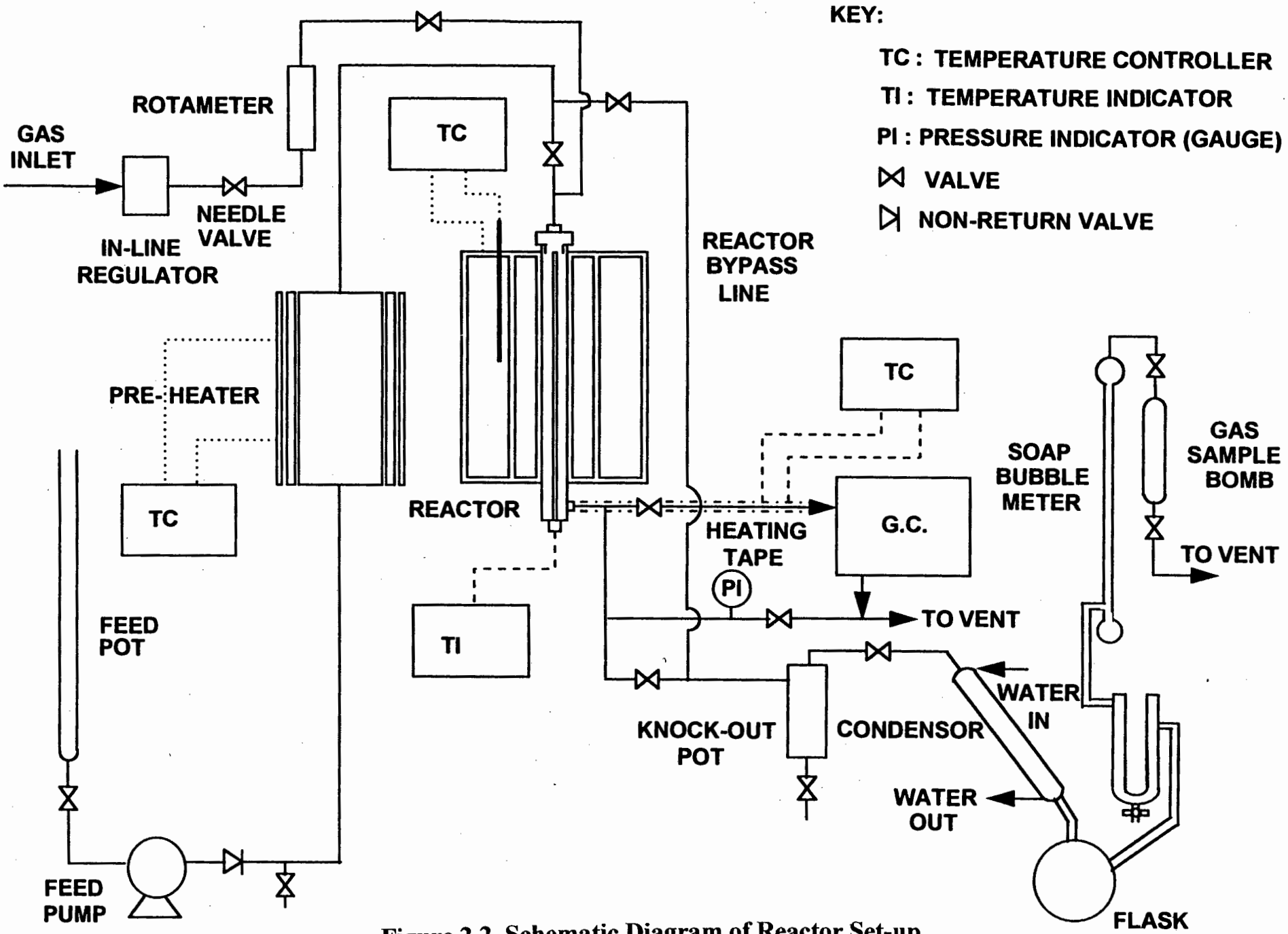

Figure 2.2. Schematic Diagram of Reactor Set-up.

2.2.3. Catalyst Pretreatment

The catalyst was heated in situ at a rate of 30°C/hr to 150°C under nitrogen at a nitrogen flowrate of 0,125 l/hr per gram of catalyst and then kept at these conditions for 24 hours. After 24 hours a 2% hydrogen in nitrogen (by volume) mixture was introduced at a flowrate of 5 l/hr and the temperature was increased at 10°C/hr to a final temperature of 180°C and maintained at this temperature for 12 hours. After reduction the hydrogen/ nitrogen mixture was replaced with nitrogen and the catalyst was heated at a rate of 30°C per hour until reaction temperature had been reached. Approximately 3 hours before the start of the reaction phase, the preheater was heated up to reaction temperature and the feed pump was switched on to allow time for the preheater to reach stable conditions. The heated feed was diverted away from the reactor via a bypass line to the product knock-out system. Once the reactor temperature was stable, the feed was switched from bypass to the reactor and allowed to flow over the catalyst.

2.2.4. Run Procedure

2.2.4.1. Start-up

After completing the reduction step, the preheated feed was switched from the bypass to the reactor. This was taken as time zero. During the initial stages of the reaction gas chromatograms of the product were taken after 1, 2, 4, 6, 12 and 24 hours on line and thereafter every 24 hours.

2.2.4.2. Steady State Operation

During steady state operation the following data were recorded at one hourly intervals;

- pressure (1 atmosphere)
- feed pump rate (ml/hr)
- reactor, preheater and heating tape temperatures (°C)
- tail gas flow rate (ml/min)
- temperature profile through the catalyst bed (°C at 1 cm intervals).

The product was collected at suitable intervals (usually every 2 hours) and the mass was recorded.

2.2.4.3. Shut-down

During shut-down the feed pump was stopped and the heating elements for the reactor and preheater as well as the heating tape were switched off. Nitrogen was allowed to flow through the reactor until the temperature had reached ambient. The reactor was blocked in by closing the valves at the inlet and outlet and the reactor tube was removed from the system. The reactor tube was opened in a glove box under nitrogen and the catalyst was removed and stored under nitrogen for later analysis.

2.2.5. Sample Analysis

2.2.5.1. Feed Analysis

The feed was analysed by means of a *Supelcowax 10*, 60 m column with a 0,32 mm column diameter and 0,5 μm film thickness. The components were detected by means of a FID detector.

The G.C. setting were as follows;

Column temperature program	:	2 min at 80°C, 6°C/min to 140°C, 5 min at 140°C, 6°C/min to 220°C, 2 min at 220°C.
Injector temperature	:	250°C
Detector temperature	:	250°C
Column pressure	:	25 psi at 80°C
Split	:	100:1 (95 ml/min)
Helium flowrate	:	60 ml/min (STP)
Hydrogen flowrate	:	30 ml/min (STP)
Air flowrate	:	300 ml/min (STP)

(Flowrates were corrected for a local pressure of 645 mm Hg)

The water content of the feed was determined by automatic titration using a Karl-Fischer titration apparatus (Mettler LD18) according to the method in ASTM E203-75 and ASTM D1744-64.

2.2.5.2. Reactor Product

The product transfer line from the reactor outlet to the sample loop of the G.C. was traced with heating tape and well lagged. The transfer line was kept at 250°C to ensure that all the components in the product remained in the vapour phase. When performing a G.C. analysis, the sample loop was flushed with product for 2 to 5 minutes. Once the sample loop had been flushed, the sample valve was switched to the inject position to transfer the sample onto the column. The same column and settings were used for the product as for the feed analysis. A typical G.C. trace of the product is given in Appendix 2. The composition of the product stream was verified by means of G.C./M.S. using the Supelcowax column used for on-line analysis. Electron-impact ionisation (EI) mass spectroscopy was used and the MSD was operated in the scan mode with a mass window of 20 to 250 amu. Components were identified with the aid of a Wiley 138 database. Chemical ionisation (CI) mass spectroscopy was used to identify the molecular ion of components not identified using E.I.-M.S. A 25 metre DBWAX column with a 0,25 mm column diameter and a film thickness of 0,25 μm was used. Methane with a pressure of 10 torr was used for bombarding the sample.

2.2.5.3. Tail Gas Samples

A glass gas sample bomb was placed in-line just before the vent (see Figure 2.2.). The gas bomb was changed every 24 hours and analysed for hydrogen by means of G.C. on a Molesieve A column at an isothermal column temperature of 120°C. The column was coupled to a TCD detector. Hydrogen gas was measured in order to accurately calculate the hydrogen component balance. The tail gas was also analysed for hydrocarbons using a PONA column with a FID detector.

2.2.5.4. Response Factors

The sensitivity of the G.C. detector is not always the same for all components in a mixture and it is necessary to compensate for this variation in sensitivity especially if the components do not have a similar volatility and molecular structure or if there is a component that is present in large amounts and is not detected e.g. water with a Flame Ionisation detector (FID). Relative response factors must be calculated for the components in the mixture and used to correct the area percentage obtained by integrating the peak areas. The relative response factor (R_f) for each component is

determined by preparing a mixture of the particular analyte and a reference compound (decane in the present case) and calculating the ratio of peak area to weight of the component relative to that of the reference compound. The ratio was calculated using the following formula;

$$R_F(A) = \frac{\text{Area of Reference}}{\text{Mass Reference}} x \frac{\text{Mass A}}{\text{Area of A}}$$

Response factors were calculated using the column and G.C. program which were usually used for the analysis of product samples. Compounds which were present in the reaction product were not all available as pure compounds and therefore compounds which are representative of the particular group of compounds (e.g. acetals) were substituted to give an indication of the response factor . The values obtained appear in Table 2.1.

Table 2.1. Response Factors

Pure Compound:	R_F for Components in the Product:	Response Factor:
Pentanal	2-me-pentanal, 2-me-2-pentenal	0,36
Propionic Acid	Propionic acid, 2-me-pentanoic aid	0,42
Propanol	Propanol	0,74
Propionaldehyde	Propionaldehyde	0,36
2-me-1-pentanol	2-me-1-pentanol	0,86
iso-Propyl Acetate	Propyl propionate	0,52
Dimethoxy Ethane	For comparison with Diethoxy ethane only	0,27
Diethoxy Ethane	Dipropoxy propane	0,53
2-me-3-Pentanone	2-me-3-Pentanone, 3-Pentanone	0,29

2.2.6. Calculations

A typical spreadsheet is given in Appendix 3.

2.2.6.1. Mass Balance

The mass balance over the reactor system was calculated using the difference between the mass of feed (water + n-propanol) fed to the pump and the combined masses of the product liquid and the

tail gas. The mass balance was expressed as follows;

$$Mass\ Balance\ (mass\ \%\ ) = \frac{(Mass\ Liquid\ Products\ +\ Mass\ Tail\ Gas)}{(Mass\ of\ Feed\ )}\ x\ 100$$

where the liquid products were measured by adding the masses of product collected over a 24 hour period and the tail gas was measured at ambient temperature and pressure by means of a soap bubble meter and converted from volume per unit time to mass using the following formula;

$$Tail\ Gas\ Flowrate\ (l\ /hr) = \frac{(\ Volume\ Travelled\ by\ Bubble\ (ml\ )}{(Time\ Taken\ (seconds)\ )}\ x\ \frac{3600}{1000}$$

The tail gas flowrate was corrected for conditions of Standard Temperature and Pressure as follows;

$$Tail\ Gas\ Flowrate\ (mole/hr\ at\ STP) = \frac{(645\ mm\ Hg\ x\ 273\ K\ x\ Flow\ Rate\ (l/hr)\ )}{(22.414\ l\ /\ mole\ x\ 760\ mm\ Hg\ x\ 298\ K)}$$

where the flow rate on the right hand side of the equation refers to the measured flow rate at ambient conditions.

The mass of tail gas was obtained by multiplying the tail gas flowrate at STP by the average molar mass of the tail gas which was calculated as follows;

$$Av.\ Molar\ Mass\ (Tail\ Gas) = \Sigma(\ Mole\ \%\ of\ Component\ i\ /\ 100\ x\ Molar\ Mass\ i)$$

The mass of the feed to the reactor was calculated using the volume pumped by the pump from a calibrated reservoir as follows;

$$Feed\ Mass\ (g/hr) = [Pump\ Rate\ (ml/hr)\ x\ \frac{VOL.\ \%\ Propanol}{100}\ x\ Density\ (Propanol)] + [Feed\ Pump\ Rate\ (ml/hr)\ x\ Volume\ \%\ Water]$$

It was assumed that the volume change due to mixing of water and n-propanol was negligible.

2.2.6.2. Conversion

The mole % conversion of n-propanol to products was calculated as follows;

$$Mole\ \%\ Conversion = \frac{[(Moles\ PrOH\ (Feed) - Moles\ PrOH\ (Product)]}{[(Moles\ PrOH\ (Feed)]} \times 100$$

where the moles of n-propanol were calculated using the following formula;

$$Moles\ Propanol.hr^{-1} = \frac{(Mass\ \%\ PrOH)}{(Molar\ Mass\ PrOH)} \times Flow\ Rate\ (g/hr)\ /\ 100$$

The flowrate used in the above calculation refers to the feed flowrate when calculating the moles of n-propanol in the feed and similarly for the product, the flowrate refers to the product flowrate.

2.2.6.3. Selectivities

The mole % selectivity of n-propanol which reacted, for each of the components in the product mixture, was calculated as follows;

$$Mole\ \%\ Selectivity\ for\ i =$$

$$\frac{[Mole\ \%\ Component\ i\ (Product) - Mole\ \%\ Component\ i\ (Feed)]}{[Mole\ \%\ PrOH\ (Feed) - Mole\ \%\ PrOH\ (Product)]} \times 100$$

2.2.6.4. Yield

The yield was expressed as the product of the conversion and the selectivity for a particular component in the product stream.

$$Yield = (Mole\ \%\ Conversion) \times (Mole\ \%\ Selectivity\ for\ Component\ i\ )\ /\ 100$$

2.2.6.5. Rate of Formation of Product

The rate of formation of the product was expressed as moles of product per mole of copper catalyst per hour.

2.2.6.6. Component Balance

A component balance was performed using the G.C. results to ensure that all the product was accounted for. The component balance was performed for hydrogen, oxygen and carbon and was

typically expressed as follows;

$$Component\ Balance\ for\ Hydrogen = \frac{Hydrogen_{Into\ Reactor}}{Hydrogen_{Out\ of\ Reactor}} \times 100$$

The Hydrogen entering the reactor was calculated using the following formula;

$$Hydrogen\ Entering =$$

$$\Sigma\ [Mole\ \%\ Component\ i\ (Feed)\ x\ Number\ of\ Hydrogens\ (Component\ i)]$$

The Hydrogens in the product were calculated in a similar way;

$$Hydrogen\ Out =$$

$$\Sigma\ [Mole\ \%\ Component\ i\ (Product)\ x\ Number\ of\ Hydrogens\ (Component\ i)]$$

2.2.7. Optimisation of Operating Conditions:

An experimental design to optimise the operating conditions so as to achieve maximum yield of propionaldehyde was performed.

2.2.7.1. Parameters:

The operating conditions which were found to affect the yield were temperature, liquid hourly space velocity (LHSV) and water partial pressure. The pressure was kept at atmospheric pressure and was not varied.

2.2.7.2. Extraneous Factors:

The effect of catalyst ageing (see section 3.3.6.) on the experimental results was minimised by loading fresh catalyst for each run and recording the results over the same time period on-line (usually the first 48 to 72 hours on stream). It must be borne in mind that other operating parameters such as higher temperatures could accelerate the rate of catalyst deactivation. No measures were taken to counter these extraneous effects. Only pure n-propanol (99.9%) and deionised water were used as feed.

In order to vary the water partial pressure without affecting the n-propanol partial pressure, an inert

was added to the feed. Dioxane was chosen as the inert (see Appendix 4) for its miscibility with the water/n-propanol mixture. Fresh feed was prepared before each run to minimise selective evaporation of the more volatile components. Sufficient feed was prepared for the duration of the run to prevent inconsistencies from having to prepare additional feed batches during the course of a particular run.

2.2.7.3. Factors Affecting the Choice of Statistical Design:

The three key operating conditions (variables) affecting the yield of propionaldehyde were identified during the initial trial runs and no further screening tests were performed.

The reproducibility was found to be good during the initial trial runs and only one repeat experiment was carried out during the optimisation series. The experiments in the series were carried out in random order to minimise extraneous effects as far as possible. The operating conditions were chosen to include as wide a range as practically possible given the temperature sensitivity of the catalyst and the equipment constraints e.g. minimum and maximum pump settings. An empirical design was chosen because the results were not going to be extrapolated.

2.2.7.4. Statistical Design and Design Matrix:

A half factorial design was chosen due to time constraints. The minimum and maximum for each of the operating conditions were set at the practical limit therefore it was not possible to carry out further experiments outside the chosen range i.e. additional block factorial analyses and the star points could not be carried out.

The limits for the three operating variables were as follows;

Temperature	:	220-320°C
LHSV	:	1-6 hr^{-1}
Water partial pressure	:	0.08-0.8 atmospheres (total pressure = 1 atmosphere)

The dehydrogenation of n-propanol does not take place below 210 °C and the copper chromite catalyst sinters above about 330 °C. The limits set for the LHSV were determined by the maximum catalyst loading possible given the reactor size and the limits of the pump. The range chosen for the water partial pressure corresponded to a molar ratio of water to n-propanol of 0.5:1 and 5: 1 at the

same total pressure. The design matrix appears in Table 2.2.

Table 2.2. Design Matrix for Optimisation Study.

y*	z*	x*	Temperature (°C)	LHSV (hr^{-1})	H_2O partial pressure (atm)	Run
-1	1	-1	320	1	0,00	A
1	-1	-1	220	6	0,08	B
-1	-1	1	220	1	0,80	C
1	1	1	320	6	0,80	D
0	0	0	270	3	0,46	E

*Note: x, y and z are the three axes of the design matrix and represent points in space. The x axis represents water partial pressure, the y axis represents LHSV and the z axis represents temperature.

Six runs were performed-the four experiments at the limit and the midpoint of the factorial design plus one repeat experiment (experiment E). It was decided to repeat the midpoint to check for the presence of any deviation due to extraneous factors not accounted for by the experimental design.

3. RESULTS AND DISCUSSION

3.1. CATALYST CHARACTERISATION

3.1.1. Catalyst Composition

The chemical composition of G-13 catalyst was verified by Atomic Absorption spectroscopy after dissolving the catalyst in a 48% hydrofluoric acid solution. The results (Table 3.1) agree well with those supplied by the manufacturer (section 2.1.1).

Table 3.1. Atomic Absorption Analysis of G-13 Catalyst.

Component:	Mass %:
Copper	37,1
Chromium	26,5
Other*	0,8

* Manganese (0,4%) and Aluminium (0,4%).

Analysis of the unreduced catalyst by X-ray diffraction indicated the presence of Ramsbeckite ($Cu_{15}(SO_4)_4(OH)_{12}.6H_2O$) and copper chromium oxide spinel ($CuCr_2O_4$).

3.1.2. BET Surface Area.

The surface area of the unreduced catalyst was determined by means of the B.E.T. method and was 39 m^2/g of catalyst.

A catalyst sample was reduced in situ in the B.E.T. surface analyser using the reduction procedure outlined in section 2.2.3.. The surface area of the catalyst increased to 74 m^2/g after reduction.

The catalyst was exposed to a 1:1 molar mixture of n-propanol and water at 320°C and a feed liquid hourly space velocity 2 hr^{-1} for 4 days. The catalyst was unloaded and transferred under nitrogen to

the B.E.T. instrument where the surface area was measured. The surface area had decreased from 74 m^2/g to 70 m^2/g. The catalyst appeared to have undergone a small degree of sintering. It should be noted that different reaction temperatures and space velocities will affect the aging of the catalyst in different ways i.e. the degree of sintering will depend on the reaction conditions.

3.1.3. Temperature Programmed Desorption.

The acidity and basicity of the reduced copper-chromite catalyst (see section 2.1.3) was determined to give a better understanding of the mechanisms involved in product formation (see section 3.3.7). The ammonia desorption profile appears in Figure 3.1. and the CO_2 desorption profile appears in Figure 3.2.

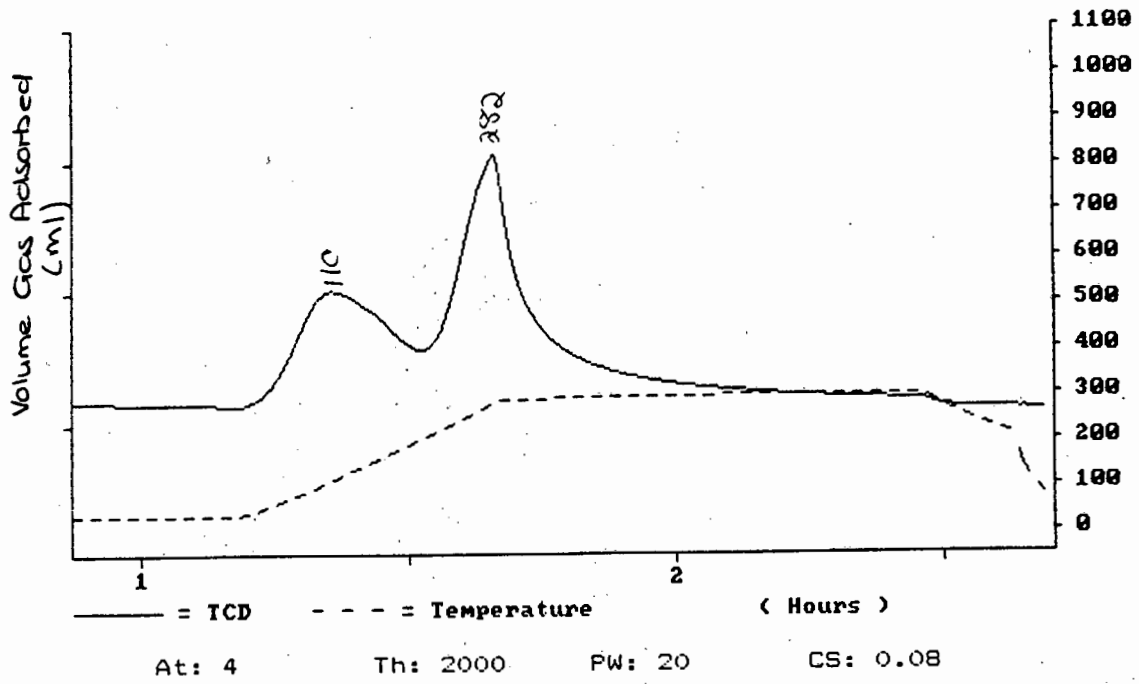

Peak Report:

Peak #:	Area:	Mass of catalyst (g)	Volume of NH_3 (ml)
1	1.081×10^4		
2	4.539×10^4		
Total:	**5.620×10^4**	**0.0915**	**2.8182**

Figure 3.1. Ammonia Desorption Profile.

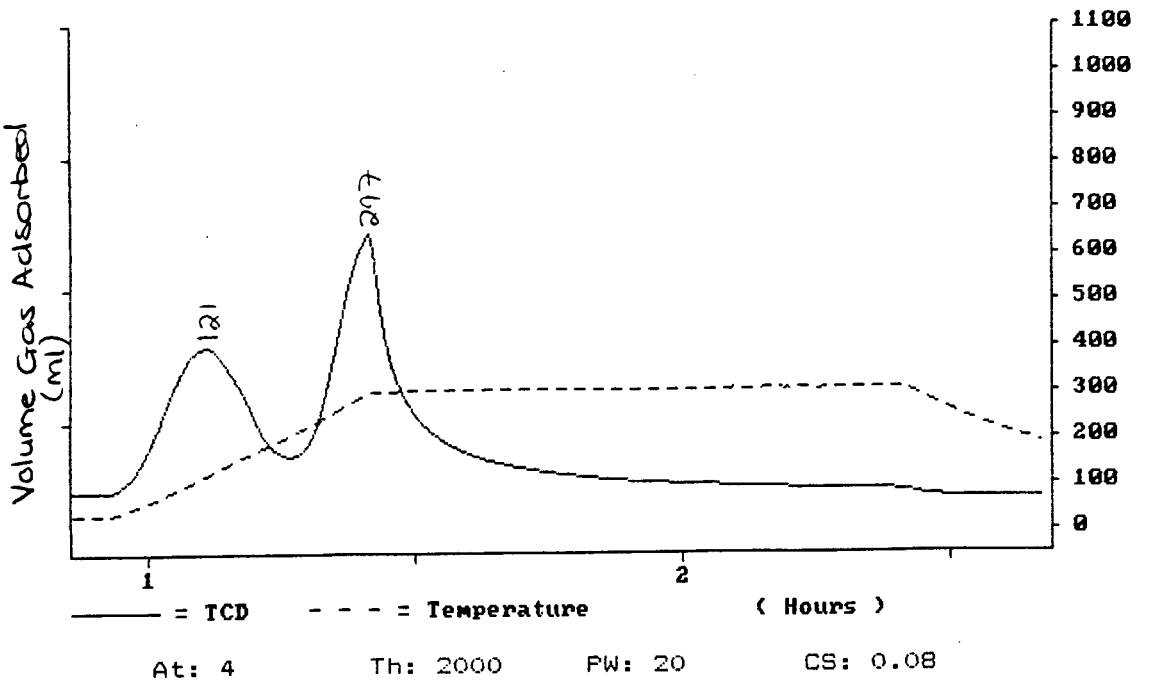

Peak Report:

Peak #:	Area:	Mass of catalyst (g)	Volume of CO_2 (ml)
1	$1.539x10^4$		
2	$3.955x10^4$		
Total:	**$5.494x10^4$**	**0.1034**	**2.903**

Figure 3.2. CO_2 Desorption Profile.

The first peak in each desorption profile is probably due to physisorption of the analyte on the surface of the catalyst. The total volume of ammonia per gram of catalyst was calculated as follows; 2.8182 ml NH_3 / 0.0915 g catalyst = 30.8 ml ammonia/g of catalyst. The area of the first peak in the ammonia desorption profile corresponded to ($1.081x10^4/5.620x10^4$ x 30.8 ml ammonia/g of catalyst) = 5.9 ml ammonia/g of catalyst. The acidity calculated from area under the second peak of the ammonia desorption profile was 24.9 ml ammonia/g of catalyst using the same method of calculation. The total volume of carbon dioxide per gram of catalyst was calculated as follows; 2.903 ml CO_2 / 0.1034 g catalyst = 28.1 ml CO_2/g of catalyst. The first peak in the CO_2 desorption profile corresponded to ($1.539x10^4/5.494x10^4$ x 28.1 ml CO_2/g of catalyst) = 7.9 ml CO_2/g of catalyst. The basicity calculated from the area under the second peak of the CO_2 desorption profile was 20.2 ml CO_2/g of catalyst.

The catalyst has roughly equal quantities of basic and acidic surface sites with slightly higher acidity than basicity. No distinction could be made between Lewis and Brönsted sites. It was presumed that the ammonia adsorbs on the Cr^{3+} sites (the chrome is not reduced to Cr^{2+} under the reduction conditions used in this study but reduces above 500°C) [40], while the CO_2 adsorbs on the reduced copper (Cu^0) which, being electron rich, is presumed to act as a base. The volume of ammonia and CO_2 adsorbed on the catalyst surface appears to exceed the volume of a monolayer of gas as determined by the B.E.T. method (17 ml/g). The volume of gas adsorbed for the acidity and basicity determination give an indication of the relative acidity and basicity only.

3.2. PRE-EXPERIMENTAL RUNS

3.2.1. Blank Runs With Inert Packing

The reactor was packed with an inert material (Carborundum powder 0,72 mm) and a run was carried out using the same experimental procedure outlined in sections 2.2.1. to 2.2.4. at a temperature set point of 250°C and a feed flow rate of 25 ml/hr with a 1:1 mole ratio feed mixture of water to n-propanol. The product was sampled at 24 hour intervals. The hydrocarbon analysis was carried out according to section 2.2.5.2. and no conversion of n-propanol was found to have taken place and no other hydrocarbons were detected. It was concluded that the reactor system was inert.

3.2.2. Temperature Profiles

The reactor was loaded and operated according to section 3.2.1. Temperature profiles were taken over the length of the reactor to establish whether a temperature gradient was present. There was a significant temperature gradient across the catalyst bed for both the blank run and the catalytic run which was clearly unsatisfactory (Figure. 3.3.).

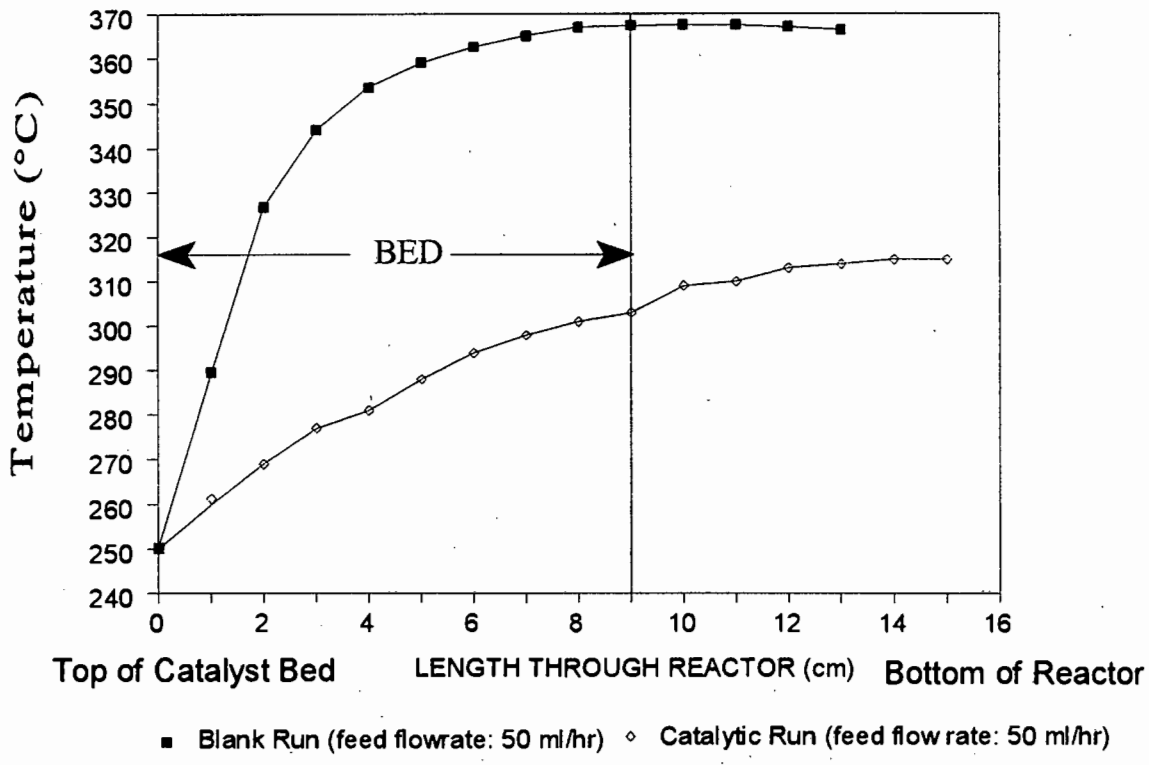

Figure 3.3. Temperature Gradient Through Reactor.

The controlling thermocouple was placed at the top of the catalyst bed and was set at 250°C. The temperature controller supplied additional power to the electric heating element to compensate for cold feed entering at the top of the bed in order to maintain the setpoint at 250°C. This resulted in the lower parts of the bed being overheated. However, it was necessary to establish if the observed gradient was solely due to the heating arrangement or whether catalytic activity contributed to the gradient. Without feed flow there was a large isothermal region in the centre of the bed for the catalytic runs. However, the size of the isothermal region and its location within the reactor tube was greatly influenced by the feed flow rate (Figure. 3.4.).

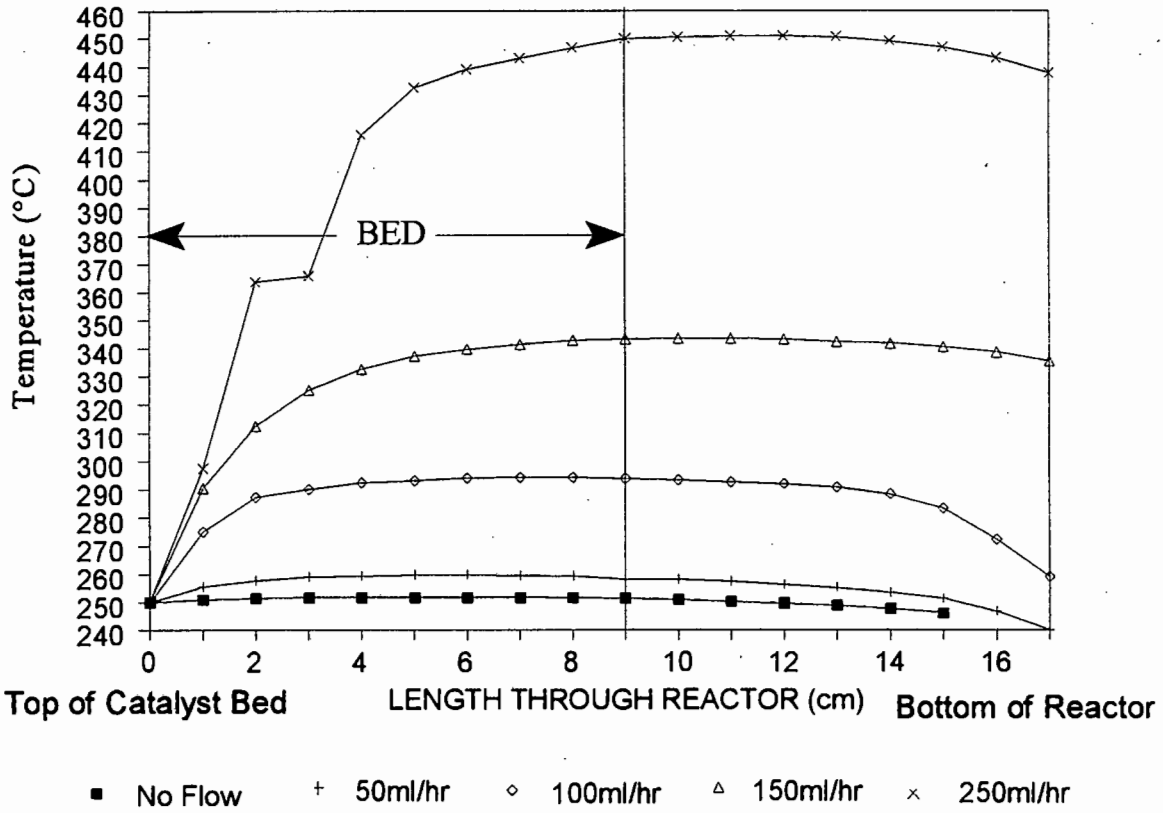

Figure 3.4. Influence of Feed Flowrate On Temperature Profile for Catalytic Runs.

The initial results suggest the need for a larger preheat zone. A separate preheater was installed. It consisted of a vessel approximately three times the diameter of the reactor tube and was packed with stainless steel distillation packing to ensure even flow and good heat transfer. The feed was introduced into the bottom of the vessel and the vaporised feed was drawn off overhead into the reactor via a well-lagged transfer line. The preheater vessel was heated by a band heater to the same temperature as the reactor temperature setpoint (Figure 2.2.). The temperature gradient across the bed improved significantly (Figure 3.5.). Although the increase in the temperature profile through the catalyst bed (e.g. Figure 3.4.) may lead one to think that the reactions taking place are overall exothermic, this is not the case (section 3.3.1.) and they are overall endothermic. The introduction of the feed preheater got rid of the temperature gradient through the bed. This is in line with the initial thoughts that the gradient was a product of the heating arrangement and that the temperature controller was overcompensating for the cold feed entering at the top of the bed. The temperature

controller responded to the cold feed entering at the top where the controlling thermocouple was situated, by supplying additional power to the electric heating element in order to maintain the setpoint at 250°C. The feed heated up rapidly in the top regions of the bed and the additional heat produced by the electric heating element caused the temperature to overshoot the set point in the lower regions of the bed. All subsequent runs were performed using the preheater arrangement to minimise temperature gradients (see Figure 3.5.).

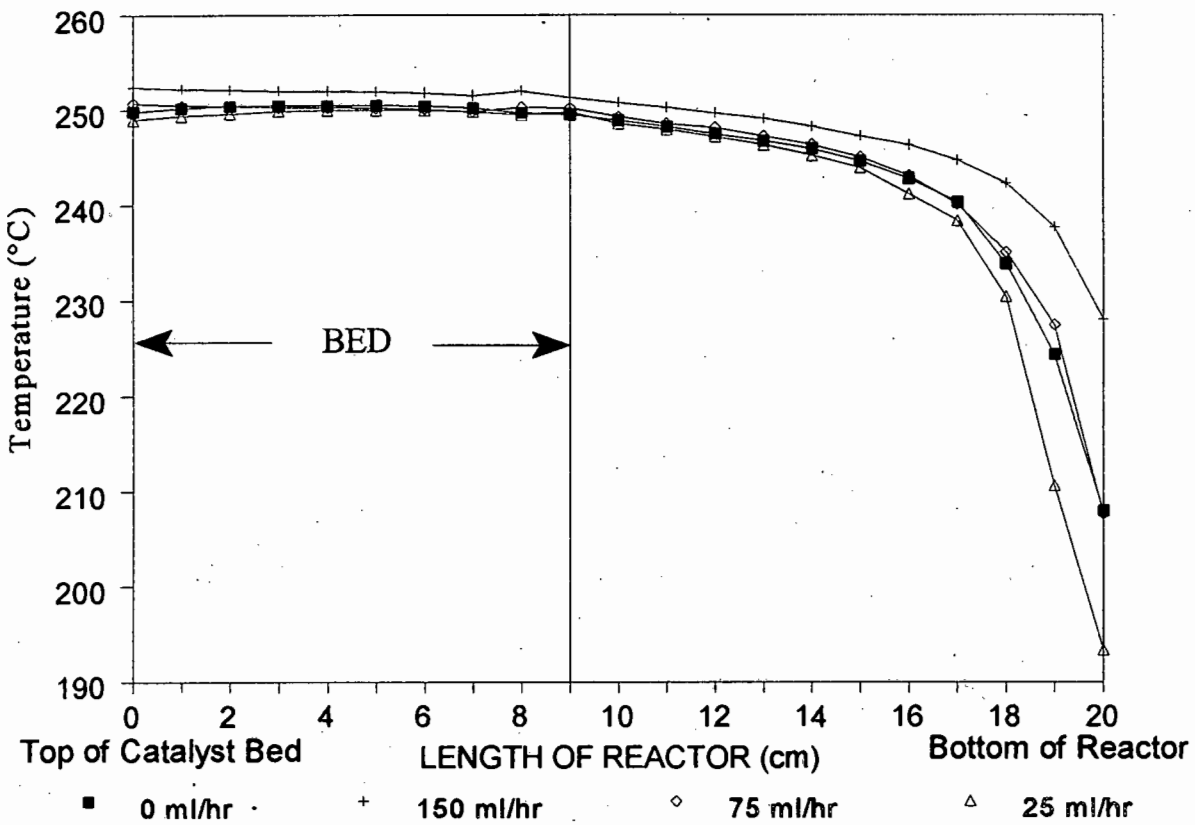

Figure 3.5. Temperature Profiles Through the Reactor After Introducing a Preheater

3.3. EXPERIMENTAL RUNS

3.3.1. Thermodynamics of n-Propanol Dehydrogenation and Associated Reactions.

The thermodynamics for the main reactions found to occur in this study were analysed to determine whether these reactions were endothermic or exothermic in order to understand the effect of temperature on product distribution.

At 298 K:

n-Propanol → Propionaldehyde + H_2

$\Delta H°_f$ propionaldehyde	=	- 45.90
$\Delta H°_f$ n-propanol	=	- (-61.55)
		+ 15.65 kcal/mol (Endothermic)

n-Propanol + Propionaldehyde → Propyl propionate + H_2

$\Delta H°_f$ propyl propionate	=	- 127.40
$\Delta H°_f$ n-propanol	=	- (-61.55)
$\Delta H°_f$ propionaldehyde	=	- (-45.90)
		- 19.95 kcal/mol (Exothermic)

n-Propanol + Propionaldehyde → 1,1-Dipropoxy Propane + H_2O

$\Delta H°_f H_2O$	=	- 57.78
$\Delta H°_f$ 1,1-Dipropoxy propane	=	- 133.0 (estimate)
$\Delta H°_f$ n-propanol	=	- (2 x -61.55)
$\Delta H°_f$ propionaldehyde	=	- (-45.90)
		- 21.78 kcal/mol (Exothermic)

n-Propanol + H_2O → Propionic acid + 2 H_2

$\Delta H°_f$ propionic acid	=	- 109.60
$\Delta H°_f$ n-propanol	=	- (-61.55)
$\Delta H°_f H_2O$	=	- (-57.78)
		+ 9.73 kcal/mol (Endothermic)

n-Propanol + Propionaldehyde → 2-Methyl-Pentanol + H_2O

$\Delta H°_f H_2O$	=	- 57.78
$\Delta H°_f$ 2-Methyl-Pentanol	=	- 96.0 (estimated from hexanol and 3-me-pentanol)
$\Delta H°_f$ n-propanol	=	- (-61.55)
$\Delta H°_f$ propionaldehyde	=	- (-45.90)
		- 46.33 kcal/mol (Exothermic)

n-Propanol + Propionaldehyde → 2-Methyl-Pentanal + H_2O

$\Delta H°_f$ H_2O	=	- 57.78
$\Delta H°_f$ 2-Methyl-Pentanal	=	- 59.0 (estimated from hexanal)
$\Delta H°_f$ n-propanol	=	- (-61.55)
$\Delta H°_f$ propionaldehyde	=	- (-45.90)
		- 9.33 kcal/mol (Exothermic)

The formation of propionaldehyde is endothermic as is the formation of propionic acid. The formation of secondary products, eg. esters and condensation products, is exothermic.

The theoretical predictions suggest that the formation of propionaldehyde, propionic acid and other acids (such as 2-methyl-pentanoic acid) will be favoured at higher reaction temperatures. The condensation products and esters are expected to be favoured at lower reaction temperatures. The formation of some of the secondary reaction products is equilibrium controlled and the increase in propionaldehyde concentration at higher reaction temperatures is likely to affect the position of the equilibrium possibly masking the effect of thermodynamics on byproduct formation.

A typical experimental run at 270°C, 1:1 mole ratio of n-propanol:water, and a LHSV of 1.95 hr^{-1} was analysed to determine whether the overall thermodynamics were endothermic or exothermic. The main products were as follows;

	Mole %:	$\Delta H°_f$ (kcal/mol)
propionaldehyde	62.10	15.65
propyl propionate	8.13	-19.95
1,1-dipropoxy propane	0.04	-21.78
propionic acid	6.16	9.73
2-me-1-pentanol	2.24	-46.33
2-me-pentenal	6.30	-9.33
Other minor byproducts	15.03	-

The overall $\Delta H°_f$ for the reaction is 7.06 kcal/mol excluding any contribution by minor byproducts. These other byproducts would have to have an average $\Delta H°_f < -47$ kcal/mol to make the overall

reaction exothermic. It was concluded that the overall reaction was probably mildly endothermic.

3.3.2. Calculation of the Theoretical Equilibrium.

It is important to know the equilibrium conversion for a reaction such as the dehydrogenation of n-propanol, since the optimisation of operating conditions is pointless if equilibrium constraints dictate a very low conversion of reactant to the desired product.

Equililbrium expressions can be used to predict the equilibrium concentration if the value of the Equililbrium constant (K_p) is known [42]. K_p can be calculated from the equation for Gibb's free energy (Table 3.2.);

$$- \Delta G_T^\circ = RT \ln K_p$$

The Gibb's free energy can be calculated from;

$$\Delta G = \Delta H - T\Delta S$$

Table 3.2 Literature Values for Thermodynamic Parameters.

COMPONENT:	ΔG°_f (kcal /mol) at 500 K	ΔG°_f (kcal /mol) at 600 K
n-Propanol	- 22,79 [43]	- 14,37 [43]
Propionaldehyde	- 20,60 [43]	- 15,07 [43]
Hydrogen	0	0

Values were converted from calories to joules using the conversion factor, 1 cal = 4,184 J.

For the reaction;

n-Propanol → propionaldehyde + hydrogen (gas)

If we assume that we start with 1 mole of n-propanol and let the propionaldehyde concentration be x at equilibrium, then;

n-propanol concentration (moles) = 1-x

propionaldehyde concentration (moles) = x

hydrogen concentration (moles) = x

Total = 1+x moles

$$K_p = \frac{(p_{propionaldehyde}).(p_{H_2})}{(p_{propanol})} = \frac{(n_{propionaldehyde}).(n_{H_2})}{(n_{propanol})} x \frac{P}{n_T}$$

where;

p	=	Partial pressure
n	=	Moles of each component
P	=	Pressure at which reaction takes place
n_T	=	Total number of moles

Performing the calculation at 500 K, using $\Delta G°_{500}$ (gas) = 9,16 kJ/mol which gives K = 0,1103 (compared to 0,1430 obtained by Connett [8]), the propionaldehyde concentration at equilibrium is 0,315 moles and the n-propanol concentration at equilibrium is 0,685 moles i.e. 68,5 % of the n-propanol is unreacted. At 600 K only 19,8 % of the n-propanol is unreacted. Although equilibrium constraints should be kept in mind during optimisation, the equilibrium does not lie so far towards the reactants that conversion is too low to be of practical value.

3.3.3. The Reactor System-Reynold's Number.

It is important to evaluate the reactor system in terms of flow regime and plug-flow behaviour to evaluate the potential effect on the experimental results. The probability of external mass transfer being present is high if the Reynold's number is low i.e. the laminar flow regime [44]. In order to get an indication of the flow regime in which the current study was undertaken, the modified Reynold's number was calculated for the reaction temperature of 320 °C. The equation was as follows [42];

$$\overline{Re} = \frac{D_p u \rho_f}{\upsilon_{mix}(1-\varepsilon)}$$

where;

D_p	=	Diameter of catalyst particle
u	=	Superficial fluid velocity
ρ_f	=	Density of fluid
μ_{mix}	=	Viscosity of a low pressure gas mixture

ε = Void fraction

The superficial fluid velocity can be expressed as follows;

$$u = \frac{m}{\rho A}$$

where;

m = Mass flow rate

ρ = Density of the fluid

A = Cross sectional area of the tube

Substituting into the expression for the modified Reynold's number gives;

$$\overline{Re} = \frac{D_p \frac{m}{A}}{\mu_{mix}(1 - \varepsilon)}$$

The following values were used;

D_p = $3x10^{-3}$ m

m = $6,03x10^{-6}$ kg/s (i.e. at a total liquid feed flowrate of 25 ml/hr)

A = $3,53x10^{-4}$ m^2

μ_{mix} = $1,53x10^{-5}$ kg/m.s

ε = 0,51

The viscosity of the fluid mixture was calculated using the following equation [42];

$$\mu_{mix} = \Sigma \frac{y_i \eta_i}{\Sigma y_i \phi_{ij}}$$

where;

$$\phi_{ij} = (\frac{M_j}{M_i})^{\frac{1}{2}} = \phi_{ji}^{-1}$$

and;

M_i	=	Molecular mass of component i
M_j	=	Molecular mass of component j
ϕ_{ij}	=	Parameter to account for different molecular masses of components in a mixture.
μ_{mix}	=	Viscosity of the low pressure gas mixture containing n components
y_i	=	mole fraction of i
η_i	=	Viscosity of pure i at the temperature of the mixture

The modified Reynold's number was calculated to be 6,8 for a total liquid feed flowrate of 25 ml/hr at a reaction temperature of 320 °C. If the maximum pump speed of 150 ml/hr is used to calculate the modified Reynold's number then, Re = 41,0.

With such low values of the Reynold's number the flow is laminar. For laboratory reactors the Reynold's number is typically around 10 or lower [45] which is true in the current case. From the value for the modified Reynold's number one would expect external mass transfer to be limiting. It is therefore necessary to verify the existence of external mass transfer effects experimentally.

3.3.4. Mass Transfer Tests

Discussion of mass transfer effects will be limited to those taking place between the bulk fluid and the surface of the catalyst particles.

A particular catalyst may be highly active but it will not be effective if the reactants cannot reach the catalytic surface quickly enough. The transfer of reactants from the bulk fluid to the catalyst surface requires a driving force to be able to take place. The concentration difference between the bulk fluid and the catalyst surface provides this driving force. If this concentration gradient is significant a falsification of kinetics is observed [46], i.e. the rate of reaction and the selectivity differ from the

values (intrinsic kinetics) that would be obtained in the absence of mass transfer limiting conditions. There are essentially three possible reaction regimes [46];

1. In the first regime the rate of reaction is low and the potential required to provide the diffusion flux is insignificant. The kinetics which are observed are the intrinsic kinetics i.e. mass transfer is not rate limiting.

2. In the second regime a significant concentration gradient exists in the catalyst pores and pore diffusion is rate limiting. The observed kinetics tend towards first order kinetics i.e. intraparticle mass transfer limitations exist.

3. In the third reaction regime there is a concentration difference between the bulk fluid and the outer catalyst surface. The kinetics of the reaction appear to be first order since mass transfer through the bulk fluid is a first order process i.e. interparticle mass transfer is rate limiting.

For the adsorption of reactants and desorption of products on the catalyst surface it is necessary to transport them through the bulk fluid. The rate of transportation depends on the temperature, pressure and gas velocity relative to the catalyst surface. The velocity profile of the bulk fluid near the catalyst surface, the physical properties of the fluid and the reaction rate, determine whether the difference in concentration between the fluid and surface will be significant or not. The fluid passing over a catalyst pellet develops a boundary layer. The velocity is zero at the surface of the catalyst and approaches the bulk velocity a short distance from the surface. Transfer of material perpendicular to the catalyst surface through the boundary layer takes place by means of molecular diffusion. Laminar flow occurs in the boundary layer. The thickness of the boundary layer varies with the flow rate in the bulk fluid, i.e. the more turbulent the flow in the bulk fluid the thinner the boundary layer and the less resistance there is to molecular diffusion.

The simplest method for determining the presence or absence of external mass transfer processes is to keep the space velocity constant but vary the linear velocity and monitor the effect that this has on the conversion (or intrinsic rate). If the conversion remains constant mass transfer is not significant [47]. The space velocity (v_0/V) is kept constant by simultaneously varying v_0 (volumetric flow rate of the feed) and V (volume occupied by the catalyst) [48].

The presence or absence of external mass transfer was verified at a fixed liquid hourly space velocity of 2,5 hr^{-1} and a temperature of 320°C. A high temperature was selected to give a high rate of reaction. Mass transfer effects should be apparent at high rates of reaction.

The catalyst loading and liquid flow rates used for this study are given in Table 3.3. and the results of the mass transfer experiments are given in Table 3.4.

Table 3.3. Operating Conditions for Mass Transfer Determination.

Volume of Catalyst (ml):	Liquid Flow Rate Setting (ml/hr):	Linear Velocity (cm/min):	Liquid Hourly Space Velocity (LHSV) (hr^{-1}):
10	25	0,12	2.5
20	50	0,24	2.5
30	75	0,36	2.5

Table 3.4. Experimental Results of External Mass Transfer Experiments.

Experiment:	3B	2BR	6B
Mass of catalyst (g)	16.0	30.0	45.0
Moles of Copper in catalyst (mole)	0.09	0.18	0.26
Actual Feed flow rate (cm^3/min)	0.40	0.83	1.21
Actual Linear velocity (cm/min)	0.11	0.24	0.35
Rate (moles propanol reacted/mole copper/hr)	2.26	1.53	1.21

The rate of reaction was plotted against linear velocity and appears in Figure 3.6.

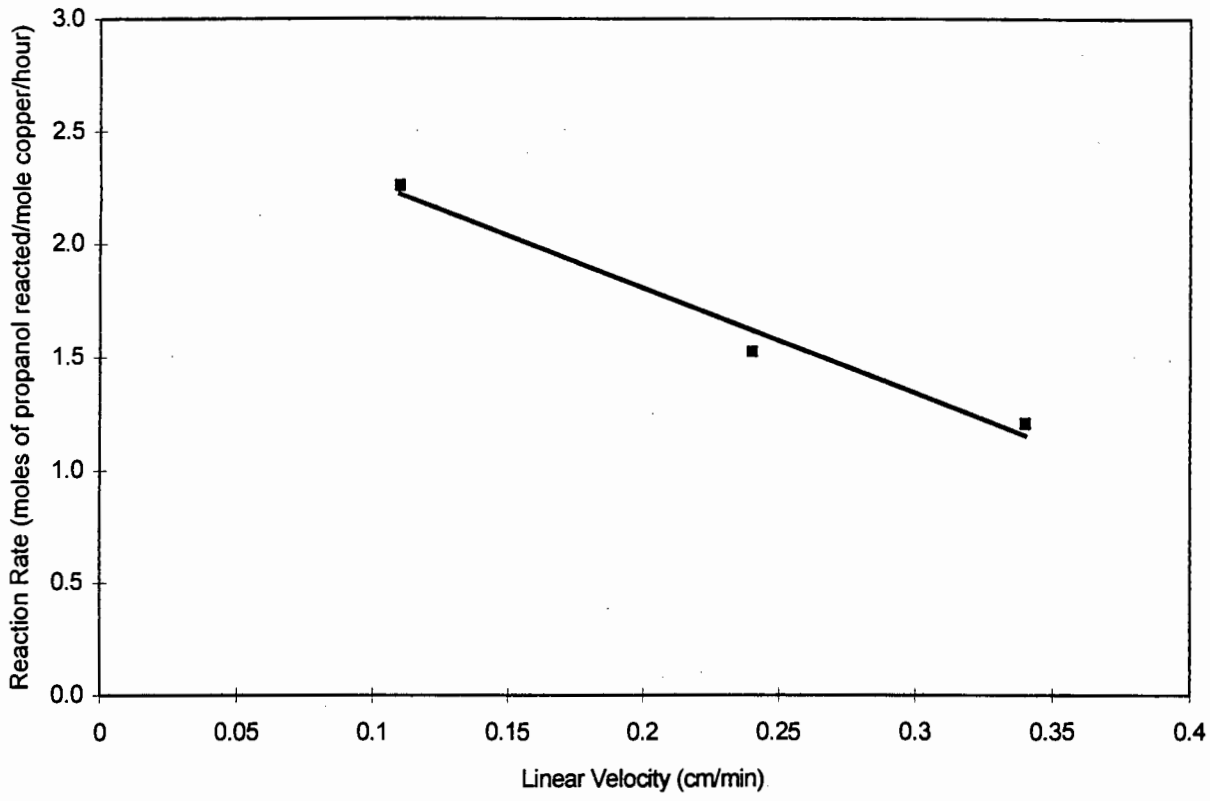

Figure 3.6. Plot of Reaction Rate versus Linear Velocity.

The intrinsic rate of reaction varies with linear velocity therefore mass transfer effects are present i.e. external mass transfer is rate limiting. This is possibly due to the reaction kinetics being faster than the rate of transfer of feed molecules across the boundary layer to the catalyst surface.

External mass transfer was rate limiting and no further experiments were carried out to check for the presence of internal mass transfer. The presence of mass transfer at the experimental conditions used for this study must be borne in mind and no intrinsic kinetic interpretations can be made using the data presented here.

3.3.5. Effect of Time-on-line on Conversion.

The effect of catalyst ageing, with time-on-line, was studied to determine the impact on the experimental results. The average values for the operating conditions used in the study are given in Table 3.5. The conversion of n-propanol was plotted against time-on-line and the result appear in Figure 3.7.

Table 3.5. Actual Operating Conditions Used for the Time-on-line Study.

Operating Conditions:	Average Value Over 7 Days:
Feed composition (Mole ratio water : n-propanol : dioxane)	1:1:0
Catalyst bed temperature (°C)	270.4
LHSV (hr^{-1}) for total feed mixture	1.95

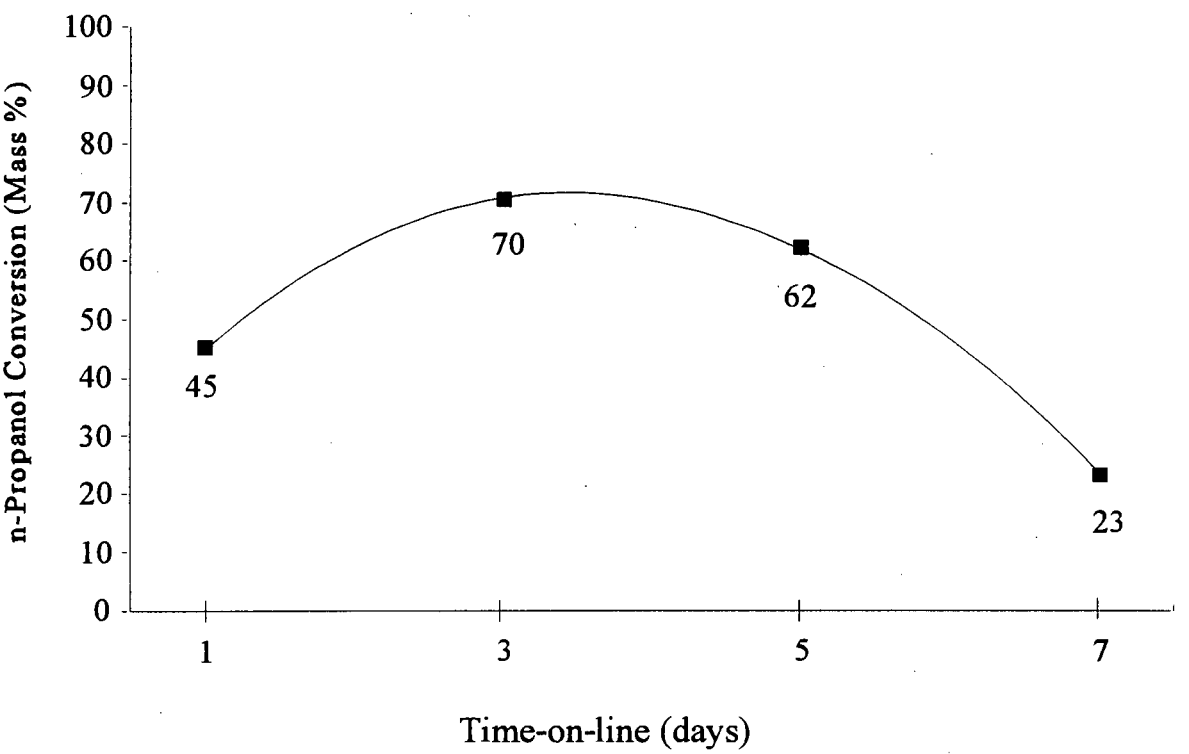

Figure 3.7. Plot of n-Propanol Conversion Against Time.

There was an initial activation period in which the catalyst activity increased with time. This may indicate that the catalyst surface had not reached a fully active state (e.g. the catalyst may not have been optimally reduced). The catalyst reached maximum activity after approximately three days on line then the activity declined rapidly. The decline in catalyst activity does not appear to be related to loss of catalyst surface area (see section 3.1.2.) and it is possible that the loss of catalytic activity could be due to fouling of the catalyst by byproducts.

Samples were taken every 6 to 8 hours and analysed. The most consistent analyses (excluding any obviously erroneous G.C. analyses) were averaged. The average values for the first 48 hours on line were used for the optimisation study so that results could be compared under similar catalyst activation/deactivation states. The operating conditions for each of the tests in the optimisation study were varied over a wide range and are expected to cause different activation/deactivation rates. Due to time constraints it was not possible to quantify the activation/deactivation profile at each set of operating conditions. However, the trend was similar over the period. This situation should be borne in mind when interpreting the results.

3.3.6. Optimisation of Operating Conditions-Contour Plot Interpretation.

The average operating conditions and experimental results for the optimisation study (see section 2.2.7.4.) are given in Table 3.6. A detailed breakdown of the results appears in Appendix 5. Data from the optimisation experiments was used to generate contour (surface area) plots (Appendix 6) using *Statgraphics* [49] to express the relationship between the reaction conditions and the conversion of n-propanol, the selectivity of n-propanol for propionaldehyde and the propionaldehyde yield. *Statgraphics* [49] is a statistical program which produces contour (density) plots using a trend fitting procedure to extrapolate the prevailing trends within the boundaries of a given set of data. The trends, while useful, do not have as much value as the hard data points. *Statgraphics* [49] like other statistical programs produces outputs which are proportional to the number of data points available i.e. the more data points in the inputs the more confidence there is in the outputs. It is important to note that unreliable data has the potential to skew the trends.

Table 3.6. Average Operating Conditions and Experimental Results for the Optimisation Study.

Run Number:	1	2	3	4	5 *	6 *	7	8
Experimental Conditions:								
Temperature (°C)	219	321	219	320	270	271	270	269
Water Partial Pressure (atm.)	0.83	0.83	0.08	0.08	0.46	0.46	0.50	0.00
LHSV (hr^{-1})	1.1	2.6	6.3	1.2	3.2	3.2	2.0	2.0
Residence Time (hr)	0.93	0.38	0.16	0.87	0.31	0.31	0.51	0.49
Experimental Results (mole%):								
n-Propanol conversion	29.5	50.9	28.4	86.2	26.3	39.6	66.5	39.5
n-Propanol selectivity to propionaldehyde	30.8	10.1	15.7	19.9	24.1	21.9	18.4	22.4
Yield of propionaldehyde	9.1	5.1	4.5	17.1	6.4	8.7	12.3	8.9
Hydrogen balance	99.3	98.8	97.0	99.5	99.4	99.4	96.5	97.9
Carbon balance	99.2	98.2	98.8	97.6	99.1	98.5	96.1	98.7
Oxygen balance	98.7	99.2	97.8	98.7	99.8	98.1	97.6	98.2

* Duplicate experiments

3.3.6.1. The Effect of Reaction Temperature on n-Propanol Conversion and on Propionaldehyde Selectivity.

The conversion of n-propanol followed the expected trend and was low at low reaction temperatures and increased as the temperature was increased (see Appendix 6.1.). The data looks somewhat scattered but at water partial pressures below 0,4 atm it appears that propionaldehyde selectivity increased with increase in temperature to a maximum at around 280°C and then decreased with further increases in temperature (see Appendix 6.4.) due to the higher rate of reaction at higher temperatures and hence greater consumption of propionaldehyde for byproduct formation.

3.3.6.2. The Effect of Liquid Hourly Space Velocity on n-Propanol Conversion and on Propionaldehyde Selectivity.

As expected, the conversion of n-propanol was found to be high at low liquid hourly space velocities and the conversion decreased as the liquid hourly space velocity was increased due to the shorter contact time on the catalyst surface (see Appendix 6.2.). The selectivity for propionaldehyde increased as the liquid hourly space velocity increased (see Appendix 6.6.) since the contact time was not sufficiently long for propionaldehyde to be converted to byproducts.

3.3.6.3. The Effect of Water Partial Pressure on n-Propanol Conversion and on Propionaldehyde Selectivity.

The n-propanol conversion was higher at low water partial pressures and decreased as the water partial pressure was increased at higher temperatures (e.g. 320°C) (see Appendix 6.1.). Water has been shown to act as a poison for copper-chromite catalysts [40]. The selectivity for propionaldehyde increased with increased water partial pressure (see Appendix 6.4. and 6.6.) except at high temperatures (e.g. 320°C see Appendix 6.4.) where temperature appears to be the driving force affecting byproduct formation. An increase in water partial pressure is expected to disfavour byproduct formation since water is a product of many of the byproduct-forming reactions.

3.3.6.4. The Effect of Operating Conditions on Propionaldehyde Yield.

3.3.6.4.1. The Effect of Temperature on Yield.

The yield increases as the temperature is increased (see Appendix 6.7, at any given water partial pressure, up to 0.6 atm, as the temperature is increased from 220°C to 320°C, the pattern gets darker). In the case of temperature vs LHSV, there are two regions of high yield (Appendix 6.8), at low temperatures (below about 250°C) and at high temperatures (above about 300°C). It is important to note that *Statgraphics* extrapolated the trend in the low temperature region (see Appendix 6.8.) although there are no data points in that area. At lower temperatures the LHSV appears to have a strong effect on the yield as can be seen from the broad band of high yield which decreases rapidly with increase in temperature (i.e. the contours are close together). The yield is high at low temperatures over a wide range of LHSV's and again at high temperature (above 300°C) and a LHSV below 2 hr^{-1}. Although the selectivity is expected to be low at low LHSV's the conversion is high and the high temperature also contributes to the high conversion which results in the yield being high.

It is important to note that few data points were used for the analysis and any dubious points could distort the *Statgrapics* plots. Only the broad trends are discussed here. More data points would be needed to draw further insights.

3.3.6.4.2. The Effect of LHSV on Yield.

At low LHSV (see Appendix 6.2 and Appendix 6.5) the conversion is high but the selectivity for propionaldehyde is low. As the LHSV is increased the conversion decreases but the selectivity increases. There is therefore a midpoint at which the yield is optimal. This appears to be between 2 and 3 hr^{-1} (i.e there is a band of consistently high yield for temperatures between 200 and 250°C). For water partial pressure vs LHSV (Appendix 6.9), at low LHSV (e.g. 1 hr^{-1}) the yield decreases with increase in water partial pressure. The conversion is high and the selectivity is low at low LHSV and the increase in water partial pressure results in the conversion and the selectivity increasing. The conversion appears to have a greater effect on the yield than the selectivity hence the yield decreases. At higher LHSV (e.g. 2-6 hr^{-1}) the yield decreases as the water partial pressure is increased. However, the effect of water partial pressure on yield appears to be less pronounced (the contours are wider apart). The high yield predicted by the contour plot (Appendix 6.9) at high LHSV and high water partial pressure is unlikely unless the effect of selectivity on the yield outweighs the effect of conversion. This does not appear to be the case. It appears that the effect of conversion on the yield is stronger than the effect of selectivity for propionaldehyde.

3.3.6.4.3. The Effect of Water Partial Pressure on Yield.

At a low water partial pressure (0.08 atm see Appendix 6.7), the yield increases with increase in temperature due to the higher conversion. At high water partial pressures (e.g. 0.8 atm) the yield decreases with increase in temperature since there is less n-propanol to be converted. The optimum yield appears to be at lower water partial pressures (see Appendix 6.9) with higher yields at 0.4 atm over a wider range of LHSV's. From Appendix 6.7. it appears that the optimum water partial pressure is between 0 and 0.4 atm for temperatures above 310°C.

The yield contour plots can be used to predict the expected yield for a particular set of conditions prior to performing an experiment. The water partial pressure appears to have a much smaller effect on the yield than the temperature and LHSV. The temperature appears to be the dominant factor affecting propionaldehyde yield with maximum yields likely at a LHSV between 2 and 3 hr^{-1}.

3.3.7. Qualitative Product Analysis

The reactor product was analysed using G.C.-M.S. (see section 2.2.5.2.). The E.I. mass spectra are given in Appendix 7. The reaction conditions are given in Table 3.7. The main components of the reactor product were identified using a Wiley 138 database and appear in Table 3.8.

Table 3.7. Reaction Conditions for Qualitative Product Analysis.

Operating Conditions:	Average Value:
Feed composition (Mole ratio water : n-propanol)	1:1
Reactor temperature (°C)	250
LHSV (hr^{-1})	1

Note: Only water and n-propanol were used as feed.

Table 3.8. Components of the Reactor Product Identified by G.C.-M.S.

Component:	Number of Peak on M.S.:	Mass %	Retention Time on G.C. Column (min):
Propionaldehyde	1	11.0	3.65
2-Methyl-3-pentanone	2	2.9	4.33
2-Methyl-pentanal	3	13.3	5.10
n-Propanol	4	5.4	5.46
Propyl propionate	5	14.2	5.62
1,1-Dipropoxy propane	6	31.6	5.88
2-Methyl-2-pentenal	7	1.0	8.15
Hexyl Propionate	8	1.0	9.19
Unknown	9	-	9.30
Unknown	10	*	10.33
2-Methyl-1-pentanol	11	*	10.33
Unknown	12	3.8	10.73
Unknown	13	-	12.13
Unknown	14	-	12.48
Propionic acid	15	5.6	17.77
2-Methyl-pentanoic acid	16	1.9	24.85

* Component 10 and 11 co-elute on the G.C. column. The total mass % for component 10 (unknown) and 11 (2-methyl-1-pentanol) is 5.4%. The total mass % for all the unknown components (excluding component 10) is about 3%. Where no value is given (i.e. -) the peaks were below the detection limit of the FID detector.

Extensive fragmentation was observed when using electron-impact ionisation (E.I.) mass spectroscopy methods for the identification of components in the product. The molecular ion was not identified for some of the components and so chemical ionisation (C.I.) mass spectroscopy was used since the bombarding ions transfer less energy to the analyte molecules than during electron bombardment. The amount of fragmentation decreased and there was an increase in the amount of the molecular ion observed. This made it possible to calculate the molecular mass of the unknown components of the product mixture. When molecules are bombarded with ions the molecules are ionised and break up into fragments. Each resulting fragment has a particular ratio of mass to charge, the m/e value. For most fragments the charge is 1 so the m/e value is the mass of the fragment [50]. The molecular mass of each fragment which is measured is the sum of the average atomic masses of the elements and peaks may be observed with molecular mass + 1 or molecular mass + 2 depending on the isotopes present.

The CI mass spectra are given in Appendix 8. The molecular ion for components 9, 10 and 12 (Table 3.9) corresponded to a molecular mass of 200 g/mole. Component 13 and 14 had a molecular mass of 100 g/mole and an empirical formula $C_6H_{12}O$. The fragmentation pattern for component 13 and 14 were almost identical and the two components eluted next to each other on the G.C. trace therefore they were assumed to be isomers of one another. The prominent fragments observed on the mass spectra of compound 13 and 14 correspond to a molecular mass of 41 g/mole, (characteristic of the fragment C_3H_5) and a fragment which has a molecular mass of 59 g/mole (corresponding to a fragment with the structure $-O-CH_2CH_2CH_3$). The isomers probably have a structure approximately as follows;

$CH_2=CH-CH_2-O-CH_2CH_2CH_3$ or $CH_3CH=CH-O-CH_2CH_2CH_3$

Components 9, 10 and 12 are also isomers of one another and have an empirical formula $C_{12}H_{24}O_2$. The characteristic peaks observed in the mass spectra are given in Table 3.9. The possible structures for the most abundant peaks are given in Table 3.10.

Table 3.9. Characteristic Peaks Observed for Each of the Unknown Compounds.

Component:	m/z Value (Mass to charge ratio):	Abundance:
Component 9	57	29 936
	75	182 650
	85	188 692
	103	44 774
	No peak corresponding to 131 or 143	
Component 10	No peak corresponding to 57	
	No peak corresponding to 73	
	89	19 176
	101	30 203
	117	6 100
	131	61 788
	143 base peak	456 295
Component 12	59	182 651
	85	361 938
	101 base peak	84 673
	No peak corresponding to 131	
	143	334 437

Table 3.10. Possible Structures for Each of the Main Fragments Observed in the Mass Spectra.

Molecular Mass of Fragment (g/mole):	Possible Structure:
41	CH_2=CH-CH_2
59	-O-C=O-CH_3 or O-$CH_2CH_2CH_3$
82	C_6H_{10}
84	C_5H_8O
102	$CH_3CH_2CH_2OC$=OCH_3
118	$C_6H_{14}O_2$

The basic structure of all three the unknown compounds (9, 10 and 12) has the following general formula since each exhibits a peak at a molecular mass between 115 and 118 depending on the number of hydrogen atoms present;

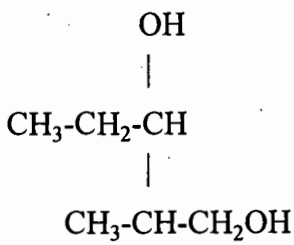

Molecular mass (M)= 118

Each of the -OH groups reacts further with a molecule of propionaldehyde with the elimination of water and addition of hydrogen. The additional propionaldehyde adduct is indicated in bold. The following structures are proposed for each of the three isomers;

1.

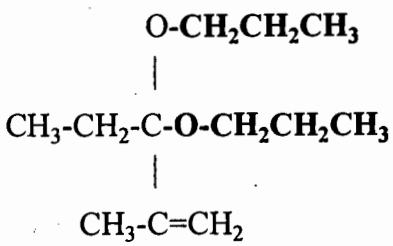

2a.

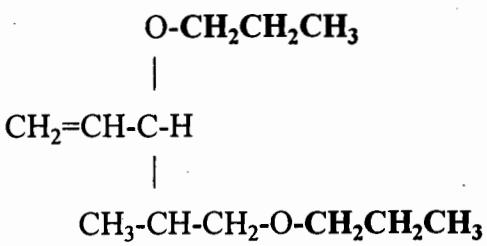

2b.

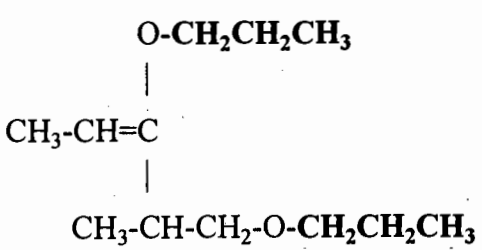

2c.

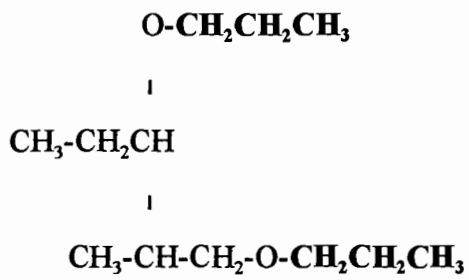

3.

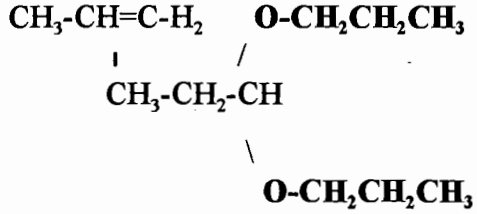

Compound 9 and compound 10 elute very close together on the G.C. trace and probably have a very similar structure. Compound 12 has a longer retention time. Although it is probably similar to compound 9 and 10, it's structure differs in some way from the others which effects it's retention timein the G.C. column. The three possible structures were examined in conjunction with the mass spectra in order to identify the three unknown components.

The following structure was assigned to component 12;

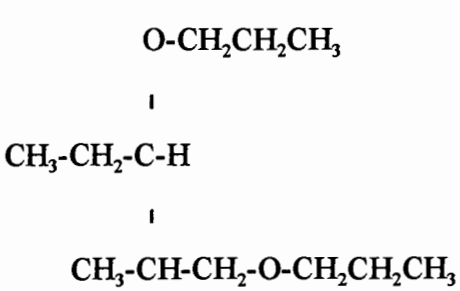

(i.e. 2c)

Component 12 differed sufficiently from the other two to elute some distance apart. This structure cannot form a fragment with a m + 1 of 131 since this would require a fragment with the following structure;

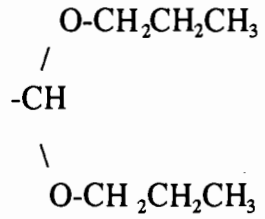

Component 9 was assigned the following structure;

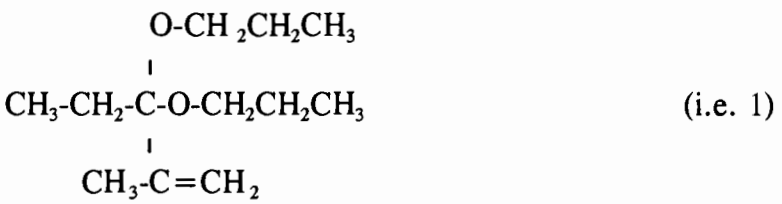

(i.e. 1)

Extensive fragmentation was observed with few high molecular mass fragments remaining intact. Component 10 was assigned the following structure;

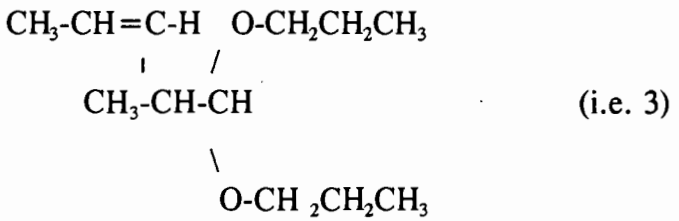

(i.e. 3)

Component 10 is a more stable structure since the electron dense double bond and the oxygens of the ether linkage are stabilised by the carbon atoms between them. The lower degree of fragmentation observed for component 10 (i.e. fragments with a molecular mass of 143 g/mole) indicate this greater stability. The structure of component 9 is less able to stabilise the electron density due to the very close proximity of the two ether groups and the double bond.

3.3.8. Change in the Relative Quantities of Products with Residence Time.

The molar percentage selectivity of each of the major byproducts was plotted against residence time. The data for the plots appears in Table 3.11. and the plots are given in Figure 3.8. and Figure 3.9. The n-propanol conversion is plotted against residence time and is given in Figure 3.10. The

runs were carried out at different temperatures and water partial pressures. The effect of residence time on molar selectivity was examined assuming that temperature and water partial pressure effects are not significant in order to examine the broad trends. These experiments, although discussed here, were carried out before the optimisation of operating conditions (section 3.3.6) in which temperature and water partial pressure were found to have significant effects. This should be borne in mind.

Table 3.11. Mole Percentage Selectivity of Byproduct Formed for Different Residence Times.

Residence Time (hr):	0.16	0.31	0.31	0.38	0.87	0.93
Temperature (°C)	219	270	271	321	320	219
Run Number:	3	5	6	2	4	1
Propionaldehyde	15.7	24.1	21.9	10.1	19.9	30.8
Propyl propionate	22.1	NA	23.0	NA	NA	22.4
Propionic acid	6.2	13.2	10.9	NA	NA	2.8
2-me-pentanal	2.1	3.2	1.1	NA	7.0	NA
2-me-1-pentanol	7.9	0.9	0.2	1.5	NA	2.1
2-me-pentanoic acid	0	0	0.2	NA	NA	0
1,1-Dipropoxy propane	NA	NA	0.4	0.2	NA	0.4

Note: NA means no analysis

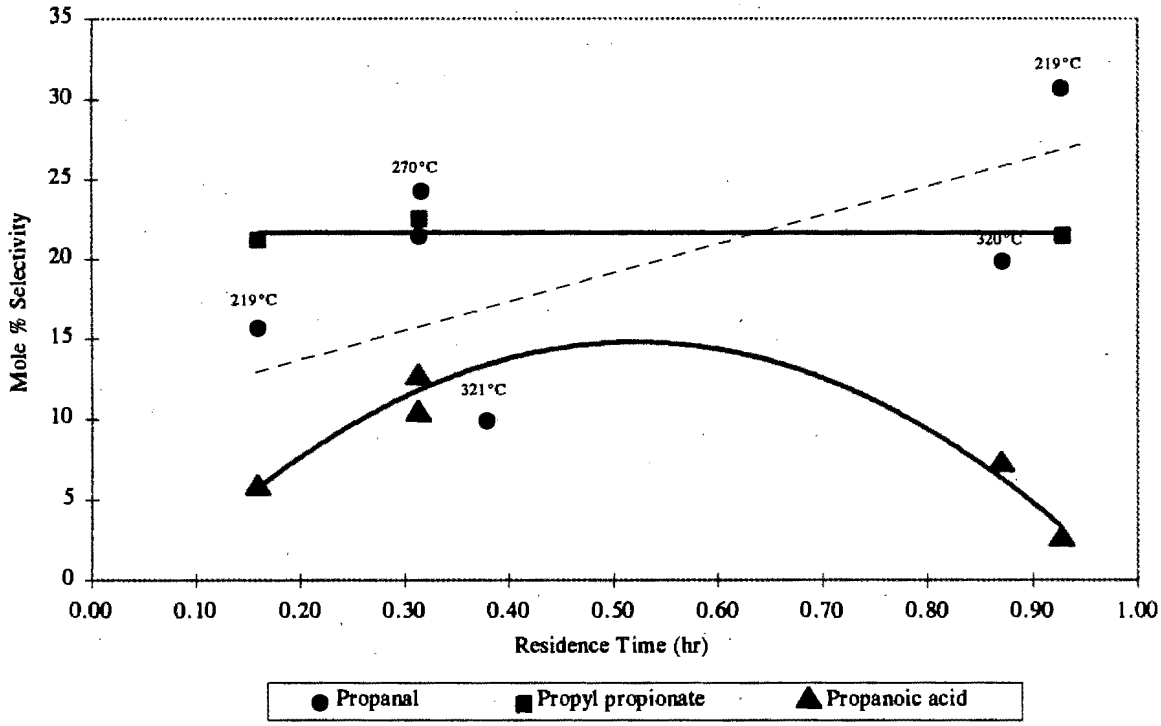

Figure 3.8. Plot of Mole Percentage Selectivity of Byproducts against Residence time for Propionaldehyde, Propyl Propionate and Propionic Acid.

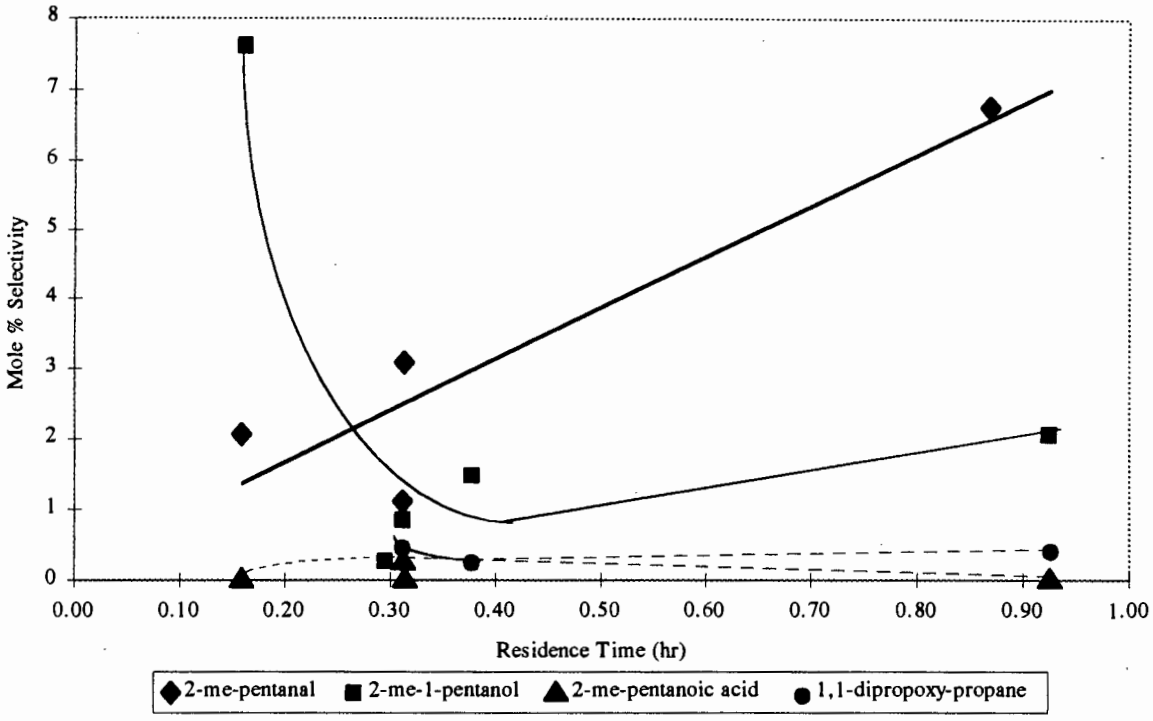

Figure 3.9. Plot of Mole Percentage Selectivity of Byproducts against Residence time.

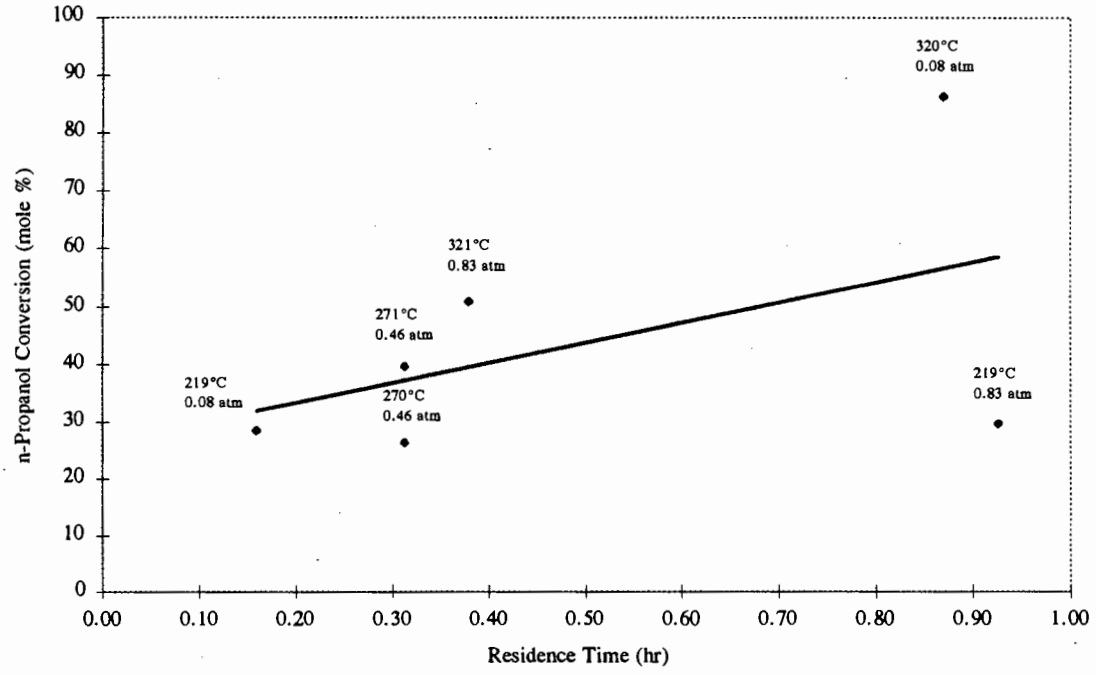

Figure 3.10. n-Propanol Conversion vs Residence Time.

There are several possible mechanisms by which propionaldehyde can be converted to byproducts. These mechanisms are outlined in Figure 3.11.

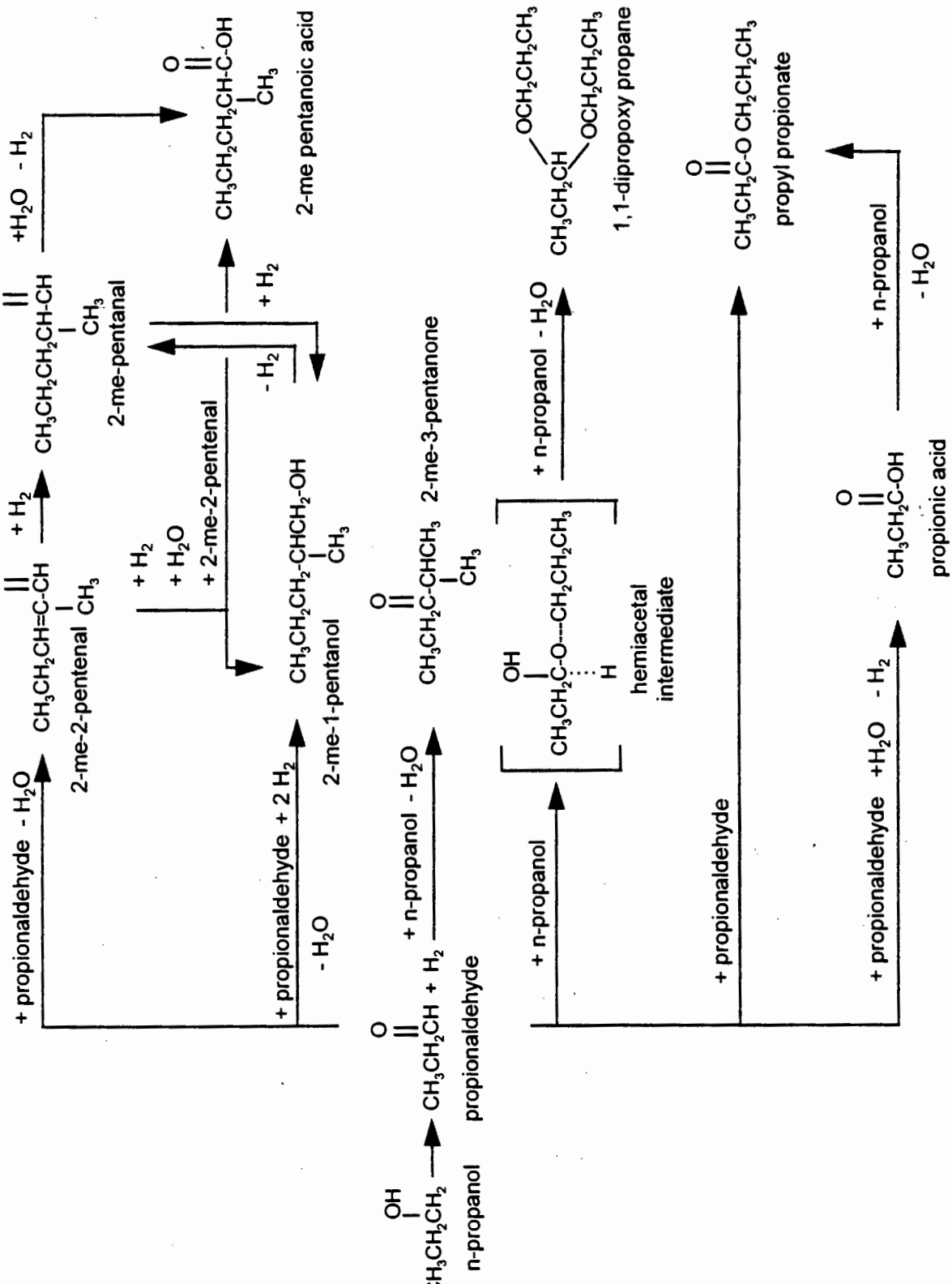

Figure 3.11. Possible Mechanisms for Byproduct Formation from Propionaldehyde.

Only the major products of n-propanol dehydrogenation which could be quantified by means of G.C. analysis are discussed below. Several of the components (such as 2-me-3-pentanone, 2-me-2-pentenal, and all the unknown components) in the reaction product, as identified by means of G.C.-M.S., were only present in low amounts and accurate quantitative data were not available.

Propyl propionate selectivity appears to remain relatively constant as the residence time increased. There are two possible routes for the formation of propyl propionate. The first possible mechanism for propyl propionate formation is via Fischer esterification where propionic acid reacts with n-propanol to form the ester. The second possible route is via the Tischenko reaction where two molecules of propionaldehyde react to form the ester. Propyl propionate is formed even at low residence times when little propionic acid is present and may initially form via the Tischenko reaction and later, when the concentration of propionic acid has increased, Fischer esterification may become more prevalent.

The selectivity for propionic acid increased initially with residence time (Figure 3.8.) and then decreased with increased residence time. The decrease in the concentration of propionic acid with increased residence time may be due to it's consumption in the formation of propyl propionate.

The selectivity for 2-me-pentanal increased with increased residence time. 2-me-Pentanal can form via the Aldol condensation of two molecules of propionaldehyde or via the dehydrogenation of 2-me-1-pentanol.

2-me-1-Pentanol has a high selectivity at low residence times however, the selectivity decreased rapidly with increased residence time. There are two possible routes for the formation of 2-me-1-pentanol. The first possible route is via the Aldol condensation of propionaldehyde and the second is via the Cannizzaro reaction between two molecules of 2-me-2-pentenal to form 2-me-1-pentanol and 2-me-pentanoic acid. One would expect roughly equal amounts of 2-me-1-pentanol and 2-me-pentanoic acid if 2-me-1-pentanol was formed by means of the Cannizzaro reaction. This was not the case and the concentration of 2-me-pentanoic acid was very low even at long residence times. The sharp decrease in the concentration of 2-me-1-pentanol with longer residence times is probably due to dehydrogenation of 2-me-1-pentanol to form 2-me-pentanal. Given that the catalyst is a dehydrogenation catalyst it is more likely that 2-me-1-pentanol is dehydrogenated to 2-me-pentanal since a rapid increase in 2-me-pentanal was observed.

The concentration of 2-me-pentanoic acid detected in the reactor product mixture was extremely low and only qualitative assumptions can be made regarding the potential route through which it is formed. The most likely route for the formation of 2-me-pentanoic acid is via reaction of 2-me-pentanal with water in a similar manner to the formation of propionic acid particularly since there is no evidence that the Cannizzaro reaction takes place to any extent.

1,1-Dipropoxy propane concentration was also extremely low and appeared to remain unchanged at longer residence times. 1,1-Dipropoxy propane is probably formed via the reaction of propionaldehyde with n-propanol to form a hemiacetal intermediate. Propyl propionate and 1,1-dipropoxy propane may be competing reactions where the hemiacetal intermediate from which they form could be converted into either of the two byproducts (see Figure 3.11).

Prasad [20] proposed that the formation of byproducts during ethanol dehydrogenation over a copper-chromite catalyst, occurs by means of a series mechanism. The complicated pore structure of the catalyst introduces a barrier to the departure of intermediates which increases the probability that they will degenerate into byproducts. It appears that the dehydrogenation step is rate determining with the condensation reaction occurring rapidly [51] under mild conditions [52]. Certain Aldol condensation products dimerise easily on standing [52] to give higher molecular mass products e.g. 1,1-dipropoxy propane. Tsuji et al [53] suggest that the rate determining step for the Aldol condensation of n-butyraldehyde is alpha-hydrogen abstraction and the active catalyst site is surface O^{2-}. Tsuji et al [53] found that all catalysts that produced Aldol condensation products had basic sites on the catalyst surface. The occurrence of condensation reactions in the presence of basic sites is confirmed by Corma [54] and by means of the TPD study carried out in the current study (see section 3.1.3.) where the G-13 copper chromite catalyst was found to have roughly equal quantities of acid and base sites. Correa Bueno et al [55] found that during ethanol dehydrogenation, the amount of carbonyl compounds formed increased with chromium content for chromium-containing copper catalysts. It was suggested that this may be due to the higher basicity of the surface of the catalyst with an increase in the availability of proton acceptor sites when chromium is added to the catalyst.

3.4. DISCUSSION

Significant byproduct formation occurs during the production of propionaldehyde by n-propanol dehydrogenation. The extensive byproduct formation is as a result of the reactivity of propionaldehyde which acts as an intermediate [51] on the copper chromite catalyst. The ammonia and CO_2 desorption profiles indicate the presence of both acidic and basic sites with slightly more acidic sites than basic sites. The catalyst composition has a significant influence on the types of byproducts which were formed [55] [57].

The possible mechanisms by which the main byproducts are formed are discussed below.

Aldehydes:

Propionaldehyde:

Propionaldehyde is the desired product of n-propanol dehydrogenation.

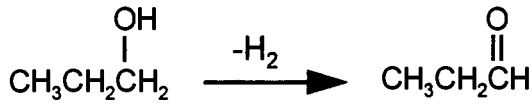

2-me-2-Pentenal:

The unsaturated aldehyde forms by Aldol condensation of propionaldehyde with the loss of water to give 2-me-2-pentenal via an intermediate (3-hydroxy-2-methylpentanal) [56]. The reaction steps are illustrated in Figure 3.11.

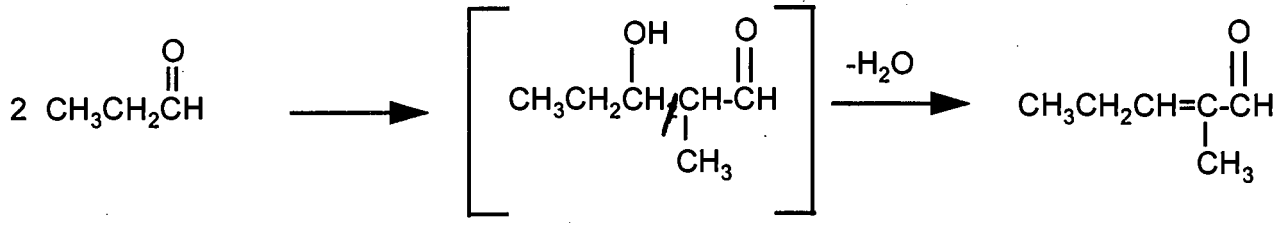

2-me-pentanal:

2-me-pentanal is the product of an Aldol condensation of propionaldehyde to form 2-me-2-pentenal which is hydrogenated to 2-me-pentanal.

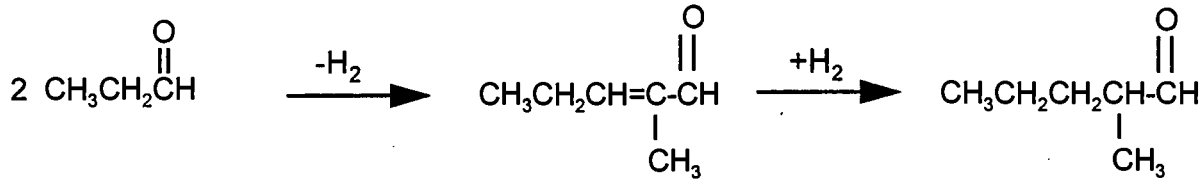

Ketones:

2-me-3-pentanone:

The ketone is formed by condensation of n-propanol and propionaldehyde via an Aldol-type reaction [57]. The carbonyl carbon of the aldehyde reacts with the carbon next to that carrying the alcohol group of n-propanol.

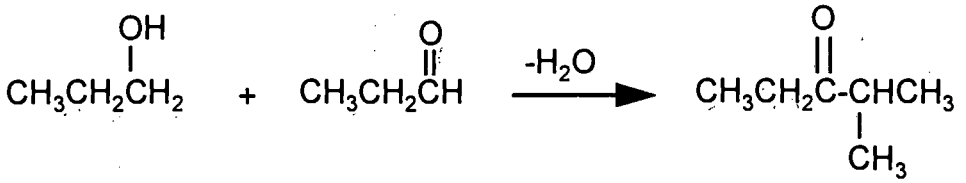

Acetals:

1,1-Dipropoxy propane:

This acetal is formed by the reaction of 2 moles of n-propanol with 1 mole of propionaldehyde to give a hemiacetal intermediate which is converted to 1,1-Dipropoxy propane with the elimination of water. An acid catalyst is needed and in the case of small unbranched aldehydes the equilibrium lies far to the right [58].

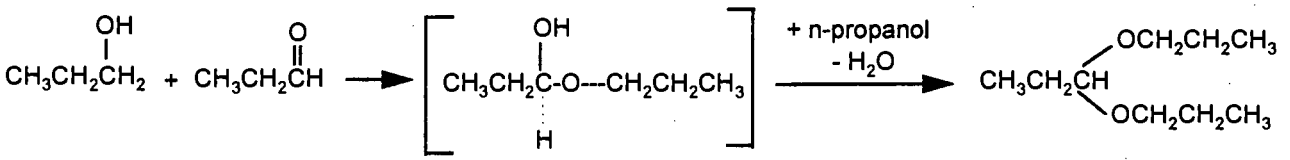

(See Figure 3.11. for preferred reaction sequence).

During the initial analysis of the reactor product problems were encountered due to separation of the product into an aqueous and an organic phase. Satisfactory separation of the two phases was not possible. Separation could be achieved by centrifuging the product mixture but it was difficult to draw off the two phases without causing mixing. It was decided to add ethanol to the reactor product as a solvent to homogenise the product prior to G.C. analysis. A 5:1 volume ratio of product to solvent alcohol was sufficient to produce a single phase. Previous analyses of the reactor product had shown the presence of the acetal, 1,1-Dipropoxy propane, and it was assumed that it formed as a byproduct of the dehydrogenation reaction. However, subsequent analyses, after the addition of the solvent alcohol to the reactor products, showed that acetal adducts of the solvent alcohols i.e. 1,1-diethoxy propane, were present in the product mixture. This was verified by means of G.C.-M.S.. The question arose as to whether the acetal formation was a result of reaction in the injector port of the G.C. or while the product was standing on the bench waiting to be analysed. A

sample of the reactor product was analysed at various injector temperatures and no significant change in the acetal concentration was observed (Table 3.12)

Table 3.12. Acetal Concentration as a Function of Injector Temperature

Injector Temperature (°C)	Mass % 1,1-Dipropoxy propane
100	5,1
150	5,7
200	5,4

(Samples were analysed by G.C.-AED on a 30 meter DBWAX column. The atomic emission line at 777 nm was monitored).

It is well known that an aldehyde in an alcoholic solution exists in equilibrium with the hemiacetal intermediate [58] [50]. In the presence of acid the hemiacetal reacts with the solvent alcohol to form the acetal. The reaction is reversible even at ambient temperature but for small unbranched aldehydes the equilibrium lies to the right (see Figure 3.12.).

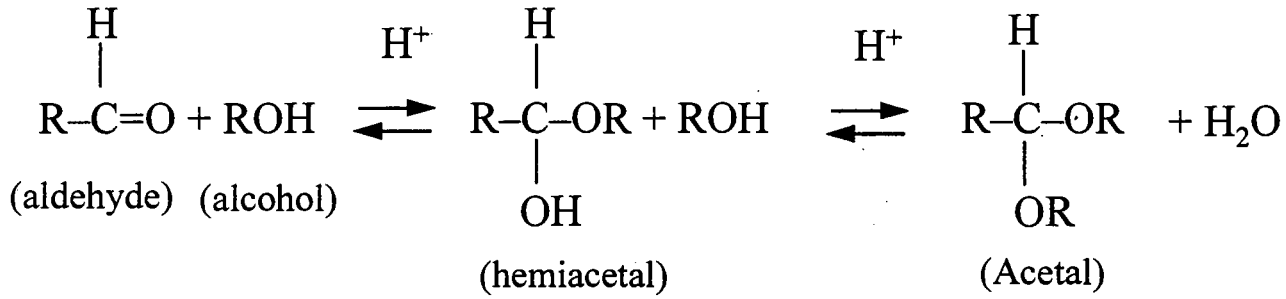

Figure 3.12. Reaction of an Alcohol with an Aldehyde to Form an Acetal.

Since acetal formation is acid catalysed, the propionic acid which formed as a byproduct during the reaction was neutralised with sodium carbonate and a sample was analysed. It was found to contain acetals suggesting that acetal formation took place prior to injection into the G.C.

A solution containing n-propanol, propionaldehyde and propionic acid in water was prepared from pure reagents and injected into the G.C. immediately after preparation. Traces of acetals were found to be present. A repeat analysis 24 hours later showed an increase in the mass percentage of acetals

present and a decrease in the mass percentage of n-propanol and propionaldehyde present. A control sample excluding the acid was analysed and no acetals were found to be present.

It appears that acetals formation occurs at room temperature in the presence of a carboxylic acids. The reaction appears to be rapid since trace amounts of acetal were detected immediately after preparation of the test mixture, and acetal formation continues if the sample is left to stand under ambient conditions. Although the temperature of the G.C. injection port may contribute to acetal formation, elevated temperatures are not a prerequisite for acetal formation. The 1,1-dipropoxy propane present in the product, as detected by means of an on-line G.C., is probably only due to acetal formation inside the reactor since the sample was analysed almost instantaneously.

Alcohols:

2-me-1-Pentanol:

There are three possible routes for the formation of 2-me-1-pentanol. The first is via Aldol condensation of propionaldehyde. The branched alcohol can also form by means of the Cannizzaro reaction in which 2 moles of 2-me-2-pentenal react, in the presence of a base, to give 2-me-1-pentanol and 2-me-pentanoic acid. The third possibility is the hydrogenation of 2-me-2-pentenal. Copper-silica catalysts are known to accelerate the Cannizzaro reaction [59].

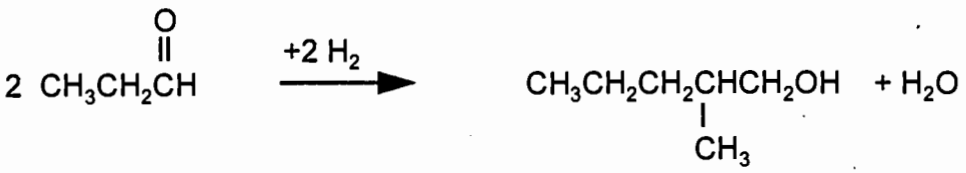

OR

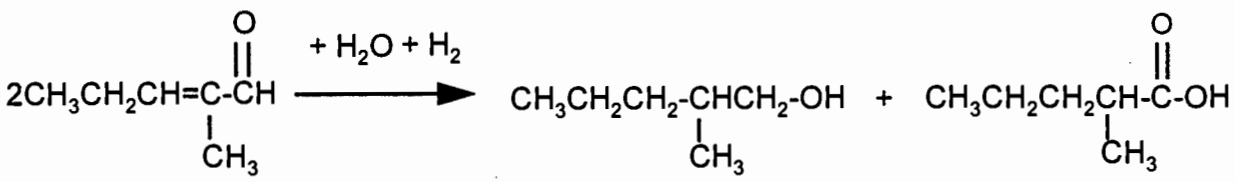

OR

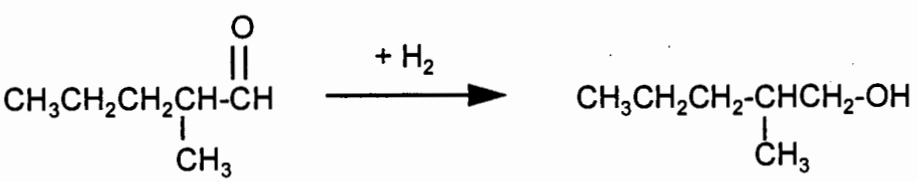

Carboxylic Acids:

Propionic acid:

Propionic acid is formed by the reaction of propionaldehyde and water.

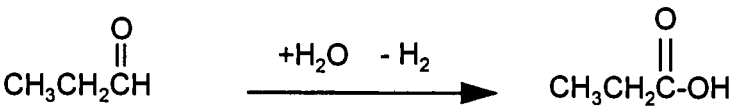

2-me-Pentanoic acid:

The branched acid can be produced via the Cannizzaro reaction in which 2 moles of 2-me-2-pentenal react to give 2-me-1-pentanol and 2-me-pentanoic acid or via the reaction of 2-me-pentanal and water.

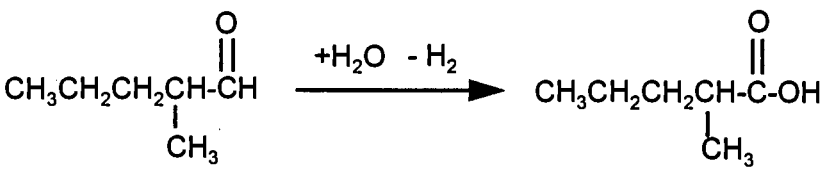

OR

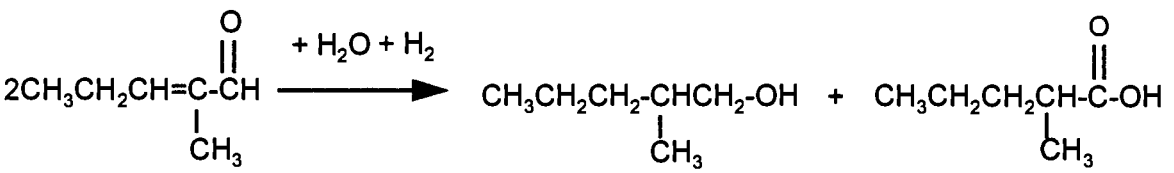

Esters:

Propyl Propionate:

Esters can form via two mechanisms. The first is Fischer esterification in which propionic acid reacts with n-propanol to give the ester [58]. The second possible route is via the Tischenko reaction in which two aldehydes react to form a hemiacetal intermediate which is dehydrogenated to the ester [55][56][57][25].

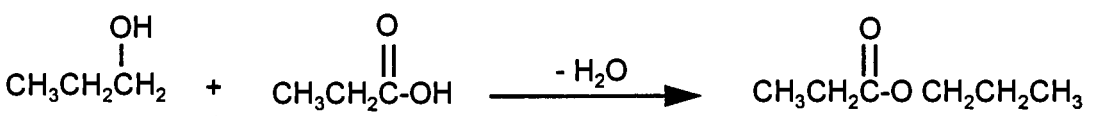

OR

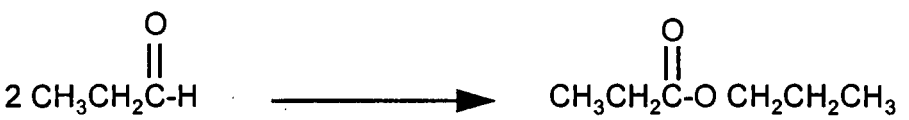

4. CONCLUSION

Propionaldehyde, the desired product in the dehydrogenation of n-propanol, is highly reactive and reacted further to form a wide variety of byproducts. Water was added to the feed to reduce byproduct formation by driving the equilibrium in favour of propionaldehyde. The selectivity of n-propanol for propionaldehyde increased with increase in water partial pressure. However, the n-propanol conversion decreased making it difficult to produce satisfactory yields of propionaldehyde.

The reaction conditions were varied in order to optimise the propionaldehyde yield. Contour plots of the effect of reaction conditions, i.e. the reaction temperature, water partial pressure and liquid hourly space velocity, on the yield were presented. A maximum propionaldehyde selectivity of 32 mole % was achieved at a reaction temperature of 219°C, a water partial pressure of 0.8 atmospheres and a liquid hourly space velocity of 1.1 hr^{-1}. The contour plots can be used as a tool to predict the yield given a set of reaction conditions.

During the study rapid deactivation of the copper-chromite catalyst was observed. The activity of the catalyst dropped to half its initial value after seven days on line. This has a significant impact on the viability of this process for commercial use especially since no catalyst regeneration process is available from the catalyst manufacturer.

The rapid deactivation of the catalyst together with the low propionaldehyde yield and the high byproduct yield make this process unattractive for industrial applications.

A single commercial dehydrogenation catalyst was investigated. It is entirely possible that a catalyst could be developed which would produce fewer byproducts and have a longer life time.

5. REFERENCES:

1. Yoo J.S.; Appl Catal. A: Gen. 102, 215-232 (1993)

2. SRI Report 11A, Menlo Park, California, 1978.

3. SRI Report 24A1, Menlo Park, California, 1975.

4. Pepe F.; Angeletti C.; De Rossi S.; Lo Jocono M.; J of Catal. 91, 69-77 (1985)

5. Cunningham J.; Alsayyed G.H.; Cronin J.A.; Fierro J.L.G.; Healy C.; Hirschwald W.; Ilyas M.; Tobin J.P.; J of Catal. 102, 160-171 (1986)

6. Kaushik V.K.; Sivaraj Ch; Kanta Rao P.; Appl. Surf. Scie. 51, 27-33 (1991)

7. Sivaraj .H.; Kantarao P.; Appl Catal. 45, 103-114 (1988)

8. Connett J.E.; J. Chem. Thermodynamics 4, 233-237 (1972)

9. Chhabra M.S.; Venkateswarlu C.; Indian Chem. Eng. 32, 73-79 (1990)

10. Ullmann's Encyclopedia of Industrial Chemistry Fifth Edition Volume 22A pg 441-452

11. Kirk-Othmer Encylopedia of Science and Technology, Vol. 1 pg 103-109

12. Chemical Economics Handbook, SRI International, Menlo Park, California, 1995, Vol. 682 pg 7000.

13. Kirk-Othmer Encylopedia of Science and Technology, Vol. 16 pg 637

14. Ullmann's Encyclopedia of Industrial Chemistry Fifth Edition Volume 18A pg 321-326

15. Kirk-Othmer Encylopedia of Science and Technology, Vol. 19 pg 221-226

16. SRI Report 24A, Menlo Park, California, 1967.

17. Industrial Organic Chemistry Second Edition, K. Weissermel and H. Arpe, pg 164 (1993)

18. SRI Report 24A2, Menlo Park, California, 1976.

19. Ullmann's Encyclopedia of Industrial Chemistry Fifth Edition Volume 16A pg 441-452

20. Prasad Y.S.; Padlia B.D.; Raman S.K.; J Chem. Tech. Biotechnol. 35A, pg 15-20 (1985).

21. Shiau G,; Chen T-W.; J of the Chin. I. Ch. E., Vol. 22, No 3, pg 141-147 (1991).

22. Pines H.; The Chemistry of Catalytic Hydrocarbon Conversions, pg 158, Academic Press (1981).

23. Tonner S.P.; Wainwright M.S.; Trimm D.L.; ; Cant N.W.; Appl. Catal. 11, 93-101 (1984)

24. Madhusudhan Rao V.; Shankar V.; Appl. Catal. 45, 335-344 (1988).

25. Cant N.W.; Tonner S.P.; Trimm D.L.; Wainwright M.S. J of Catal 91, 197-207 (1985)

26. Tonner S.P.; Trimm D.L.; Wainwright M.S.; Cant N.W.; Ind. Eng. Chem. Prod. Res. Dev. 23, 384-388 (1984)

27. Doca N.; Segal E.; React. Kinet. Catal. Lett. 28 (1), 123-129 (1985).

28. Klier K.; Advances in Catalysis Vol. 31, pg 243, Academic Press (1982).

29. Volta J.C.; Turlier P.; Trambouze Y.; J. of Catalysis 34, 329-337 (1974)

30. Schulz K.H.; Cox D.F.; J Phys. Chem. 97, 647-655 (1993)

31. Kaushik V.K.; Sivaraj Ch; Kanta Rao P.; Appl. Surface Scie. 51, 27-33 (1985)

32. Gulkava; Kraus; J Mol. Cat. Vol. 87, pg 47-55, (1994).

33. Buckley E.; Cox J.D.; Trans. Faraday Soc. 63, (1967)

34. Echevin B.; Teichner S.J.; Bull. Soc. Chim. Fr. 1495, (1975)

35. Kanoun N.; Astier M.P.; Pajonk G.M.; Appl. Catal 70, 225-236 (1991)

36. Kanoun N.; Astier M.P.; Pajonk G.M.; React. Kin. and Catal. Lett. 44, 51-56 (1991)

37. Chinchen G.C.; Denny P.J.; Jennings J.R.; Spencer M.S.; Waugh K.C.; Appl. Catal. 36, 1-65 (1988)

38. Pospisil M.; Taras P.; Collect. Czech. Chem. Commun. 42, 1266-1277 (1977)

39. Dunbar R.E.; Arnold M.R.; J. Org. Chem. 10, 501 (1945)

40. Eley D.D.; Pines H. and Weisz P.B. (Editors); Advances in Catalysis and Related Subjects, Vol 20, Chemisorptive and Catalytic Behaviour of Chromites; Burwell R.L.; Haller G.L.; Taylor K.C.; Read J.F.; pg 13-27; Academic Press, New York and London (1969).

42. Perry R.H.; Green D.W.; Maloney J.O.; Perry's Chemical Engineers' Handbook, 5th Edition, pg 4-4, McGraw-Hill

43. Stull D.R.; Westrum E.F.; Sinke G.C.; The Chemical Thermodynamics of Organic Compounds, John Wiley and Sons (1969).

44. Carberry J.J.; Chemical and Reaction Engineering, pg 111, McGraw-Hill, (1976).

45. Anderson J.R. and Pratt K.C.; Introduction to the Characterisation and Testing of Catalysts, pg 1-49, Academic Press (1985).

46. Satterfield C.N.; Mass Transfer in Heterogeneous Catalysts, pg 2-9, M.I.T. Press (1970).

47. Chambers R.P. and Boudart M; J. Catalysis Vol. 6, 141-145 (1966).

48. Froment G.F. and Bischoff K.B.; Chemical and Reactor Analysis and Design, pg 336-337 and 524-529, 2nd Edition, John Wiley and Sons (1990).

49. Statgraphics, Manugistics ANC, Rockwell, Maryland, USA.

50. Morrison R.T. & Boyd R.N. Organic Chemistry, pg 570, 5th Edition (1987)

51. Dolgov B.N. and Nizovkina T.V.; J. Gen. Chem. (USSR) 19, 1119 (1949).

52. Comprehensive Organic Synthesis, pg 136-140, Vol. 2, Trost B.M.; Fleming I; Heathcock C. H. (Editors), Pergamon Press (1989).

53. Tsuji H.; Yagi F.; Hattori H.; Kita H.; J. Catalysis, 148, 759-770 (1994).

54. Corma A.; Fornes V.; Rey F.; J Catalysis, 148, 205-212 (1994).

55. Correa Bueno J.M.; Goncalves C.M.; Vaccari A.; Appl. Cat. A: Gen. 103, 69-78 (1993).

56. Elvers B.; Hawkins S.; Russey W.; Schulz G. (Ed's); Ullmann's Encyclopedia of Industrial Chemistry, 5th Edition, Vol. A22, pg 157-161, V.C.H. Publishers.

57. Takeshita K.J.; Sci. Hiroshima Univ. Ser. A: Phys. Chem. 54 (1), 99-123 (1990).

58. March J.; Advanced Organic Chemistry, pg 789, 2nd Edition McGraw-Hill, (1977).

59. Comprehensive Organic Synthesis, Vol. 8, pg 86-87, Fleming I (Volume editor), Pergamon Press (1989).

APPENDIX 1.

CALIBRATION CURVES FOR ROTAMETER CALIBRATION.

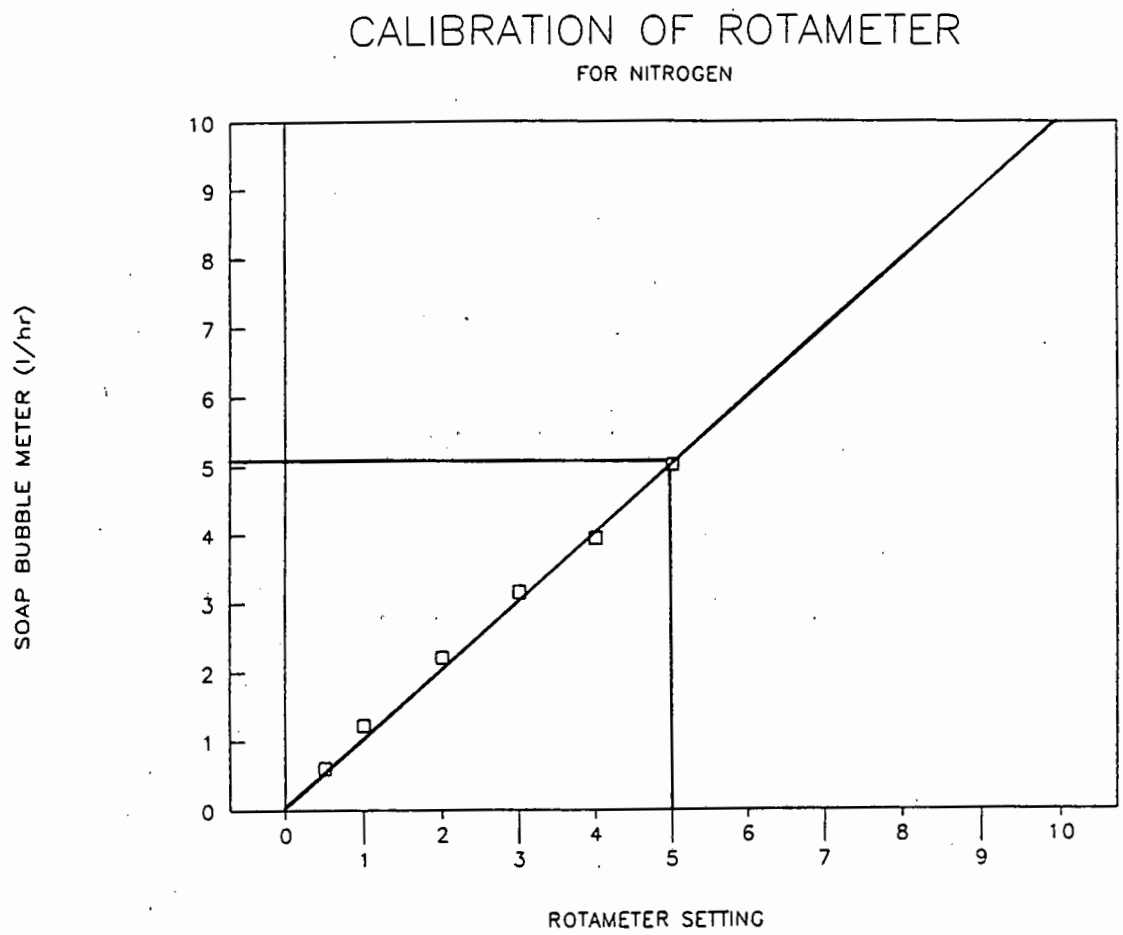

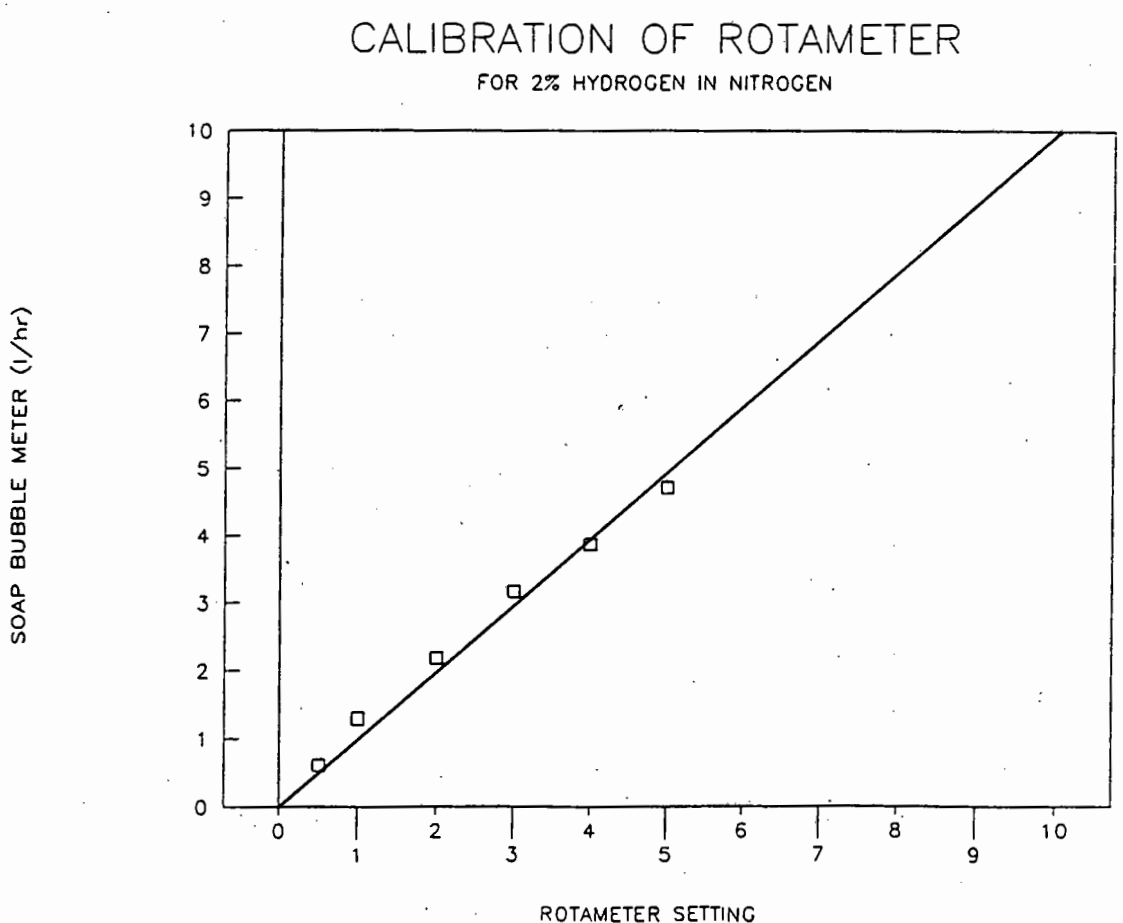

APPENDIX 2.

TYPICAL G.C. TRACE OF REACTOR PRODUCT.

/ARIAN 3400 GAS CHROMATOGRAPH

PEAK NO.	PEAK NAME:	RESPONSE TIME (MIN)	RESULT (AREA %)	AREA (COUNTS)
1	Unknown	2.989	2.0619	11363
2	Propionaldehyde	3.65	11.017	60713
3	Unknown	3.771	0.2138	1128
4	2-Methyl-3-pentanone	4.333	2.8945	15951
5	2-Methyl-pentanal	5.102	13.3287	73452
6	n-Propanol	5.461	5.3685	29585
7	Propyl propionate	5.619	14.1899	78198
8	1,1-Dipropoxy propane	5.884	31.6426	174377
9	2-Methyl-2-pentenal	8.151	0.977	5384
10	Hexyl Propionate	9.19	1.011	5571
11	Unknown + 2-Methyl-1-pentanol	10.331	5.4108	29818
12	Unknown	10.726	3.7769	20814
13	Propionic acid	17.768	5.6474	31122
14	2-Methyl-pentanoic acid	24.849	1.8566	10231
15	Unknown	28.198	0.6027	3321
	TOTALS:		100.00	551085

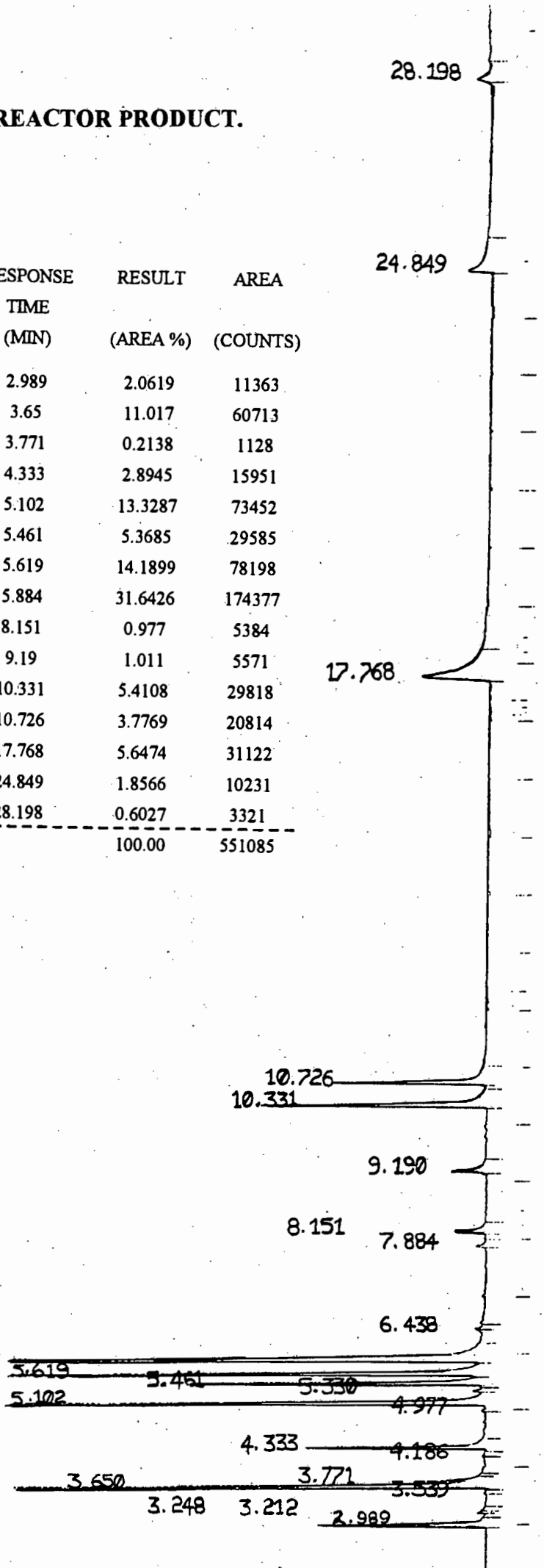

APPENDIX 3.

TYPICAL SPREADSHEET FOR ENTERING EXPERIMENTAL DATA.

RUN NAME:	7				
THEORETICAL FEED RATIO (DIOXANE:H2O:PrOH)(MOLES):	0:5:1				
TEMPERATURE SETPOINT ():	220.0				
PRESSURE (kPa) (abs):	85				
FEED FLOWRATE SETPOINT (ml\hr)	25.0				
OVERALL AVERAGE FEED FLOWRATE (ml\hr):	26.9				
VOL. CATALYST LOADED (ml):	25.0				
MASS OF CATALYST LOADED (g):	37.5				
OVERALL AVERAGE LHSV (hr-1):	1.1				
FEED COMPOSITION:					
MOLES WATER:	3.3				
MOLES PROPANOL:	0.7				
MOLES DIOXANE:	0.0				
MASS % WATER:	60.0				
MASS % PROPANOL:	40.0				
MASS % DIOXANE:	0.0				
VOLUME WATER (ml):	60.0				
VOLUME PROPANOL (ml):	49.8				
VOLUME DIOXANE (ml):	0.0				
VOLUME % WATER:	54.7				
VOLUME % PROPANOL:	45.3				
VOLUME % DIOXANE:	0.0				
REACTION PHASE:					
DATE:	17/12/94				
TIME:	13h00	14h00	15h00	16h00	
SOAP BUBBLE VOL (ml):	25.0	25.0	25.0	25.0	
SOAP BUBBLE TIME (s):	43.1	39.2	40.8	29.7	
TAIL GAS FLOWRATE (l/hr):	2.1	2.3	2.2	3.0	
GAS FLOWRATE AT STP (mol/hr):	0.1	0.1	0.1	0.1	
AVERAGE GAS MOLECULAR MASS (g/mol):	2.1	2.1	2.1	2.1	
GAS FLOWRATE (g/hr):	0.2	0.2	0.2	0.2	
REACTOR TEMPERATURE (øC):	215.4	218.8	219.9	221.5	
FEED PUMP RATE (ml/hr):	26.0	27.0	26.8	26.8	
PROPANOL FLOWRATE IN (g/hr):	9.5	9.8	9.8	9.8	
PROPANOL MOLAR FLOWRATE (mole/hr):	0.2	0.2	0.2	0.2	
WATER FLOWRATE IN (g/hr):	14.2	14.8	14.7	14.7	
DIOXANE FLOWRATE (g/hr):	0.0	0.0	0.0	0.0	
FEED MASS IN (g/hr):	23.7	24.6	24.4	24.4	
LIQUID PRODUCT OUT. (g/hr)	22.0	22.0	20.8	20.8	
MASS OF HC'S OUT (LIQUID) (g/hr)	7.8	7.3	6.1	6.1	
LIQUID MASS BALANCE (mass %):	93.0	89.5	85.0	85.0	
OVERALL MASS BALANCE (mass %):	93.6	90.2	85.7	86.0	
LHSV (hr^-1):	1.0	1.1	1.1	1.1	
PREHEATER TEMP.:	220.0	220.0	220.0	220.0	

TEMPERATURE PROFILE FOR REACTOR:
CATALYST BED LENGTH (cm):

cm:	0	221.8
	1	222.0
	2	222.3
	3	222.2
	4	221.8
	5	221.1
	6	220.0
	7	218.4
	8	216.5

FEED FLOWRATE IN (g/hr):	23.7	24.6	24.4	24.4
HYDROCARBON FLOWRATE IN (g/hr):	9.5	9.8	9.8	9.8
WATER FLOWRATE IN (g/hr):	14.2	14.8	14.7	14.7
Hydrogen (C=0 H=2 O=0 M=2.02):	0.0	0.0	0.0	0.0
Propene (C=3 H=6 O=0 M=42.08):	0.0	0.0	0.0	0.0
Propanal (C=3 H=6 O=1 M=58.08):	0.0	0.0	0.0	0.0
n-Propanol (C=3 H=8 O=1 M=60.10):	40.0	40.0	40.0	40.0
2-Methyl-propanal (C=4 H=8 O=1 M=72.1)	0.0	0.0	0.0	0.0
2-Methyl pentanal (C=6 H=12 O=1 M=100.16):	0.0	0.0	0.0	0.0
1,1-Diethoxy Propane (C=7 H=16 O=2 M=132.2)	0.0	0.0	0.0	0.0
2-Methyl-2-Pentenal (C=6 H=10 O=1 M=98.09):	0.0	0.0	0.0	0.0
Propyl propanoate (C=6 H=12 O=2 M=116.16):	0.0	0.0	0.0	0.0
2-Methyl-1-Pentanol (C=6 H=14 O=1 M=102.18):	0.0	0.0	0.0	0.0
2-Methyl-Propanal (C=4 H=8 O=1 M=72.1)	0.0	0.0	0.0	0.0
1,1-Dipropoxy Propane (C=9 H=20 O=2 M=160.26):	0.0	0.0	0.0	0.0
1-Propoxy-1-Propene (C=6 H=12 O=1 M=100.16)	0.0	0.0	0.0	0.0
Unknowns:	0.0	0.0	0.0	0.0
Water (C=0 H=2 O=1 M=18):	60.0	60.0	60.0	60.0
Propanoic acid (C=3 H=6 O=2 M=74.08)	0.0	0.0	0.0	0.0
Dioxane (C=3 H=8 O=1 M=88.11)	0.0	0.0	0.0	0.0
9	0.0	0.0	0.0	0.0
10	0.0	0.0	0.0	0.0
12	0.0	0.0	0.0	0.0
13	0.0	0.0	0.0	0.0
14	0.0	0.0	0.0	0.0
2-Me-Pentanoic acid (C=6 H=12 O=2 M=116)	0.0	0.0	0.0	0.0
TOTAL :	100.0	100.0	100.0	100.0

LIQUID PRODUCTS (MASS %):

TIME:	13h00	14h00	15h00	16h00
PRODUCT FLOWRATE (g/hr):	22.0	22.0	20.8	20.8
Hydrogen (C=0 H=2 O=0 M=2.02):	0.0	0.0	0.0	0.0
Propene (C=3 H=6 O=0 M=42.08):	0.0	0.0	0.0	0.0
Propanal (C=3 H=6 O=1 M=58.08):	1.5	4.1	2.6	5.7
n-Propanol (C=3 H=8 O=1 M=60.10):	15.9	33.4	34.7	30.2
2-Methyl-propanal (C=4 H=8 O=1 M=72.1)	0.0	0.0	0.0	0.0
2-Methyl pentanal (C=6 H=12 O=1 M=100.16):	0.0	0.0	0.0	0.0
1,1-Diethoxy Propane (C=7 H=16 O=2 M=132.2)	0.0	0.0	0.0	0.0
2-Methyl-2-Pentenal (C=6 H=10 O=1 M=98.09):	0.0	0.0	0.0	0.0
Propyl propanoate (C=6 H=12 O=2 M=116.16):	21.1	1.4	1.7	3.7
2-Methyl-1-Pentanol (C=6 H=14 O=1 M=102.18):	0.0	0.1	0.0	0.0
1,1-Dipropoxy Propane (C=9 H=20 O=2 M=160.26):	0.1	0.1	0.1	0.1
1-Propoxy-1-Propene (C=6 H=12 O=1 M=100.16)	0.0	0.0	0.0	0.0
Unknowns:	0.2	0.8	0.4	0.1
Water (C=0 H=2 O=1 M=18):	60.0	60.0	60.0	60.0
Propanoic acid (C=3 H=6 O=2 M=74.08)	1.0	0.0	0.2	0.0
Dioxane (C=3 H=8 O=1 M=88.11)	0.1	0.0	0.0	0.3
9	0.0	0.0	0.0	0.0
10	0.0	0.0	0.2	0.0
12	0.0	0.0	0.0	0.0
13	0.0	0.0	0.0	0.0
14	0.0	0.0	0.0	0.0
2-Me-Pentanoic acid (C=6 H=12 O=2 M=116)	0.0	0.0	0.0	0.0
TOTAL (MASS %)	100.0	100.0	100.0	100.0

GAS COMPOSITION (MASS %):

DAY:	13h00	14h00	15h00	16h00
MASS GAS (mole %/hr):	0.2	0.2	0.2	0.2
Hydrogen (C=0 H=2 O=0 M=2.02):	99.9	99.9	99.9	99.9
Propene (C=3 H=6 O=0 M=42.08):	0.0	0.0	0.0	0.0
Propanal (C=3 H=6 O=1 M=58.08):	0.1	0.1	0.1	0.1
n-Propanol (C=3 H=8 O=1 M=60.10):	0.0	0.0	0.0	0.0
2-Methyl-propanal (C=4 H=8 O=1 M=72.1)	0.0	0.0	0.0	0.0
2-Methyl pentanal (C=6 H=12 O=1 M=100.16):	0.0	0.0	0.0	0.0
1,1-Diethoxy Propane (C=7 H=16 O=2 M=132.2)	0.0	0.0	0.0	0.0
2-Methyl-2-Pentenal (C=6 H=10 O=1 M=98.09):	0.0	0.0	0.0	0.0
Propyl propanoate (C=6 H=12 O=2 M=116.16):	0.0	0.0	0.0	0.0
2-Methyl-1-Pentanol (C=6 H=14 O=1 M=102.18):	0.0	0.0	0.0	0.0
1,1-Dipropoxy Propane (C=9 H=20 O=2 M=160.26):	0.0	0.0	0.0	0.0
1-Propoxy-1-Propene (C=6 H=12 O=1 M=100.16)	0.0	0.0	0.0	0.0
Unknowns:	0.1	0.1	0.1	0.1
Water (C=0 H=2 O=1 M=18):	0.0	0.0	0.0	0.0
Propanoic acid (C=3 H=6 O=2 M=74.08)	0.0	0.0	0.0	0.0
Dioxane (C=3 H=8 O=1 M=88.11)	0.0	0.0	0.0	0.0
9	0.0	0.0	0.0	0.0
10	0.0	0.0	0.0	0.0
12	0.0	0.0	0.0	0.0
13	0.0	0.0	0.0	0.0
14	0.0	0.0	0.0	0.0
2-Me-Pentanoic acid (C=6 H=12 O=2 M=116)	0.0	0.0	0.0	0.0
TOTAL (Mole %)	100.0	100.0	100.0	100.0
AVERAGE MOLECULAR MASS:	2.1	2.1	2.1	2.1
MASS BALANCE (INCLUDING HYDROGEN):				
MASS IN (g/hr):	23.7	24.6	24.4	24.4
MASS OUT (g/hr):	22.2	22.2	20.9	21.0
OVERALL MASS BALANCE (MASS %):	93.6	90.2	85.7	86.0
MOLAR VALUES IN AND OUT:				

FEED (MOLES):				
DAY:	13h00	14h00	15h00	16h00
Hydrogen (C=0 H=2 O=0 M=2.02):	0.0	0.0	0.0	0.0
Propene (C=3 H=6 O=0 M=42.08):	0.0	0.0	0.0	0.0
Propanal (C=3 H=6 O=1 M=58.08):	0.0	0.0	0.0	0.0
n-Propanol (C=3 H=8 O=1 M=60.10):	0.2	0.2	0.2	0.2
2-Methyl-propanal (C=4 H=8 O=1 M=72.1)	0.0	0.0	0.0	0.0
2-Methyl pentanal (C=6 H=12 O=1 M=100.16):	0.0	0.0	0.0	0.0
1,1-Diethoxy Propane (C=7 H=16 O=2 M=132.2)	0.0	0.0	0.0	0.0
2-Methyl-2-Pentenal (C=6 H=10 O=1 M=98.09):	0.0	0.0	0.0	0.0
Propyl propanoate (C=6 H=12 O=2 M=116.16):	0.0	0.0	0.0	0.0
2-Methyl-1-Pentanol (C=6 H=14 O=1 M=102.18):	0.0	0.0	0.0	0.0
1,1-Dipropoxy Propane (C=9 H=20 O=2 M=160.26):	0.0	0.0	0.0	0.0
1-Propoxy-1-Propene (C=6 H=12 O=1 M=100.16)	0.0	0.0	0.0	0.0
Unknowns:	0.0	0.0	0.0	0.0
Water (C=0 H=2 O=1 M=18):	0.8	0.8	0.8	0.8
Propanoic acid (C=3 H=6 O=2 M=74.08)	0.0	0.0	0.0	0.0
Dioxane (C=3 H=8 O=1 M=88.11)	0.0	0.0	0.0	0.0
9	0.0	0.0	0.0	0.0
10	0.0	0.0	0.0	0.0
12	0.0	0.0	0.0	0.0
13	0.0	0.0	0.0	0.0
14	0.0	0.0	0.0	0.0
2-Me-Pentanoic acid (C=6 H=12 O=2 M=116)	0.0	0.0	0.0	0.0
PRODUCT (MOLES):				
Hydrogen (C=0 H=2 O=0 M=2.02):	0.2	0.1	0.1	0.1
Propene (C=3 H=6 O=0 M=42.08):	0.0	0.0	0.0	0.0
Propanal (C=3 H=6 O=1 M=58.08):	0.0	0.0	0.0	0.0
n-Propanol (C=3 H=8 O=1 M=60.10):	0.1	0.1	0.1	0.1
2-Methyl-propanal (C=4 H=8 O=1 M=72.1)	0.0	0.0	0.0	0.0
2-Methyl pentanal (C=6 H=12 O=1 M=100.16):	0.0	0.0	0.0	0.0
1,1-Diethoxy Propane (C=7 H=16 O=2 M=132.2)	0.0	0.0	0.0	0.0
2-Methyl-2-Pentenal (C=6 H=10 O=1 M=98.09):	0.0	0.0	0.0	0.0
Propyl propanoate (C=6 H=12 O=2 M=116.16):	0.0	0.0	0.0	0.0
2-Methyl-1-Pentanol (C=6 H=14 O=1 M=102.18):	0.0	0.0	0.0	0.0
1,1-Dipropoxy Propane (C=9 H=20 O=2 M=160.26):	0.0	0.0	0.0	0.0
1-Propoxy-1-Propene (C=6 H=12 O=1 M=100.16)	0.0	0.0	0.0	0.0
Unknowns:	0.0	0.0	0.0	0.0
Water (C=0 H=2 O=1 M=18) (CORRECTED):	0.8	0.7	0.7	0.7
Propanoic acid (C=3 H=6 O=2 M=74.08)	0.0	0.0	0.0	0.0
Dioxane (C=3 H=8 O=1 M=88.11)	0.0	0.0	0.0	0.0
9	0.0	0.0	0.0	0.0
10	0.0	0.0	0.0	0.0
12	0.0	0.0	0.0	0.0
13	0.0	0.0	0.0	0.0
14	0.0	0.0	0.0	0.0
2-Me-Pentanoic acid (C=6 H=12 O=2 M=116)	0.0	0.0	0.0	0.0
MOLE % CONVERSION, SELECTIVITY AND YIELD:				
DATE:	17/12/94	17/12/94	17/12/94	17/12/94
DAY:	1.0	2.0	3.0	4.0
MOLE % CONVERSION OF PROPANOL	63.1	25.3	26.2	35.9
MOLE % SELECTIVITY OF PROPANOL FOR PROPANAL	6.0	37.7	21.8	34.6
YIELD OF PROPANAL	3.8	9.5	5.7	12.4
MOLE % SELECTIVITY OF PROPANOL FOR:	17/12/94	17/12/94	17/12/94	17/12/94
Propene	0.0	0.0	0.0	0.0
Propanal	6.0	37.7	21.8	34.6
2-Methyl-propanal	0.0	0.0	0.0	0.0
2-Methyl pentanal	0.0	0.0	0.0	0.0
1,1-Diethoxy Propane	0.0	0.0	0.0	0.0
2-Methyl-2-Pentenal	0.0	0.0	0.0	0.0
Propyl propanoate	80.5	13.1	14.3	22.4
2-Methyl-1-Pentanol	0.1	1.3	0.0	0.0
1,1-Dipropoxy Propane	0.3	0.5	0.9	0.7
1-Propoxy-1-Propene	0.0	0.0	0.0	0.0
Propanoic acid	3.0	0.0	1.4	0.0
Unknowns:	0.5	4.3	2.0	0.4
9	0.0	0.0	0.0	0.0
10	0.0	0.0	0.5	0.0
12	0.0	0.0	0.0	0.0
13	0.0	0.0	0.0	0.0
14	0.0	0.0	0.0	0.0
2-Me-Pentanoic acid (C=6 H=12 O=2 M=116)	0.0	0.0	0.0	0.0
TOTAL SELECTIVITY:	90.4	57.0	40.8	58.1
COMPONENT BALANCE (MOLE %):	17/12/94	17/12/94	17/12/94	17/12/94
DAY:	13h00	14h00	15h00	16h00
Hydrogen:	100.7	93.9	89.6	91.0
Carbon:	94.2	89.3	85.1	85.6
Oxygen:	97.4	89.8	85.4	85.8
IN				
Hydrogen:	2.8	2.9	2.9	2.9
Carbon:	0.5	0.5	0.5	0.5
Oxygen:	0.9	1.0	1.0	1.0
OUT				
Hydrogen:	2.9	2.8	2.6	2.7
Carbon:	0.4	0.4	0.4	0.4
Oxygen:	0.9	0.9	0.8	0.8

APPENDIX 4.

G.C. TRACES FOR WATER/N-PROPANOL/DIOXANE FEED MIXTURE AND REACTOR PRODUCT.

VARIAN 3400 GAS CHROMATOGRAPH

PEAK NO.	PEAK NAME:	RESPONSE TIME (MIN)	RESULT (AREA %)	AREA (COUNTS)
1	Propionaldehyde	3.4	0.1051	1002
2	n-Propanol	5.333	77.6817	741191
3	Dioxane	5.946	22.2131	211943
	TOTALS:		100.00	954138

VARIAN 3400 GAS CHROMATOGRAPH

PEAK NO.	PEAK NAME:	RESPONSE TIME (MIN)	RESULT (AREA %)	AREA (COUNTS)
1	Propionaldehyde	3.422	10.725	40360
2	n-Propanol	5.308	64.7239	243567
3	Unknown	5.437	1.1315	4258
4	Dioxane	5.964	22.7915	85768
5	Unknown	7.609	0.6279	2362
	TOTALS:		100.00	376316

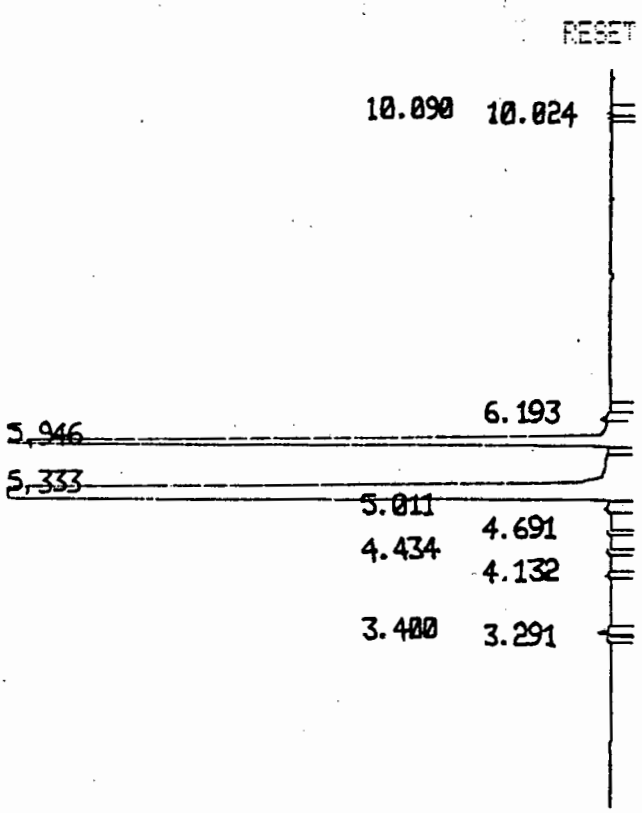

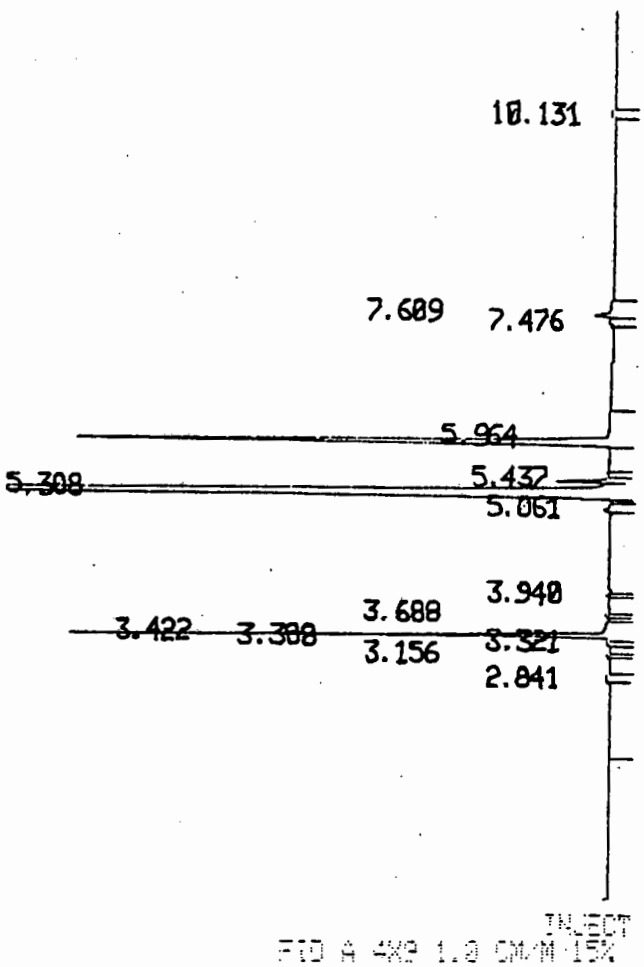

APPENDIX 5.

EXPERIMENTAL RESULTS FOR THE OPTIMISATION STUDY (Table 3.6.)[1]

Run 1	Sample 1	Sample 2	Sample 3	**Average:**
Conversion	25.51	26.51	36.59	***29.54***
Selectivity	37.33	21.54	33.63	***30.83***
Yield	9.52	5.71	12.31	***9.11***

Run 2	Sample 1	Sample 2	Sample 3	Sample 4	Sample 5	**Average:**
Conversion	52.29	43.21	52.24	54.81	51.86	***50.88***
Selectivity	6.57	10.44	10.95	8.91	13.37	***10.05***
Yield	3.44	4.51	5.72	4.88	6.93	***5.11***

Run 3	Sample 1	Sample 2	**Average:**
Conversion	29.73	27.1	***28.42***
Selectivity	15.28	16.17	***15.73***
Yield	4.54	4.38	***4.47***

Run 4	Sample 1	Sample 2	Sample 3	**Average:**
Conversion	80.86	91.72	85.88	***86.15***
Selectivity	19.57	20.84	19.13	***19.85***
Yield	15.82	19.11	16.43	***17.10***

Run 5	Sample 1	Sample 2	Sample 3	**Average:**
Conversion	31.1	24.73	23.14	***26.32***
Selectivity	21.67	32.08	18.68	***24.14***
Yield	6.74	7.93	4.32	***6.36***

Run 6	Sample 1	Sample 2	Sample 3	Sample 4	Sample 5	**Overall Average:**	**Average Sample 1 & 2**	**Average Sample 3, 4 & 5**
Conversion	50.55	50.37	25.26	33.12	38.85	***39.63***	***50.55***	***32.41***
Selectivity	18.2	21.28	27.16	28.34	14.67	***21.93***	***19.74***	***23.99***
Yield	9.20	10.72	6.86	9.39	5.70	***8.69***	***9.96***	***7.32***

Run 7	Sample 1	Sample 2	**Average:**
Conversion	70.6	62.4	***66.50***
Selectivity	15.84	21.01	***18.43***
Yield	11.18	13.11	***12.25***

Run 8	Sample 1	Sample 2	Sample 3	Sample 4	Sample 5	**Average:**
Conversion	47.36	41.78	31.79	39.10	37.63	***39.53***
Selectivity	22.35	19.08	24.14	17.48	28.97	***22.40***
Yield	10.58	7.97	7.67	6.83	10.90	***8.86***

Conversion : Mole % n-propanol converted to propionaldehyde
Selectivity : Mole % selectivity of n-propanol for propionaldehyde
Yield : Mole % yield of propionaldehyde

APPENDIX 6.

6.1. CONTOUR PLOTS: N-PROPANOL CONVERSION AS A FUNCTION OF TEMPERATURE AND WATER PARTIAL PRESSURE.

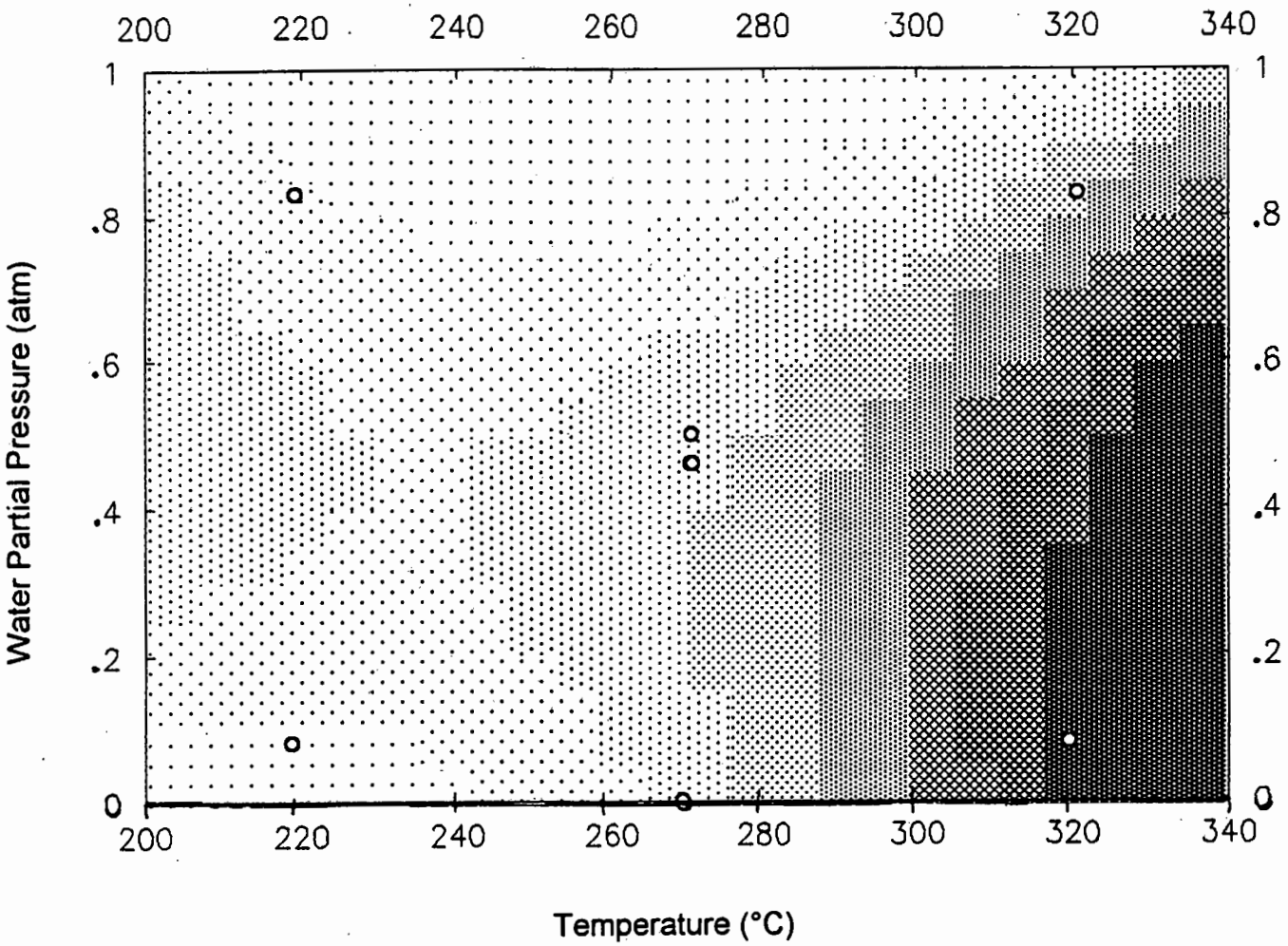

6.2. CONTOUR PLOTS: N-PROPANOL CONVERSION AS A FUNCTION OF TEMPERATURE AND LIQUID HOURLY SPACE VELOCITY.

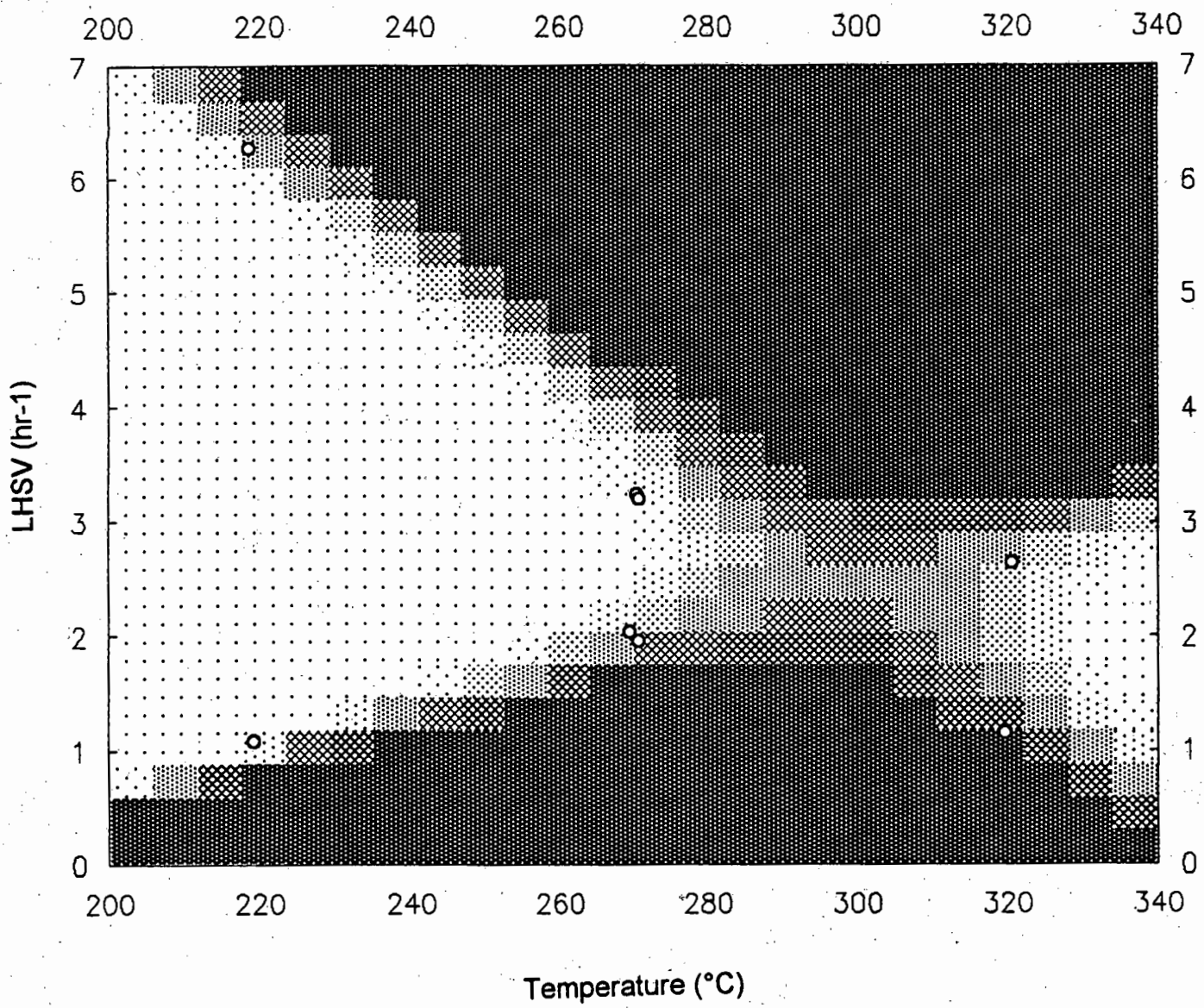

6.3. CONTOUR PLOTS: N-PROPANOL CONVERSION AS A FUNCTION OF WATER PARTIAL PRESSURE AND LIQUID HOURLY SPACE VELOCITY.

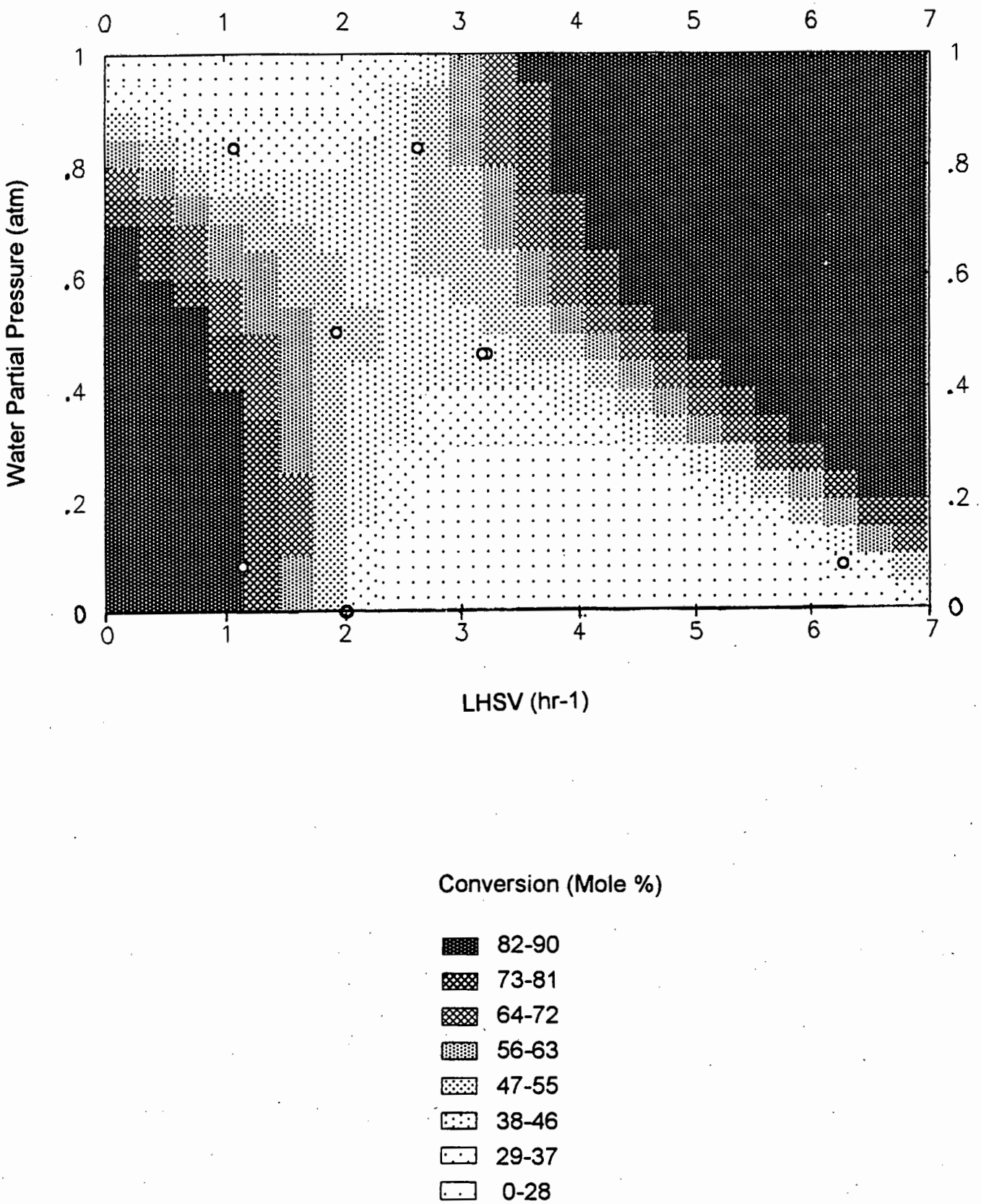

6.4. CONTOUR PLOTS: PROPIONALDEHYDE SELECTIVITY AS A FUNCTION OF TEMPERATURE AND WATER PARTIAL PRESSURE.

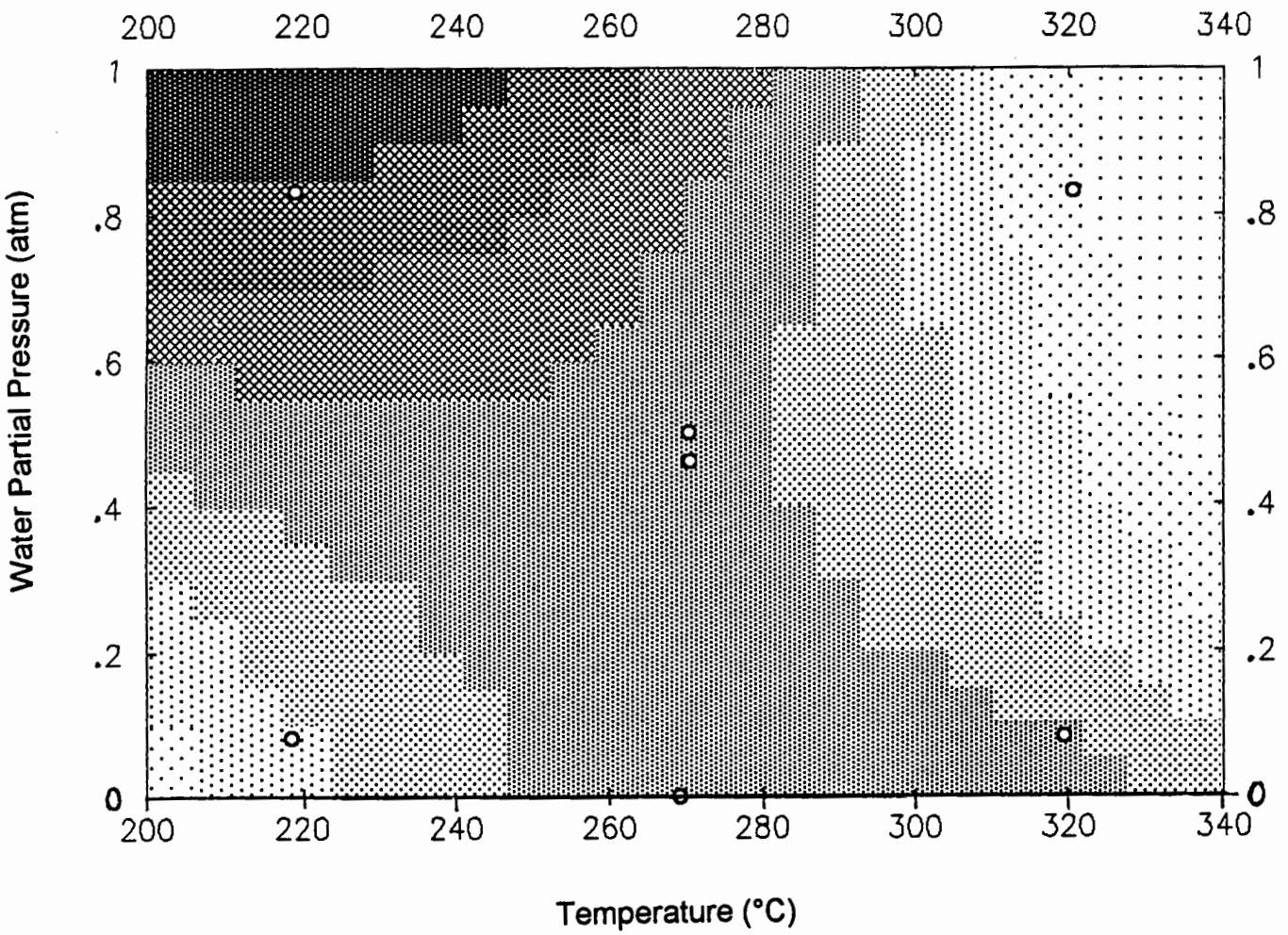

Selectivity (Mole%)

- 32-35
- 28-31
- 24-27
- 21-23
- 17-20
- 13-16
- 9-12

6.5. CONTOUR PLOTS: PROPIONALDEHYDE SELECTIVITY AS A FUNCTION OF TEMPERATURE AND LIQUID HOURLY SPACE VELOCITY.

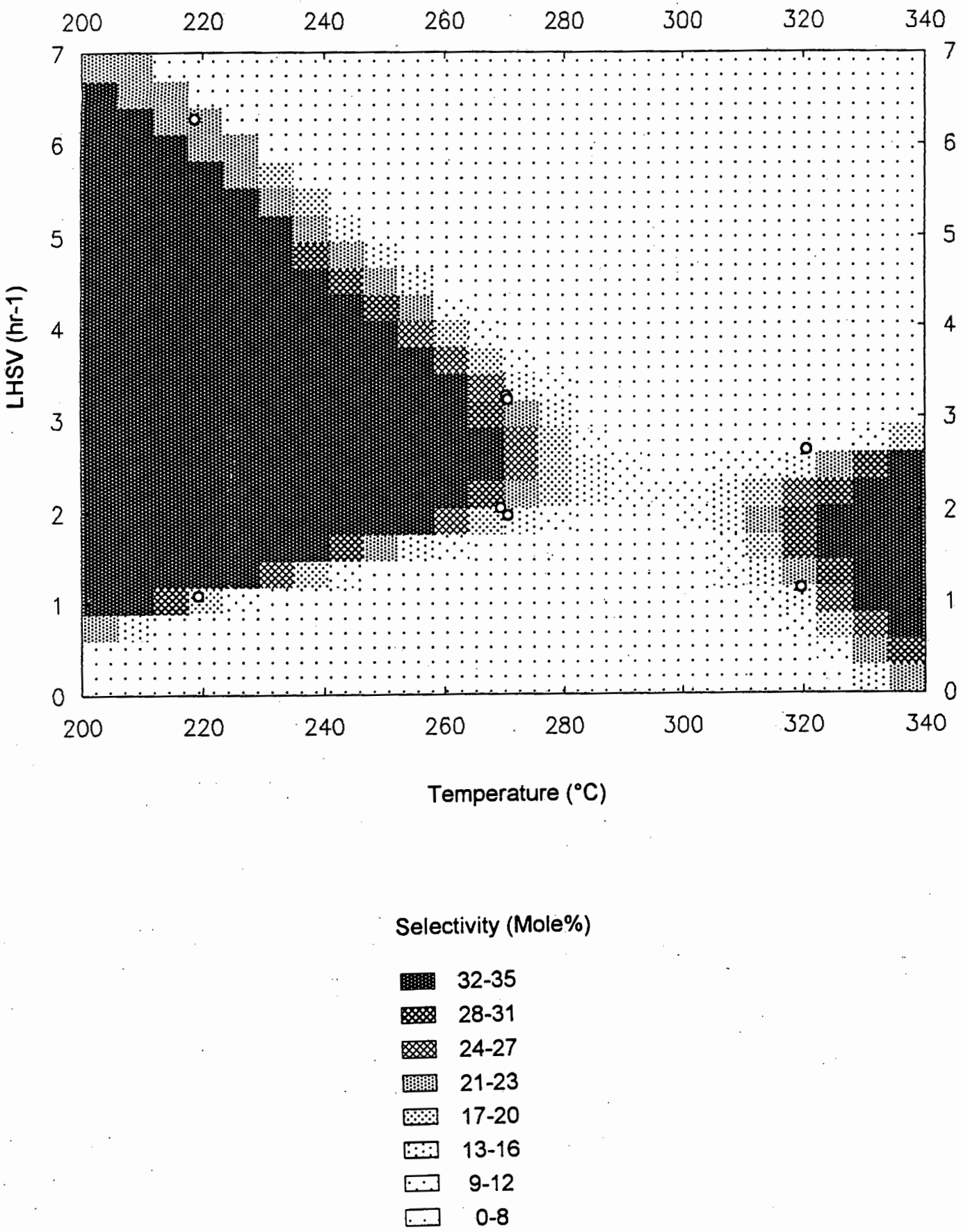

6.6. CONTOUR PLOTS: PROPIONALDEHYDE SELECTIVITY AS A FUNCTION OF WATER PARTIAL PRESSURE AND LIQUID HOURLY SPACE VELOCITY.

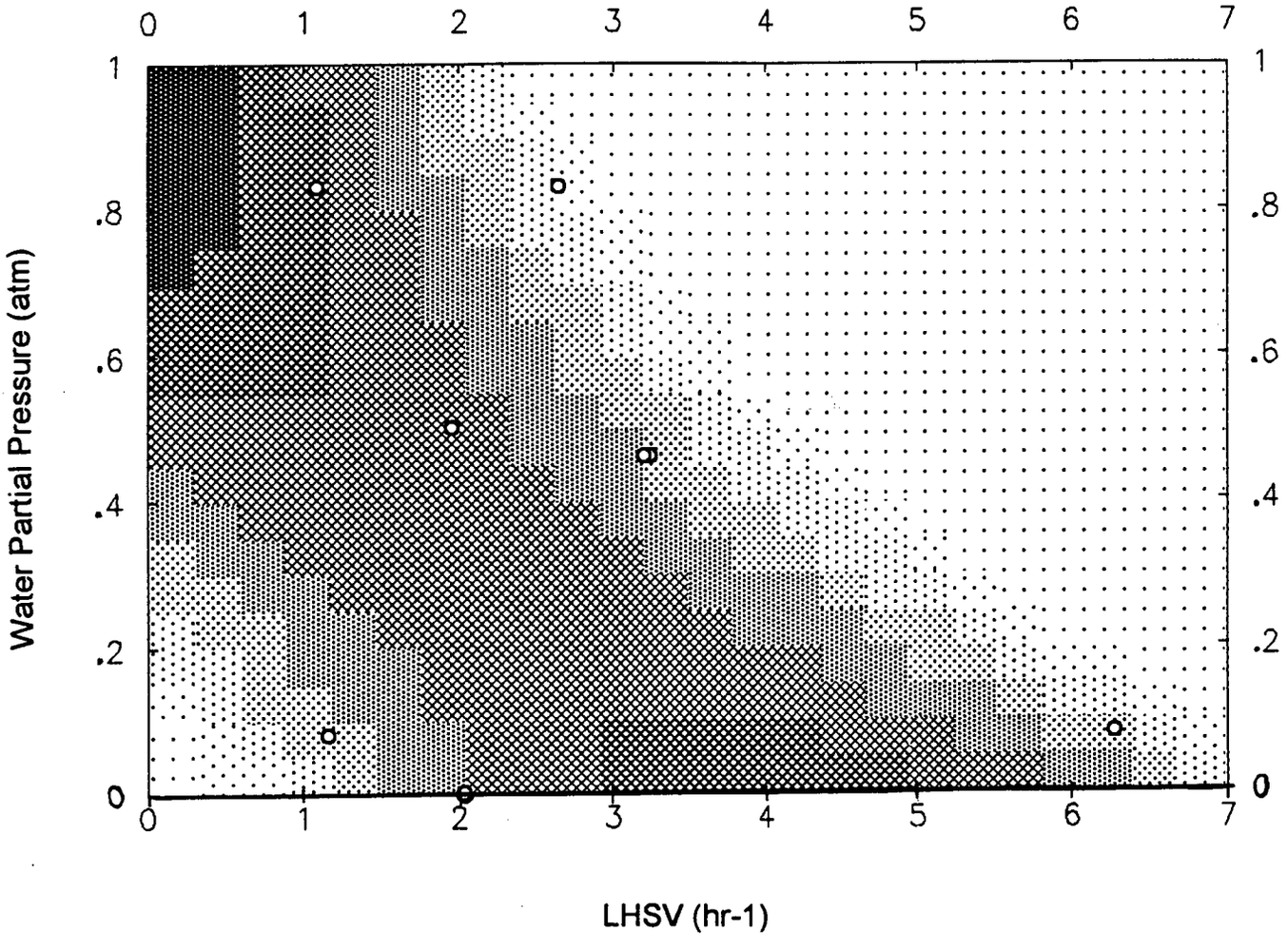

Selectivity (Mole%)

- 32-35
- 28-31
- 24-27
- 21-23
- 17-20
- 13-16
- 9-12
- 0-8
- 9-10
- 7-8
- 5-6
- 0-4

6.8. CONTOUR PLOTS: PROPIONALDEHYDE YIELD AS A FUNCTION OF TEMPERATURE AND LIQUID HOURLY SPACE VELOCITY.

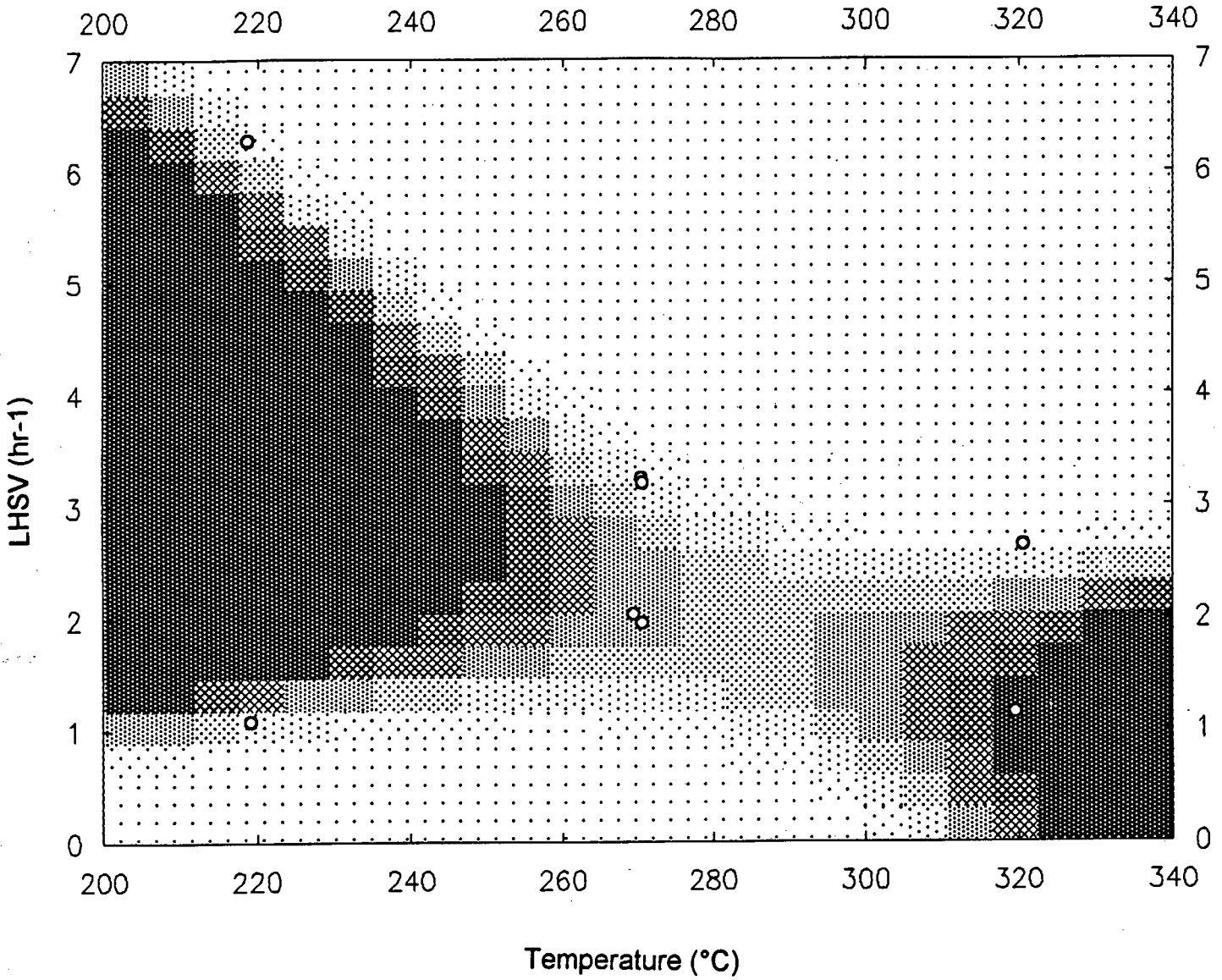

6.9. CONTOUR PLOTS: PROPIONALDEHYDE YIELD AS A FUNCTION OF WATER PARTIAL PRESSURE AND LIQUID HOURLY SPACE VELOCITY.

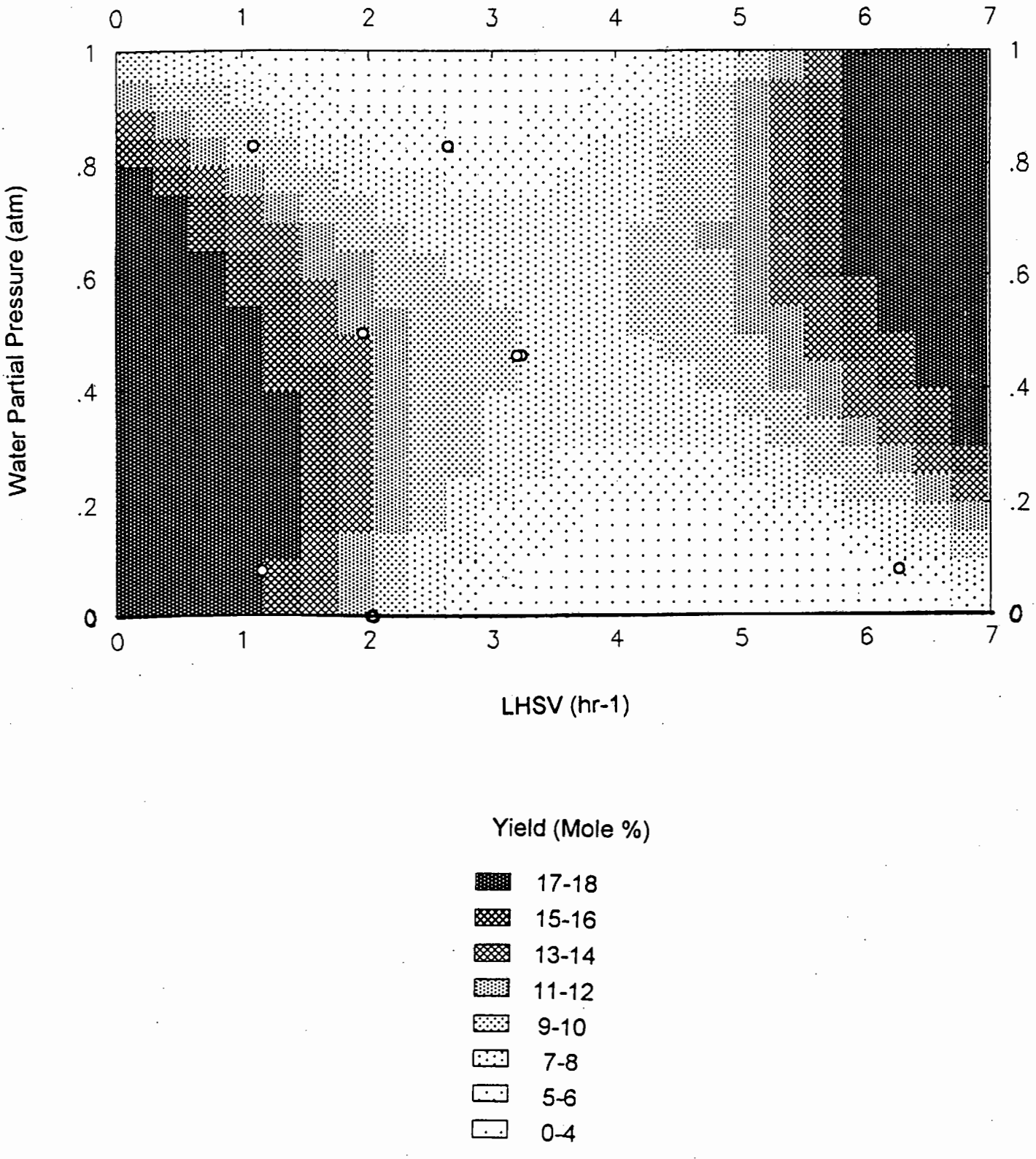

APPENDIX 7.

E.I.-MASS SPECTRA OF REACTOR PRODUCT.

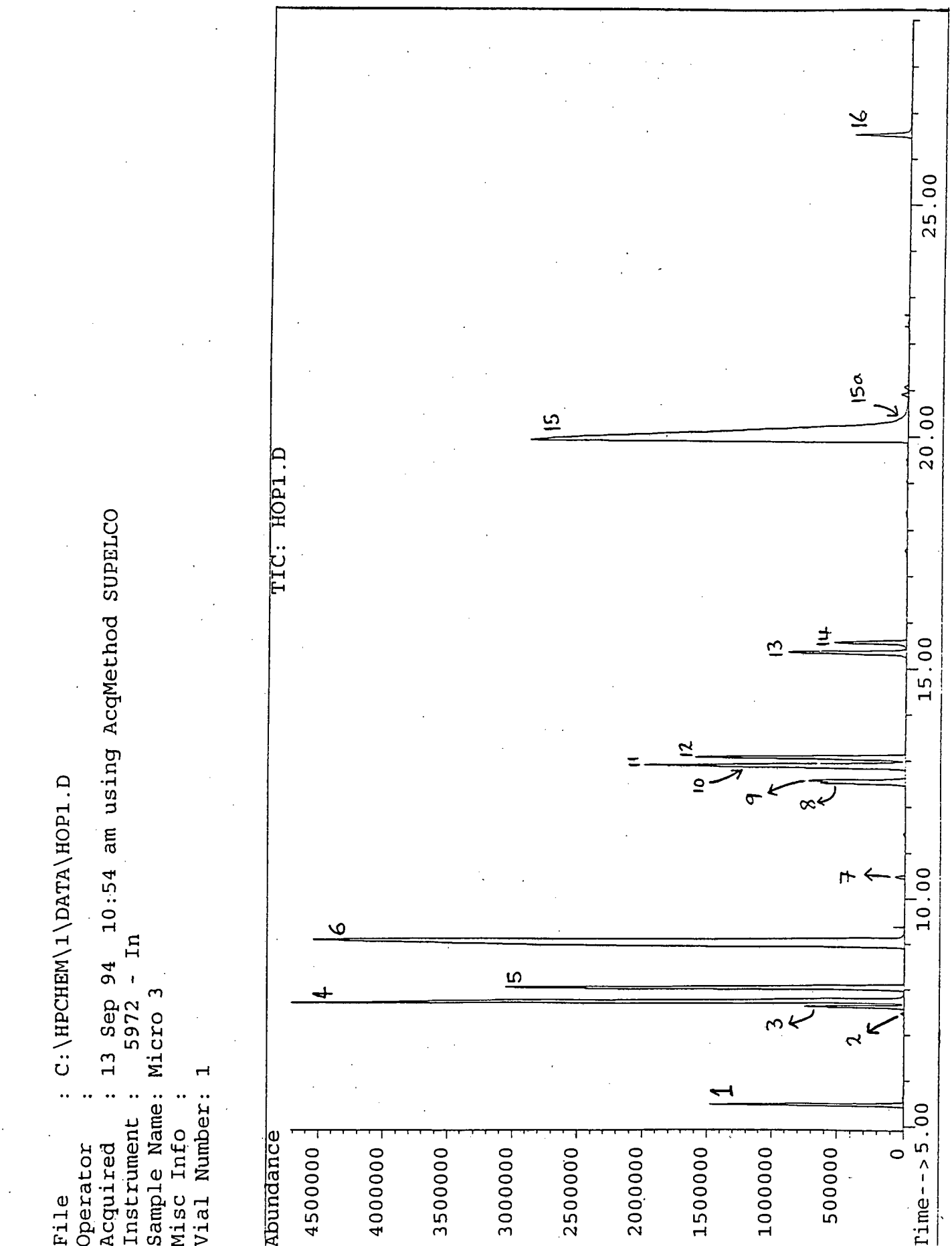

APPENDIX 8.

C.I.-MASS SPECTRA OF COMPONENT 9 (Table 3.14.)

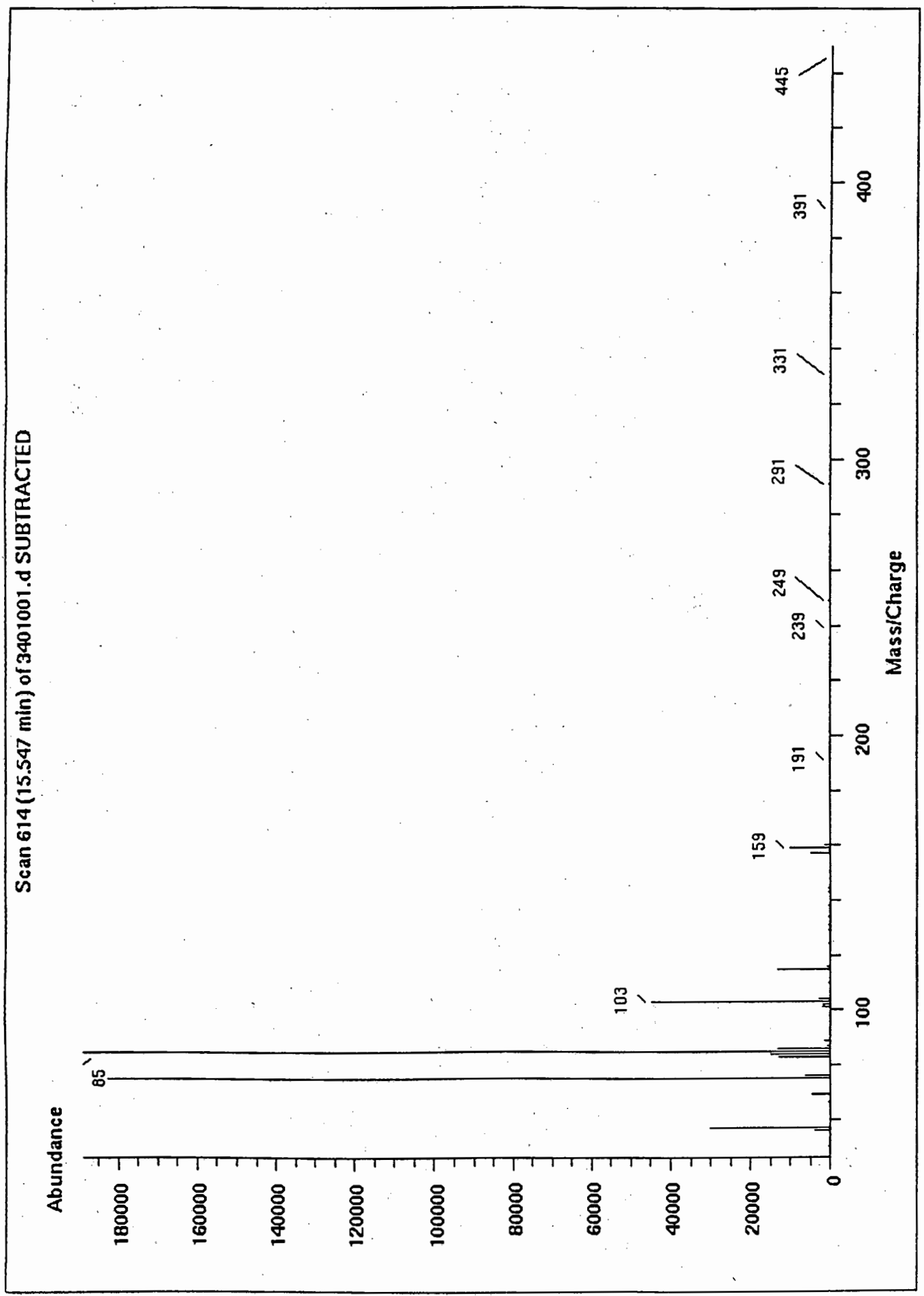

Scan 614 (15.547 min) of 3401001.d
SASTECH,5x,CI
Modified: Subtracted

m/z	abund.	m/z	abund.	m/z	abund.	m/z	abund.
50.20	185	104.15	2661	160.20	1445	250.70	64
56.20	3757	106.40	83	176.60	89	254.30	158
57.20	29936	110.25	354	180.70	62	256.25	94
61.80	83	115.15	13004	184.20	108	262.30	154
64.20	60	116.15	590	191.30	130	265.25	61
66.20	186	124.45	259	194.25	94	268.30	52
69.20	4499	126.10	153	196.15	44	272.30	157
75.20	182650	129.20	363	198.55	93	275.80	53
76.20	6125	131.15	408	199.85	39	278.40	68
83.25	12551	132.20	120	216.25	43	280.50	37
84.25	14828	134.40	214	218.30	10	284.20	100
85.25	188692	138.40	359	226.35	73	288.10	85
86.25	12927	143.20	492	230.75	21	290.40	91
87.25	856	143.90	12	232.25	33	291.30	229
89.20	1438	144.35	189	238.05	93	294.25	38
92.15	153	146.25	63	239.30	124	294.85	11
94.15	154	148.15	23	240.30	49	295.15	25
101.25	1520	157.20	4743	244.20	39	295.45	69
102.25	1804	158.25	483	248.40	80	316.35	46
103.25	44774	159.20	10128	249.30	208	321.25	63

Scan 614 (15.547 min) of 3401001.d
SASTECH,5x,CI
Modified: Subtracted

m/z	abund.	m/z	abund.	m/z	abund.	m/z	abund.
324.15	104	363.90	28	373.40	15	395.40	49
331.25	48	364.25	24	391.25	66	430.35	26
343.35	36	367.40	28	392.30	22	445.55	36
359.50	25						

C.I.-MASS SPECTRA OF COMPONENT 10 (Table 3.14.)

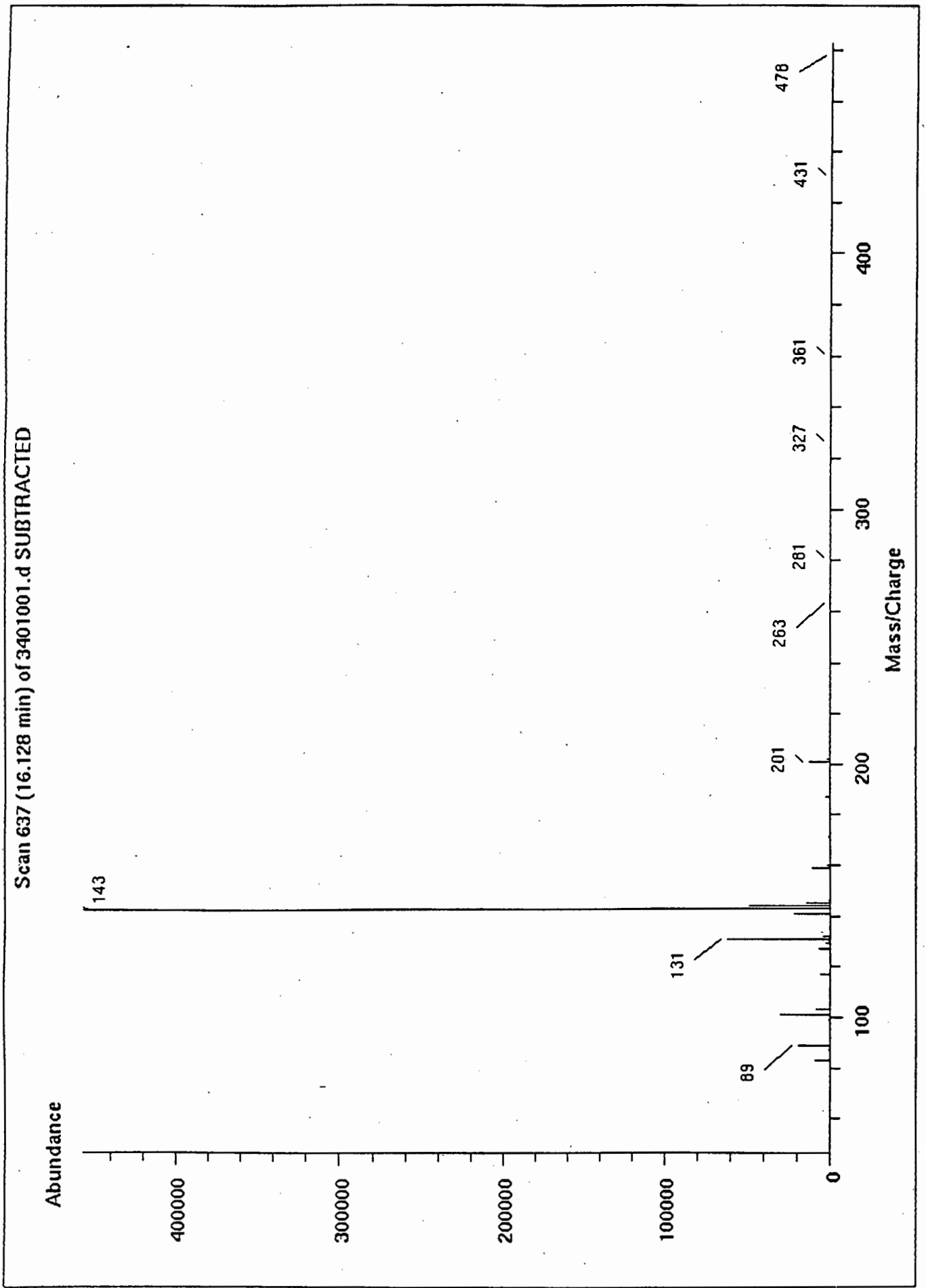

Scan 637 (16.128 min) of 3401001.d
SASTECH,5x,CI
Modified: Subtracted

m/z	abund.	m/z	abund.	m/z	abund.	m/z	abund.
50.50	43	128.20	217	187.25	2119	263.40	247
51.40	261	129.25	2255	188.25	201	267.25	8
51.70	229	130.25	1145	190.55	71	277.25	31
52.05	144	131.15	61788	196.35	54	281.30	193
65.80	31	132.15	3815	201.25	12675	299.25	132
66.20	179	141.30	21628	202.25	1681	299.85	36
78.00	158	143.30	456295	206.65	121	302.65	37
83.25	9428	144.30	48596	208.30	44	303.65	3
87.25	805	145.30	14018	210.15	4	305.05	35
89.25	19176	146.20	960	214.20	22	306.25	48
99.20	1066	150.20	190	214.35	121	309.35	76
101.25	30203	154.00	93	214.65	79	311.35	35
103.25	8676	154.30	150	223.20	106	311.85	25
104.20	232	158.20	88	224.25	51	313.85	29
106.20	22	159.20	10832	230.25	23	327.25	95
108.35	221	160.20	1554	238.65	49	331.65	23
109.75	145	171.25	1167	239.75	35	331.95	35
113.20	380	172.20	294	256.30	194	335.15	30
117.25	6100	176.20	138	260.40	137	337.35	80
127.15	7029	184.50	61	262.35	71	353.30	76

Scan 637 (16.128 min) of 3401001.d
SASTECH,5x,CI
Modified: Subtracted

m/z	abund.	m/z	abund.	m/z	abund.	m/z	abund.
354.70	37	367.35	9	400.15	25	431.25	66
355.30	101	392.60	26	417.95	31	478.40	17
361.40	102	397.15	26	428.35	21		

C.I.-MASS SPECTRA OF COMPONENT 12 (Table 3.14.)

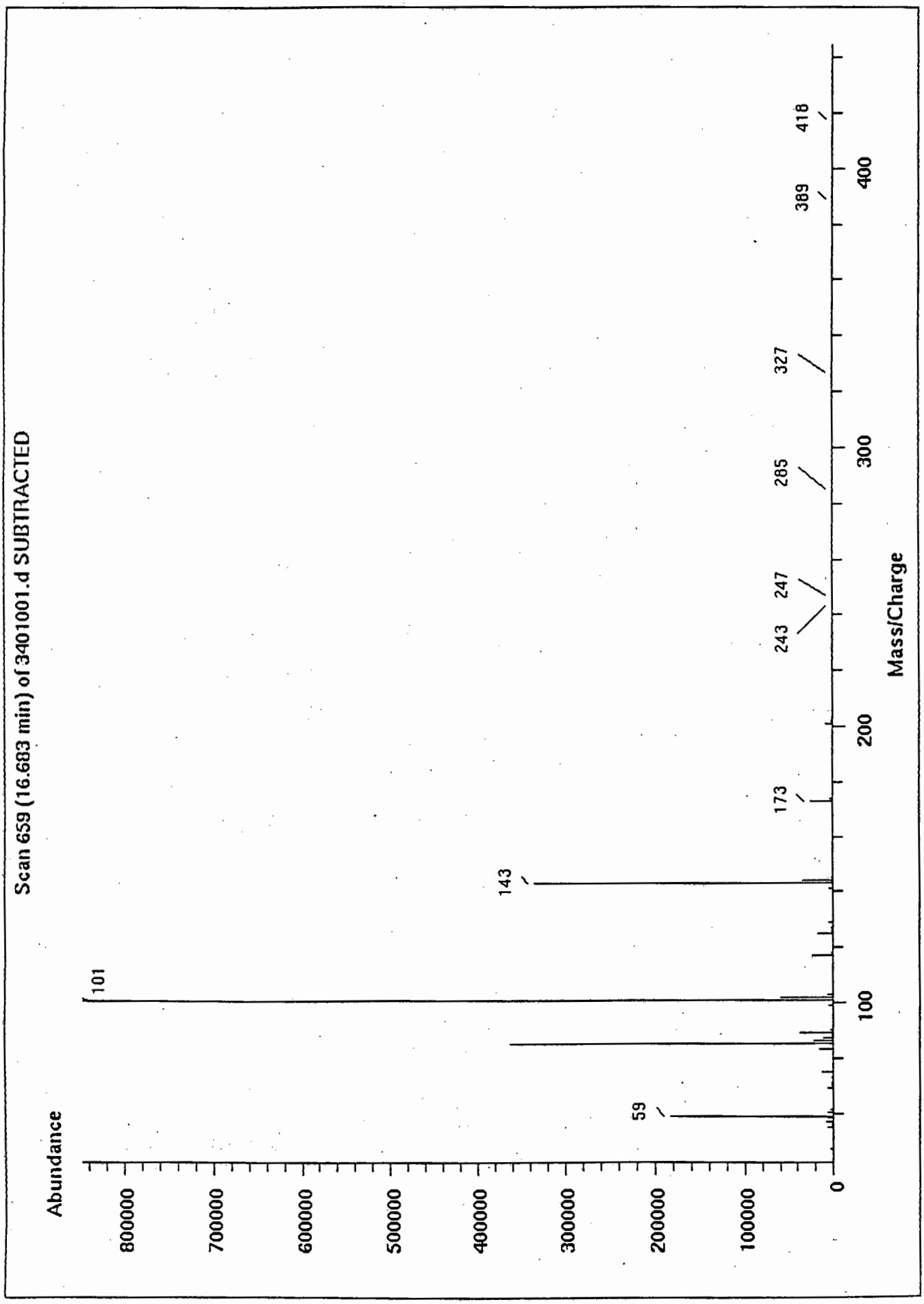

Scan 659 (16.683 min) of 3401001.d
SASTECH,5x,CI
Modified: Subtracted

m/z	abund.	m/z	abund.	m/z	abund.	m/z	abund.
46.30	183	71.20	2101	98.20	41	122.15	135
47.20	3854	73.20	1620	98.45	515	123.15	218
48.10	324	74.20	258	99.25	5140	125.25	17200
49.20	140	75.20	12856	101.25	846973	126.25	1445
49.90	52	76.10	216	102.25	59340	127.20	1277
52.45	124	79.10	296	103.25	5921	128.20	97
53.20	520	81.20	327	104.20	120	129.15	5192
55.20	5400	83.25	15143	105.85	142	130.15	699
56.20	1324	85.25	361938	106.25	147	131.20	420
57.20	8352	86.25	21812	106.55	188	132.10	69
58.30	6429	87.25	10248	107.75	50	133.15	63
59.20	182651	88.15	814	109.20	373	135.20	240
60.20	6391	89.25	37180	111.20	23	136.20	37
61.20	2720	90.25	2447	112.15	338	137.20	62
62.15	187	91.20	80	113.20	321	138.30	142
65.15	57	94.25	350	115.15	628	139.25	216
66.30	92	95.25	159	115.95	401	140.15	62
67.20	321	95.85	111	117.15	23052	140.40	175
69.20	6692	96.25	12	118.15	1418	141.20	4517
70.25	902	97.25	262	119.20	306	143.30	334437

Scan 659 (16.683 min) of 3401001.d
SASTECH,5x,CI
Modified: Subtracted

m/z	abund.	m/z	abund.	m/z	abund.	m/z	abund.
144.30	33784	179.20	325	208.15	117	260.35	33
145.20	2087	180.30	192	213.25	121	261.25	93
150.25	137	183.15	146	215.20	11	265.20	55
154.00	79	185.20	664	221.25	345	265.60	37
156.30	72	186.25	221	227.25	5	269.25	98
159.30	649	187.35	97	230.25	153	270.80	106
160.25	207	188.35	125	232.25	135	275.30	49
164.20	227	189.25	93	237.30	34	276.30	70
166.30	148	193.35	194	239.95	95	281.80	29
167.25	102	195.25	297	240.20	93	283.30	6
168.20	84	196.25	157	241.20	103	284.00	61
169.30	174	198.30	27	242.40	197	284.20	77
170.20	79	199.25	127	243.30	694	285.25	196
171.20	677	200.35	75	244.35	174	288.30	21
173.20	24691	201.25	8019	246.20	150	290.20	27
174.20	2575	202.35	975	247.35	206	295.45	70
175.20	247	203.25	10	250.30	91	297.20	10
176.20	258	204.30	9	254.30	67	297.35	138
177.15	17	206.35	65	255.30	76	298.15	38
177.90	138	207.20	26	258.30	25	300.20	6

Scan 659 (16.683 min) of 3401001.d
SASTECH,5x,CI
Modified: Subtracted

m/z	abund.	m/z	abund.	m/z	abund.	m/z	abund.
303.45	103	327.25	97	355.40	94	389.30	64
305.25	62	331.25	32	357.30	37	396.70	34
306.75	37	342.75	23	377.30	47	397.10	33
307.05	80	351.20	64	379.40	49	418.25	43
308.60	43	352.30	73	382.50	17	427.25	18
313.45	63	355.10	18	387.30	46	440.35	15
319.15	21						

C.I.-MASS SPECTRA OF COMPONENT 13 (Table 3.14.)

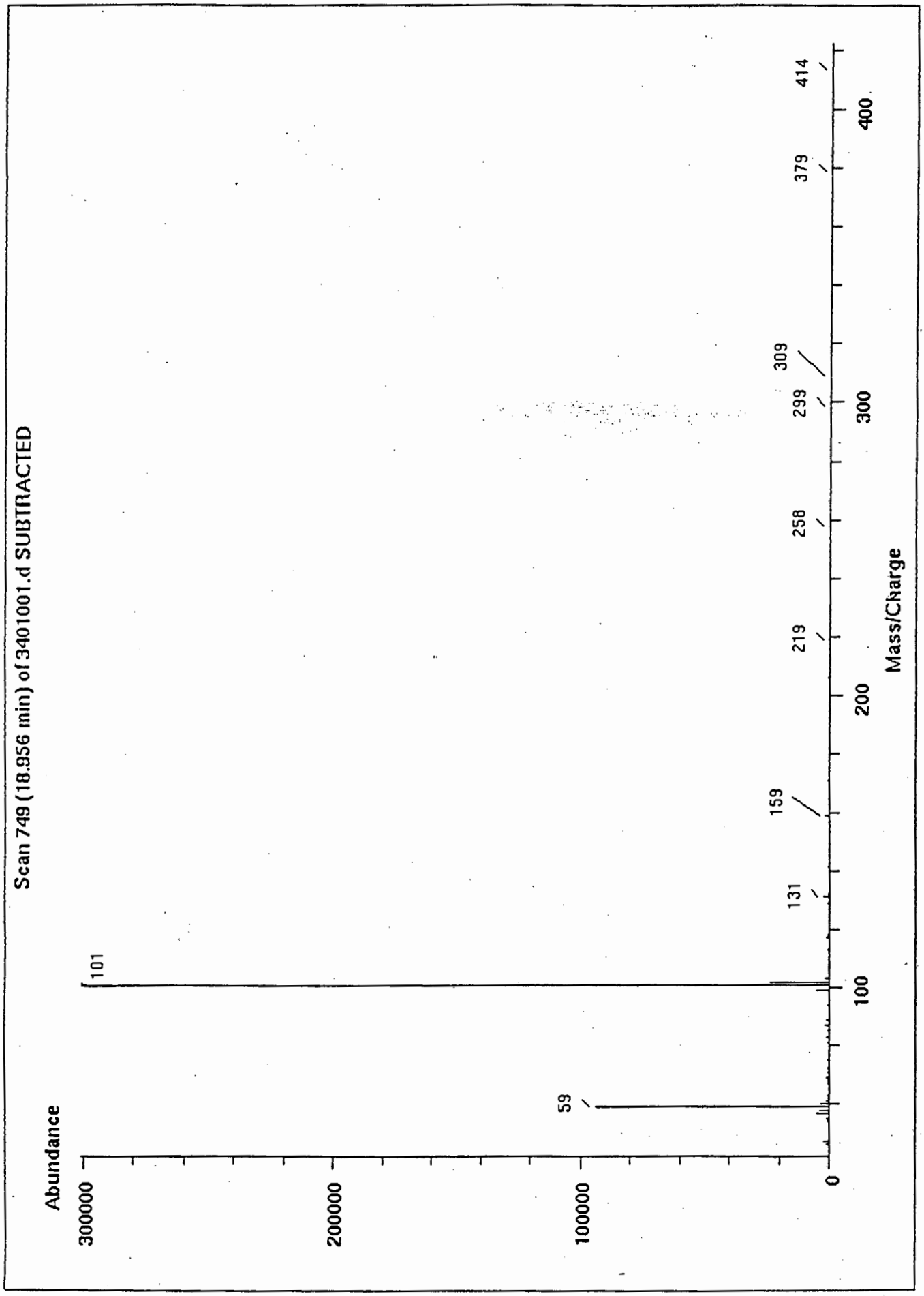

Scan 749 (18.956 min) of 3401001.d
SASTECH,5x,CI
Modified: Subtracted

m/z	abund.	m/z	abund.	m/z	abund.	m/z	abund.
46.25	1178	71.20	606	104.10	257	131.15	2099
47.20	2311	72.20	657	110.15	138	132.15	350
48.20	73	73.20	7	112.20	151	133.15	55
49.20	175	75.20	515	113.25	287	134.15	33
50.20	202	78.00	26	114.20	242	138.25	104
52.25	128	81.20	294	115.15	91	139.20	247
54.20	685	83.25	1187	116.20	35	141.25	396
55.20	939	84.25	24	117.15	1239	142.20	68
57.20	5024	85.25	305	118.15	401	144.30	93
58.20	3782	87.25	1600	119.20	105	145.25	63
59.20	93859	88.15	207	119.85	127	146.25	53
60.20	3515	89.20	945	120.35	200	147.25	139
61.20	1188	90.20	191	121.15	154	152.20	50
62.10	334	92.65	109	123.20	17	158.15	59
63.20	292	94.25	366	124.20	81	159.20	1413
64.10	130	95.25	79	126.20	15	160.20	251
65.15	46	99.25	5049	127.25	130	162.20	175
67.20	279	101.25	300586	129.15	445	163.15	25
68.30	295	102.25	23571	130.15	119	165.25	1
69.20	979	103.25	1521	130.35	228	168.20	134

Scan 749 (18.956 min) of 3401001.d
SASTECH,5x,CI
Modified: Subtracted

m/z	abund.	m/z	abund.	m/z	abund.	m/z	abund.
169.30	147	217.25	9	256.35	21	290.20	42
171.20	458	218.15	187	257.25	220	293.35	9
173.20	119	219.15	369	258.40	262	295.45	86
175.20	148	220.25	231	259.30	25	298.25	7
179.20	145	221.25	22	264.20	81	299.25	178
184.50	88	222.35	84	266.30	74	300.35	123
186.25	81	223.20	134	267.30	128	301.50	12
188.20	10	227.20	46	268.20	48	305.15	62
190.35	240	228.35	92	269.25	117	308.35	43
191.25	61	234.65	21	270.30	94	309.25	158
192.25	135	238.15	87	272.35	26	311.25	38
195.25	35	239.35	1	273.30	82	313.35	92
196.35	144	241.20	147	275.25	112	314.35	90
197.95	69	242.20	93	277.40	93	314.55	89
198.25	94	242.40	79	280.30	43	316.40	25
201.20	134	246.35	26	281.30	158	325.35	37
206.15	349	247.25	155	284.20	144	325.75	61
209.45	149	250.90	75	285.30	168	328.35	45
210.20	46	252.60	62	286.20	6	329.45	59
215.05	216	254.20	95	287.20	58	332.35	22

Scan 749 (18.956 min) of 3401001.d
SASTECH,5x,CI
Modified: Subtracted

m/z	abund.	m/z	abund.	m/z	abund.	m/z	abund.
338.35	55	353.20	37	365.60	40	414.05	188
340.15	60	363.30	75	379.40	77	418.35	26
347.30	62	364.45	26	401.85	16		

C.I.-MASS SPECTRA OF COMPONENT 14 (Table 3.14.)

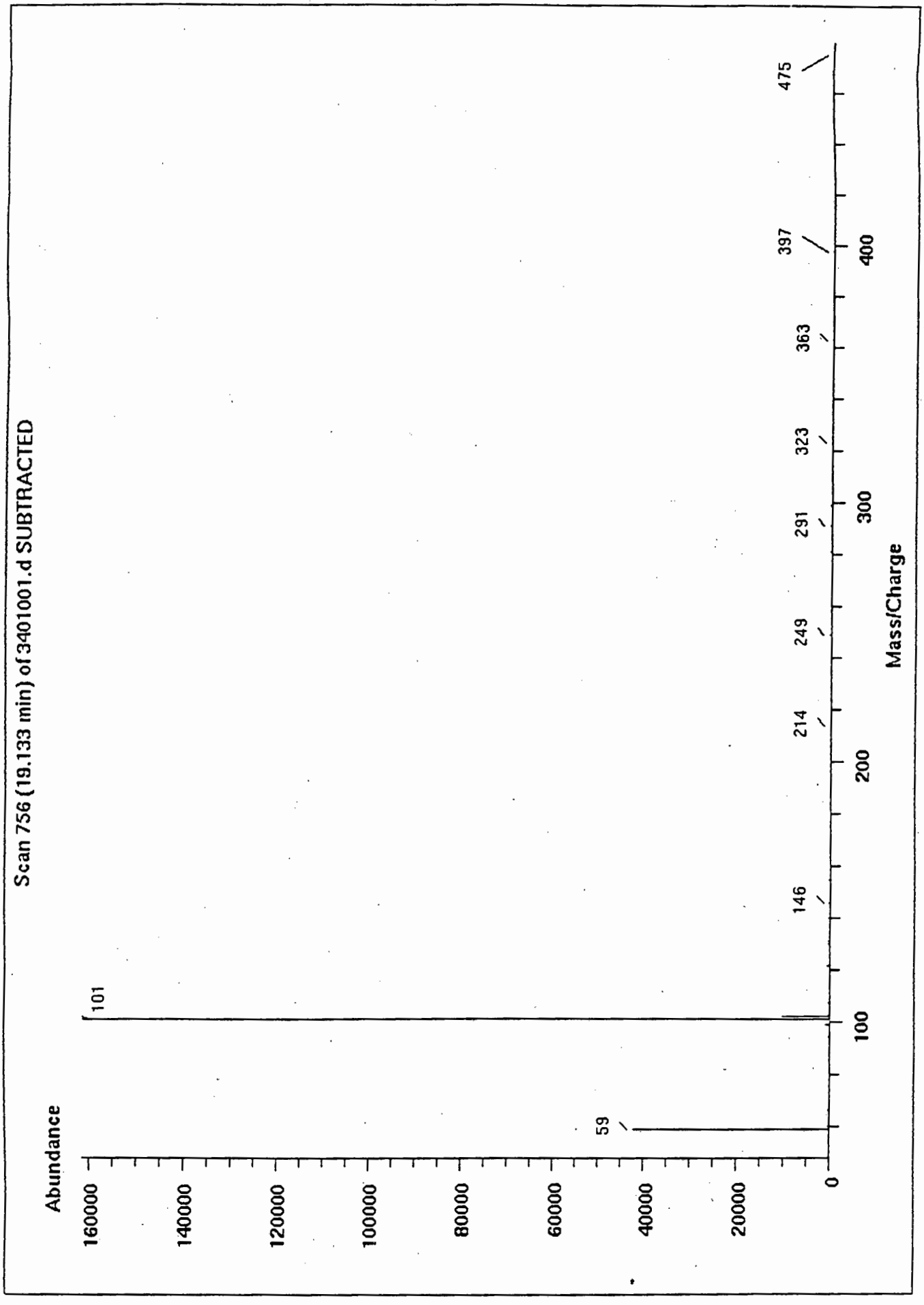

Scan 756 (19.133 min) of 3401001.d
SASTECH,5x,CI
Modified: Subtracted

m/z	abund.	m/z	abund.	m/z	abund.	m/z	abund.
52.30	54	131.20	370	224.25	72	308.35	25
58.20	127	138.15	88	237.20	7	309.40	23
59.20	42112	140.30	156	237.45	88	313.85	47
60.25	432	144.40	8	239.20	35	323.15	85
66.40	92	146.25	183	249.30	224	324.35	38
66.60	154	155.20	149	250.35	110	324.65	46
78.15	17	156.20	27	256.30	36	326.25	51
89.20	30	159.20	87	262.40	33	332.05	51
91.75	32	166.10	49	265.30	3	332.25	54
94.25	56	168.25	9	267.30	53	348.50	31
94.55	187	170.25	53	279.15	81	362.50	43
96.15	114	176.20	103	280.20	40	362.90	67
99.25	1008	186.30	66	281.10	155	363.25	12
101.25	161403	186.60	46	284.30	16	377.20	25
102.25	10335	189.95	87	291.30	214	389.35	43
103.20	298	197.20	21	295.30	39	397.30	82
107.85	238	202.25	40	298.30	13	403.25	26
122.15	441	209.75	65	299.15	183	414.65	26
127.85	120	214.20	115	307.45	84	475.60	20
130.15	300	223.25	131				